To the Graduate Council:

I am submitting herewith a thesis written by Wesley Andrew Underwood entitled "A Novel Free Form Femoral Cutting Guide." I have examined the final electronic copy of this thesis for form and content and recommend that it be accepted in partial fulfillment of the requirements for the degree of Master of Science, with a major in Biomedical Engineering.

Mohamed Mahfouz , Major Professor

We have read this thesis
and recommend its acceptance:

Richard Komistek

William R. Hamel

Accepted for the Council

Carolyn R. Hodges
Vice Provost and Dean of the Graduate School

A Novel Free Form Femoral Cutting Guide

A Thesis

Presented for the

Master of Science Degree

The University of Tennessee, Knoxville

Wesley Andrew Underwood

December 2011

Dedicated to my parents and friends

who have made this work possible.

Acknowledgement

I want to thank Dr. Mohamed Mahfouz and Dr. Richard Komistek for employing me in the Center for Muskuloskeletal Research. The instruction and challenges that I received from them has made this work possible. I also want to thank my coworkers for mentoring me through undergrad and graduate school. Their insight, guidance, and friendship has been invaluable.

Abstract

Knee arthoplasty is a common procedure that requires the removal of damaged bone and cartilage from the distal femur so that a reconstructive implant may be installed. Traditionally, a five planar resection has been accomplished with a universal cutting box and navigated with either metal jigs or optically tracked computer navigation systems. Free form, or curved, resections have been made possible with surgical robots which control the resection pathway and serve as the navigation system. The free form femoral cutting guide serves as a non powered framework to guide a standard surgical drill along an anatomically defined pathway, resulting in the removal of distal femoral cartilage. It is fixed via attachment to a bone mounted base component, which is positioned with a patient specific jig. To operate, the surgeon slides the surgical drill along a pair of interlocked tracks. One track controls motion in the anteroposterior (AP) direction and one track controls motion in the mediolateral (ML) direction. Combining both motions results in the removal of cartilage from the area of the distal femur for unilateral or total knee arthoplasty.

Contents

List of Tables

List of Figures

Chapter 1

Introduction

Currently, most knee arthoplasty techniques require a five planar femoral resection, which is not bone sparing. While in some cases the bone resected is degenerate, this is not the rule for all. Some patients may possess healthy bone and require only an artificial replacement for their cartilage. The requirements of this group have been addressed by patient specific implant companies such as ConformIs, whos iFit femoral components rest over top of the femoral surface after the cartilage has been manually removed by the surgeon. While this technique works, it is part of a larger manual implant generation system, capable of only unilateral and bicompartmental arthoplasties. The work of this thesis presents a patient specific cutting tool for the removal of cartilage from the distal femur for either unilateral or total knee arthoplasty. It is generated from patient specific contours generated by the automated IDAS and iCS systems [1].

1.1. Motivation

Multiple techniques and instruments have been developed to allow a more effective repair of the knee. Historically, the process began with a standing radiograph of the affected knee, which the surgeon then used to assess its varus or valgus deformity and prescribe a corrective angle to restore the mechanical axis of the knee [2]. Intraoperatively, the surgeon would identify boney landmarks located on the femur and tibia and set the orientation of the resection cutting blocks with respect to these landmarks. An oscillating saw was then passed through the slots of the cutting blocks to finish the resection and allow the implantation procedure to continue [2]. Traditionally, unilateral and total femoral components have required a five planar resection.

While this approach was acceptable, the surgeon was responsible for correctly identifying the boney landmarks to place the resection and align the implant. This human element introduced variation in patient outcomes as correct implant alignment is partly related to its performance [3]. Advances in computer hardware and software allowed the surgeons the choice between using traditional metal alignment jigs and the newer optically tracked navigation systems. Although the optically tracked navigation systems allowed surgeons to improve their surgical precession, resections were still created through a planar cutting guide. In addition, the surgical staff must take care to not block the line of sight from the tracking cameras and bone mounted markers [4].

Robotic systems have appeared in the operating rooms of orthopedic surgeons. One of the most successful is Mako Sugical's RIO robotic arm. Unlike the systems mentioned, it allows a curved femoral resection. It is able to achieve this because due to its optically tracked navigation system, haptic feedback system, and exquisitely responsive joints [5]. Despite its expense, this surgical arm is only capable of accommodating unilateral implants [6].

Recently, patient specific instrumentation and implants have been developed. Patient specific jigs allow cutting blocks to be positioned according to a pre operatively planned virtual resection without the intraoperative registration time required by optical navigation systems [7]. Patient specific femoral implants are designed specifically for the patient's knee. The bone contacting surface of the patient specific implant is matched to the surface of the distal femur [8]. The purpose of the implant is to essentially replace the volume of the cartilage and as such an accurate cartilage model is required. Accurate cartilage models are also required for patient specific jigs.

Accurate patient specific instrumentation requires accurate bone and cartilage models to build the instrumentation from. Currently, most orthopedic companies obtain their bone and cartilage models through either a patient's MRI, which contains bone and cartilage data, or CT, which requires the patient to be injected with a cartilage contrasting agent for the cartilage geometry to be captured [9]. After the imaging process, the DICOM images are then segmented to create a model of the bone and cartilage. The manual segmentation process is labor intensive and adds considerable production time. A solution to this is to employ an automatic segmentation process.

This work describes a novel patient specific cutting tool which guides a surgical drill along tool paths generated from the outputs of the Implant Design and Analaysis Suit (IDAS) and Intelligent Carilage System (iCS). It is intended to remove cartilage from the distal femur in preparation for a patient specific implant. Other patient specific implants, such as ConformIs's Ifit system, require the surgeon to manually removing cartilage from the distal femur before the implant may be fit [10]. With future work it can be incorporated in the software package Deformable Articulating Template (DAT) and developed further into a microsurgical robot.

1.2. Thesis outline

This thesis describes a novel free form femoral cutting tool for either total or unilateral knee arthoplasty. Its inputs are derived from two systems, Intelligent Cartilage System (iCS) and Implant Design and Analysis Suit (IDAS). iCS is a semi automated system that accepts either MRI, CT, or bi-planar x-ray images and generates a patient specific bone and cartilage model along with a virtual resection plan. This bone and cartilage model and virtual resection is then inspected by the patient's surgeon who then approves that a patient specific jig be made from it according to his surgical plan. The femur model is then passed to IDAS, which creates anteroposterior profiles of the medial and lateral condyles as well as the sulcus[11]. Mediolateral contours of the distal femur are also generated. The patient specific cutting tool is intended to be incorporated into the Deformable Articulating Template (DAT) so that it may be used to resurface the distal femur in preparation for a patient specific implant.

With the inputs of the femur model with cartilage, profile set and contour set, the cutting tool was generated in NX4. The tool functions by limiting the motion of a surgical drill to along a mediolateral tool path interlocked to an anteroposterior tool path. In this way, the surgical drill may move over the femoral surface in both the anteroposterior and mediolateral directions.

The anteroposterior tool paths were created from the medial, lateral and sulcus profiles. The mediolateral tool paths were created by selecting representative contours from the mediolateral contour set and determining best fit curvatures through an approximating spline. Once the tool paths were created, the cutting area was simulated by sweeping each mediolateral tool path along its corresponding anteroposterior tool path. After a satisfactory simulated resection was obtained, the tool paths were transformed to solid models and manufactured. The simulated resection was then verified experimentally with the manufactured components and femur model with cartilage. This qualitative analysis involved comparing the thickness of the cartilage removed virtually to the thickness of cartilage removed from the physical, resin bone and cartilage model.

1.3. Contribution of the Work

Currently, manual methods must be used through the entire process of creating a patient specific implant. ConformIs and other patient specific implant companies begin implant creation by manually segmenting MRI data, which contains cartilage information, or manually segmenting CT data that includes cartilage information only by injecting the patient with a contrasting agent before the CT scan is conducted. These companies are not able to utilize bi-planar x-rays to create a patient bone model with cartilage, which is a limitation. This work is compatible with a system that automatically segments and creates a bone model with cartilage from all three mentioned modalities with the additional benefit of not requiring a CT contrasting agent.

Chapter 2

Knee Arthoplasty Techniques

The objective of a knee arthoplasty is to restore normal knee kinematics. To reach this goal, several approaches have been created to allow the needs of most patients to be met. Depending on the extent of degeneration from one compartment to all compartments of the knee, unilateral and total knee replacements have been developed. Cruciate retaining (CR) or posterior stabilizing (PS) implants have been developed to facilitate patients that can and cannot stabilize their knee naturally. To address the soft tissue demands of the PS and CR systems, the techniques of measured resection and gap balancing were created.

2.1. Total Knee Arthoplasty

Total knee arthroplasty is indicated for patients with advanced arthritis in more than one compartment. The procedure corrects varus or valgus deformity and the patient is not required to have both collateral ligaments healthy. The knee is typically exposed according to the medial parapatellar approach Figure 2.1. The incision length range of a typical primary TKA has been reported in a 331 patient study as being 18cm-32cm while in extension and 22cm-39cm in flexion, with averages of 24cm and 29.6cm respectively [12]

Figure 2.1 Medial parapatellar approach {1}

Minimally invasive methods have also been developed, with incision length ranging from 8cm-15cm and an average of 10.5cm [13]. Typical minimally invasive and traditional incision lengths are depicted in Figure 2.2. A minimally invasive procedure is not suitable for the work presented in this thesis due to a lack of surgical area to anchor the instrument.

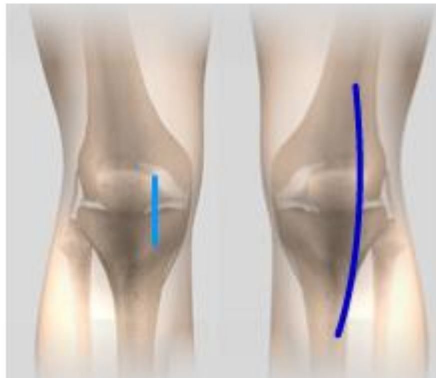

Figure 2.2 Minimally invasive and traditional incision lengths {2}

After the femur and tibia are exposed, the distal femur and proximal tibia are resected. A total, or tri compartmental, resection of the femur results in a five planar surface. A total tibial resection results in a single planar surface. The femoral prosthesis replaces the anterior surface of the femur, which contacts the patella, and both condyles. It may also incorporate structures which are designed to replace the mechanism of the posterior cruciate ligament. The tibial prosthesis replaces the proximal tibial surface [14].

2.2. Soft Tissue Techniques

Depending on the needs of the patient and the choice of surgeon, either a posterior stabilized (PS) or cruciate retaining (CR) system are used. Depending on the knee system chosen, special attention must be given to the medial, lateral, anterior and posterior ligaments so that either joint laxity or over tension is prevented. The techniques developed to address these concerns are measured resection and gap balancing.

Measured resection was developed for use with cruciate retaining implants Figure 2.3, which require healthy posterior cruciate ligaments and emphasize restoration of the joint line for proper function. The joint line is maintained by removing enough tissue from the distal femur to equal the thickness of the femoral component [15]. The goal is that this will adequately tension the PCL, resulting in the PCL functioning normally and controlling rollback during flexion [2]. If the joint line is improperly restored then either slack or excessive tightness will be present in the PCL. Although measured resection does require the additional surgical consideration to adequately tension the PCL, measured resection should require less bone to be removed than gap balancing with a PCL substituting implant because the implant itself, rather than polyethylene spacers, is used to tension the ligaments[2].

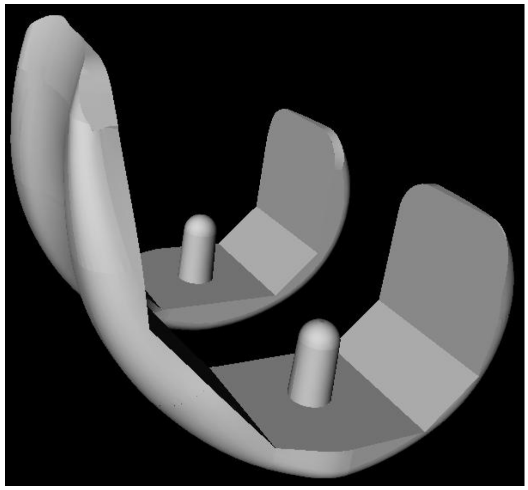

Figure 2.3 Johnson and Johnson Depuy PFC cruciate retaining femoral implant

Gap balancing was developed for PCL substituting implants and emphasizes maintaining equal collateral ligament tension at flexion and extension. This is partly achieved by managing the gap distance between the resected proximal tibia and distal and posterior femur. The constraints provided by the cruciate ligaments are replaced an interlocking cam and post between the tibial and femoral components Figure 2.4. The gap balancing technique requires additional instrumentation to accurately tension the collateral ligaments [2].

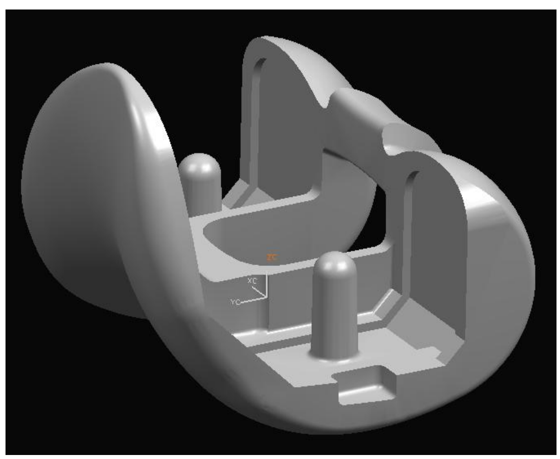

Figure 2.4 Zimmer NexGen LPS Flex cruciate substituting femoral implant

2.3. Unilateral Knee Arthroplasty

Unilateral knee arthroplasty has more restrictive patient requirements than total knee arthoplasty. The patient must have healthy collateral ligaments and healthy cartilage in one compartment. The goal of the partial knee arthoplasty is to correct the effects of diseased cartilage and slight varus or valgus deformity [16]. The minimally invasive incision begins medial to the apex of the patella and extends distally to slightly below the joint line.

The partial implants themselves do not possess the features necessary to replace the functions of the collateral ligaments. If damage to the collateral ligaments develops or arthritis appears in the unaffected compartment then a total knee replacement is usually advised [17. During the procedure, the affected femoral condyle and tibial compartment is resected and replaced with prosthesis.

2.4. Patient Specific Knee Arthoplasty

Unlike traditional implants, which are only matched to the patient in terms of size and also gender, patient specific implants are matched to the patient anatomy. They are reconstructive in that damaged bone and cartilage is replaced in function and form by the implant. To create a patient specific implant, the model of the patient bone and cartilage must be obtained by segmenting either MRI or cartilage contrasted CT. The implant is then tailored to the bone surface and is not thicker than the cartilage removed. In this way the joint space is maintained. During implantation the cartilage is removed from the femoral surface by a rasp [10]. The ConformIs implants are bone sparing as they do not require the five planar resection of traditional implants but are only available for unilateral and bicompartmental procedures Figure 2.5.

Figure 2.5 ConformIs iUni and iDuo {3}

Chapter 3

Surgical Navigation

Proper implant alignment is related to implant performance. It has been shown that femoral component malalignment in the coronal plane can increase the occurrence of abnormal knee function such as lift off of one condyle from the polyethylene implant during rollback [18]. Resections are created after the cutting guides are placed on the bone with reference to bone landmarks. For the resections to be created, the landmarks must be properly identified.

3.1. Landmarks

The mechanical axis is a line defined as originating at the center of the femoral head, through the center of the knee, and ending at the center of the ankle Fig. It can be thought of as the axis along which the leg supports bodyweight when standing. In the normal knee it passes through the center of the knee Figure 3.1 while in the abnormal knee it may shift to the lateral compartment (valgus knee) or more commonly the medial compartment (varus knee) Figure 3.2 [19].

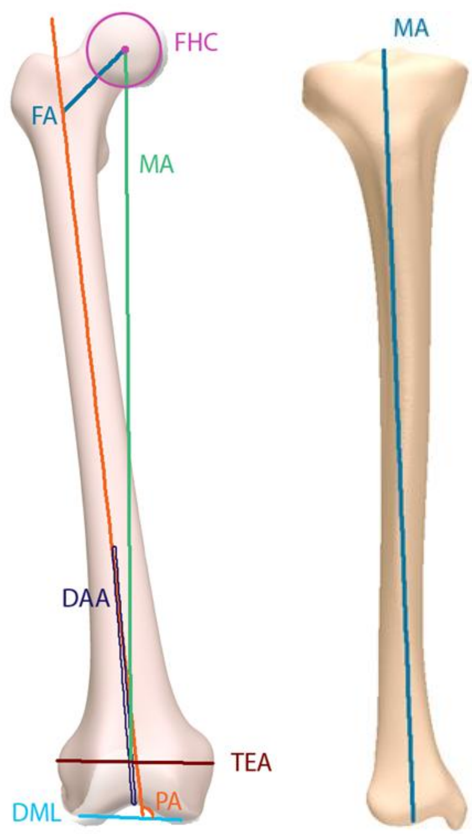

Figure 3.1 Mechanical axis of the femur and tibia {4}

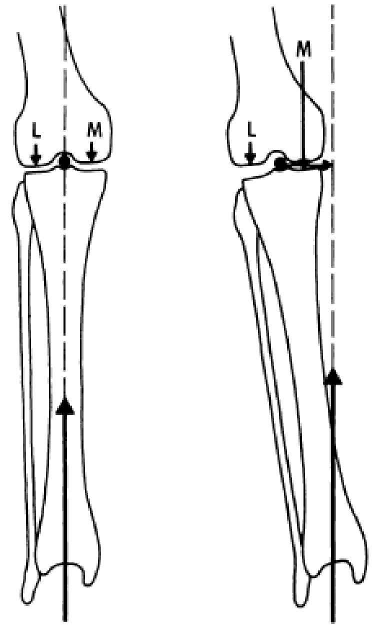

Figure 3.2 Ground reaction forces in the static normal knee and varus knee {4}

The mechanical axis must be restored in the patient because if it is not kinematic and implant wear abnormalities will result due to uneven joint loading. The natural or anatomic axis is defined as a line passing axially through the intramedullary canal of the femur or tibia. This allows the intramedullary canals of the femur and tibia to be used as reference landmarks for instrument placement.

The corrective angle with which the knee is resected is considered to be the angle between the natural and mechanical axis. In practice, this angle is found by taking a standing anteroposterior radiograph of the patient's lower body, marking the natural and mechanical axis by noting the center of the femoral head and ankle and intramedullary canals, and determining the angle between the natural axis of the femur and mechanical axis. The distal femur is typically resected at this angle with respect to the femoral intramedullary canal [2].

Two techniques exist which result in acceptable restoration of the mechanical axis. In the classic alignment of the knee, the tibia can be thought of as rising perpendicularly while the femur is 6 degrees valgus (knock kneed) with respect to the mechanical axis. This alignment is achieved by resecting the proximal tibia perpendicular to the tibial shaft and resecting the distal femur 6 degrees valgus to the femoral shaft. This results in an overall, natural 6 degree valgus knee angle. The method of anatomic alignment introduces a 3 degree varus (bow legged) angle resection of the proximal tibia with respect to the tibial shaft and a 9 degree valgus angle distal resection to the femoral shaft. In the case of the anatomic alignment the difference between the 3 degree varus tibia and 9 degree valgus femur is also the natural 6 degree valgus knee [2].

Axial plane alignment of the femoral implant can be determined with multiple landmarks: the trans-epicondylar axis, the tibial shaft axis, the anteroposterior trochlear sulcus (Whiteside's line), or the posterior condyles. The transepicondylar axis is a line with endpoints located at the center of the medial and lateral epicondyles [11]. Alignment with respect to the transepicondylar axis requires the universal cutting box to be positioned with its length parallel to the axis. The tibial shaft axis extends from the tibial shaft and is perpendicular to the transepicondylar axis. Alignment utilizing the tibial shaft requires the length of the cutting box to be perpendicular to the shaft. The anteroposterior trochlear sulcus lies in the trochlear groove and is also perpendicular to the transepicondylar axis. As such, cutting box alignment to Whiteside's line is similar to alignment referencing the tibial shaft. The posterior condylar axis is defined as the axis extending from the most posterior points of the medial and lateral condyles. Cutting box alignment referencing the posterior condylar axis is similar to referencing the transepicondylar axis. While all described reference axis are valid, the surgeon must be aware of wear of the posterior condyles when using them as reference. Damage to the posterior condyles shifts the axis that would be found normally, resulting in an abnormal reference axis and malalignment. Axial alignment of the tibial component can be determined multiple ways in flexion or extension. As an example, in flexion the anterior or posterior surfaces of the cut tibia and ankle can be used as reference [2].

3.2. Instrumentation

Instrumentation has developed to increase the precision and accuracy of the resections. Originally, the cutting blocks used to create the resections were positioned with generic mechanical jigs that are adjusted to fit to the patient's landmarks. After the surgeon was satisfied with this fit, the cutting blocks were then installed and used. Because the accuracy of this system depends on the individual ability of the surgeon to correctly identify landmarks, variation from surgeon to surgeon and patient to patient existed. These mechanical jigs were then replaced by passive surgical navigation systems that indicate in real time the orientation of the patient's limb. Finally, advances in rapid prototyping allowed the creation of patient specific jigs which eliminate the variability of mechanical jigs and registration time of optical navigation systems.

3.2.1. Universal Cutting Blocks

Universal cutting blocks are slotted metal boxes fixed to the bone with respect to boney landmarks. They may only create planar cuts and is similar to the miter box used in woodworking. To remove bone, the surgeon fits an oscillating saw into the slot and pushes it through the bone until the cut is complete. The slots of the box provide the constraint required by the oscillating saw. Originally, a separate cutting box was necessary for each cut, requiring the surgeon to refit a new cutting box for each plane. Universal cutting boxes were then developed, which allowed the anterior and posterior planes and chamfers Figure 3.3. This reduced surgical time by reducing the number of instrument adjustments, but a separate cutting box is still required to create the distal cut [20]. They are aligned to the bone with either mechanical jigs or optical navigation systems.

Figure 3.3 Universal cutting block and use with an oscillating saw {5}

3.2.2. Mechanical Jigs

Intramedullary or extramedullary rods align the femoral and tibial cutting boxes to the femur and tibia. Extramedullary rods do not utilize the intramedullary canal of the femur and tibia while intramedullary rods do. While both types of alignment rods may be used for either the femur or tibia, it is more common for the surgeon to choose to use a femoral intramedullary rod and tibial extramedullary rod [2]. Reasons for this include that the extramedullary femoral rods rely establishing alignment from bone landmarks, which may be difficult to locate accurately. By definition, intramedullary guides require the intramedullary canal to be reamed, increasing the patient risk of bone fracture and fat embolism as a result [21]. It has also been found that intramedullary rods lose accuracy when used on a valgus tibia [2]. Because the combination of intramedullary femoral rod and extramedullary tibial rod is more common, it is considered further.

The intramedullary femoral rod is the reference to which the distal femur cut guide and cutting box attach. It is inserted in a hole reamed about 1 cm anterior to the PCL's origin and into the intramedullary canal Figure 3.4 [20]. Preoperatively, a standing radiograph of the patient's lower body is taken and the intramedullary canal is observed and the corrective angle of the distal cut is determined with respect to the intramedullary canal and mechanical axis. Once the intramedullary rod is placed, the distal cut guide is attached Figure 3.5 and set to the resection angle determined in the preoperative radiograph.

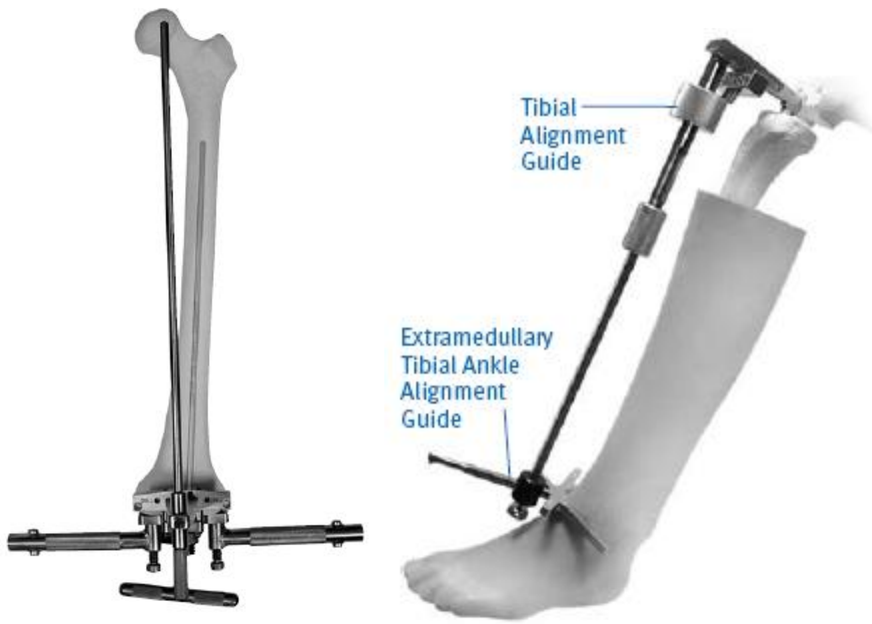

Figure 3.4 Example femoral IM alignment guide and tibial extramedullary guide {5}

The extramedullary tibial rod attaches distally to the tibia via a clamp around ankle proximal to the malleoli. Proximally, the rod is positioned with respect to the tibial tuberocity and the center of the tibial plateau. The rod is aligned to the tibial shaft by adjusting the distal ankle clamp so that it is parallel to the transmalleolar axis and then translated medially to place it in the center of the tibia [22]. The proximal tibia cut guide can then be attached and set to its preoperatively determined correction angle Figure 3.4. The cutting blocks for the femur and tibia guide the oscillating saw during the osteotomy. The femur distal cut guide is responsible for coronal plane alignment of the femoral component Figure 3.6 [2].

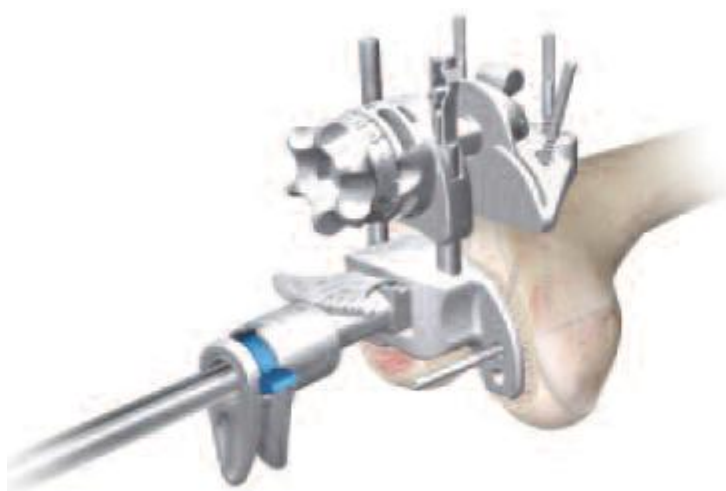

Figure 3.5 Distal femur cut guide positioned and attached to IM alignment rod {6}

Figure 3.6 Distal femur cut guide and anterior/posterior/chamfer cutting box use with an oscillating saw {6}

The anterior and posterior cuts as well as the chamfers are usually guided by a single universal cutting box that attaches to the distal femur after the distal cut has been made Figure 3.6. The alignment of the universal cutting box is responsible for rotation of the femur component in the axial plane and is rotated so that the cutting box is parallel to the trans-epicondylar axis.

The tibia proximal cutting guide attaches to either the intra or extra medullary rod. It is responsible for the coronal plane alignment of the tibial component and its coronal and sagittal cut angles are adjustable Figure 3.7. This allows the surgeon the ability to perform either natural or classic alignment in the coronal plane and also allows the tibial component to be installed with an anterior to posterior slope in the sagittal plane if desired [22].

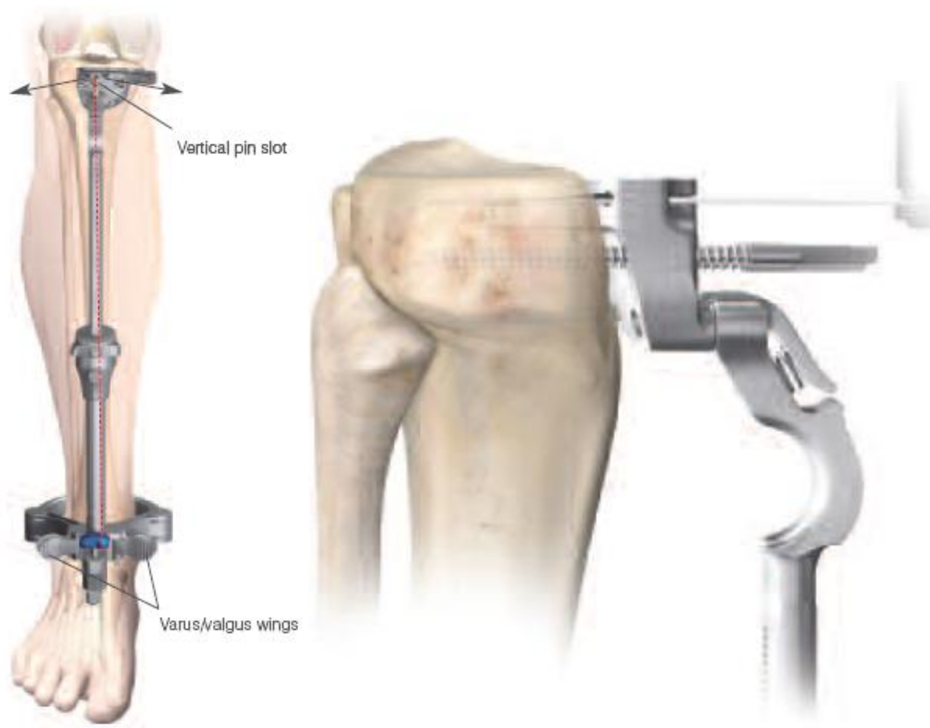

Figure 3.7 Distal tibial cut guide with extramedullary alignment rod and use with an oscillating saw {6}

3.2.3. Optical Navigation

Implant alignment may also be realized with computer rather than mechanical systems. Image free surgical navigation systems do not require intraoperative imaging to observe bone positions but rather track the femur, tibia, and surgical instruments with optically tracked rigid markers and a stylus. While several image free technologies exist, optically based navigation is the most prevalent.

A typical optically tracked navigation system consists of a 3d camera composed of either two or three cameras, depending on the manufacturer, positioned a known, fixed distance apart. The camera system is typically mounted on a cart containing the navigation computer and remains fixed throughout the operation Figure 3.8. The markers are rigid posts with at least three active infrared LEDs or reflective spheres whose positions relative to one another is known. With the system active, the infrared LEDs strobe in a known sequence and is detected by the 3d camera. Because the relative positions of the LED lights and strobe sequence is known, the navigation system is able to triangulate the marker's orientation in space. Markers are placed on the surgical instrumentation, allowing it to be tracked throughout its use Figure 3.8 [23].

Figure 3.8 Stryker image free navigation system and instrumentation {7}

Most computer navigation systems utilize virtual bone models that the system analyzes and then creates the surgical plan, consisting of the necessary resection levels, angles and rotations that the surgeon will apply. For the computerized bone and generated surgical plan to have meaning in the real world, they must be matched to the patient's bone through registration. Registration may be either fiducial based or bone shape based. Fiducial registration requires fiducial screws to be placed into the femur and tibia in prescribed locations pre operatively and remain in place while a CT scan is made and throughout the operation [24]. This form has fallen out of favor to shape based registration, which will be the focus.

Shape based registration uses information gathered from the patient bone surface to create correspondence between the real and model bone. To register the bones, the navigation system instructs the surgeon to palpate either single points or point clouds over landmarks. The navigation system may either then use the points directly to create the surgical plan or pass the points through an additional process called bone morphing. Bone morphing statistically fits a mean bone model to the inputed point cloud to create the patient bone model, rather than requiring preoperative imaging [24]

Optically tracked image free navigation has been used successfully. While each system requires specialized education and incorporates slight differences in methodology, the overall objective of a navigation system is the same as that of mechanical jigs. As the name implies, a surgical navigation system does not take control or decisions from the surgeon, but rather augments his knowledge of the situation in real time. After the patient's anatomy is registered to the navigation system, the system displays pertinent information such as varus/valgus angle, flexion/extension angle, and resection level [24].

3.2.4. Robotic Navigation

Advances in surgical computing lead to development of computer navigated and robotically controlled cutting guides. One advanced robot is the Mako RIO surgical robot, which is comprised of an optical navigation system and a surgical drill mounted to a robotic arm. Another, simpler system is PiGalileo, which is essentially a motorized universal cutting block. A third is Praxiteles, which, like PiGalileo, is only capable of planar cuts.

Active navigation systems have seen limited use, due in part to their expense. The Mako surgical arm Figure 3.9 has been approved for unilateral knee replacement. The free end of the robotic end, the effector, is fitted with a surgical drill and round headed bur. Like passive navigation systems, tracking is achieved with optical markers, which are placed on the patient femur and tibia and are mounted on the effector. The patient bone models are derived from a segmented CT scan. The registration method is similar to those described previously, with kinematic evaluation of the leg to define the center of the femoral head and palpation of the bone surface with an optically tracked probe to define landmarks [25].

The robot is equipped with a haptic feedback system, which provides the surgeon with touch feedback based on the position of the drill tip. During the operation, the navigation system monitors movement input from the effector and position input from the optical markers. If the tool is not detected in a boundary area the haptic feedback systems supports the weight of the arm and moves the arm along with the surgeon, providing a feeling in the hand of weightlessness. When the navigation system detects that the tool is moving close to the boundary area, the arm provides increasing resistance, giving the surgeon the sensation of trying to push the tool against a wall and preventing the drill tip from advancing further [5].

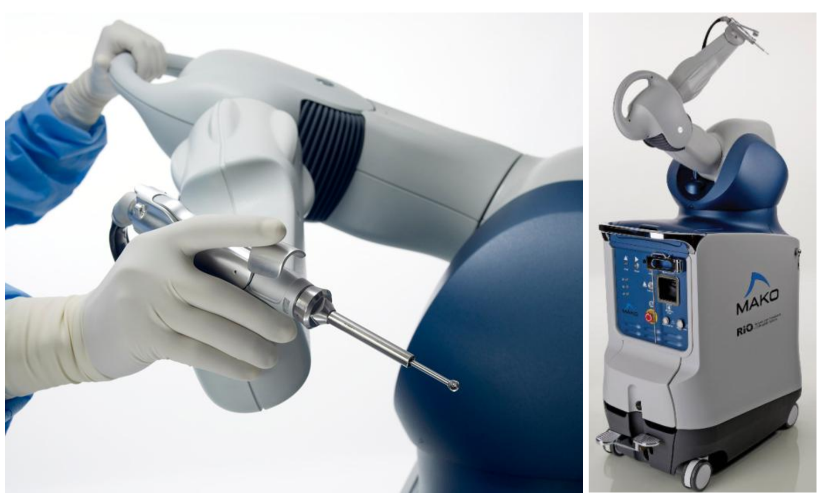

Figure 3.9 Mako Surgical RIO robot {8,9}

Smith and Nephew's PiGalileo surgical robot Figure 3.10 provides the surgeon assistance with ligament balancing and also positions a slotted cutting guide for the five planar cuts required by a typical TKA [26]. It clamps directly to the anterior of the femur and uses an optical navigation system to derive the bone landmarks used in the virtual resection. The system's awareness of the position of the motorized cutting guide with respect to the femur allows the navigation system to position the plane of the cutting guide in line with the plane indicated by the virtual resection. Due to its size, PiGalileo must be placed proximally, which is not suitable for minimally invasive techniques due to its surgical space requirement. Like a universal cutting box, it may only create planar cuts.

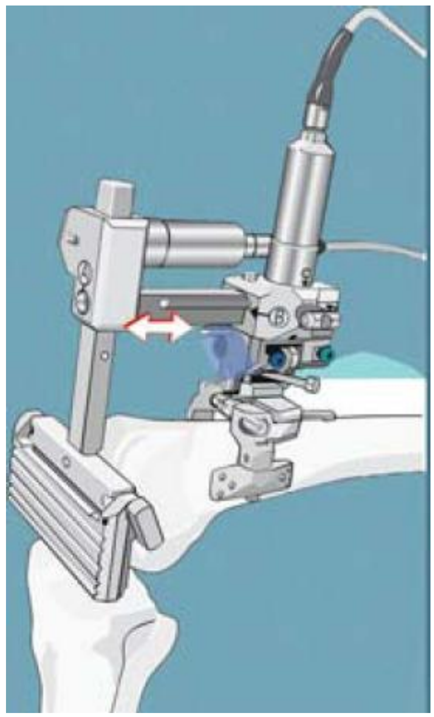

Figure 3.10 PiGalileo surgical robot {10}

Praxiteles is another robotic cutting guide and functions by sequentially rotating the surgical milling tool around its attachment point on the side of the medial condyle Figure 3.11. Its base is fixed to the bone with two pins. As indicated by the authors, the medial, rather than lateral, side was used for fixation to avoid vascular and nerve damage [27]. The robot functions by sequentially rotating the surgical milling tool around its bone fixation point as each of the five planar resections are created. The cutting plane of the surgical tool is limited by the yellow arm Figure 3.11 Two parallel motors oppose movement of the assembly and provide the force to rotate the cutting tool into position. This creates two degrees of freedom available to the surgeon: in and out motion of the milling shaft and rotation about the swivel point along the shaft. Like a universal cutting box, it may only create planar cuts. Unlike PiGalileo, which requires an oscillating saw, the cutting tool is a round milling bur. This is necessary as the rotating arm of the robot would obstruct the straight path required by an oscillating saw. Praxiteles is compatible with minimally invasive techniques and femur implants with planar, not curved inner profiles. Its position with respect to the femur is tracked optically and adjustments to its motors are controlled with feedback from the optical system [27].

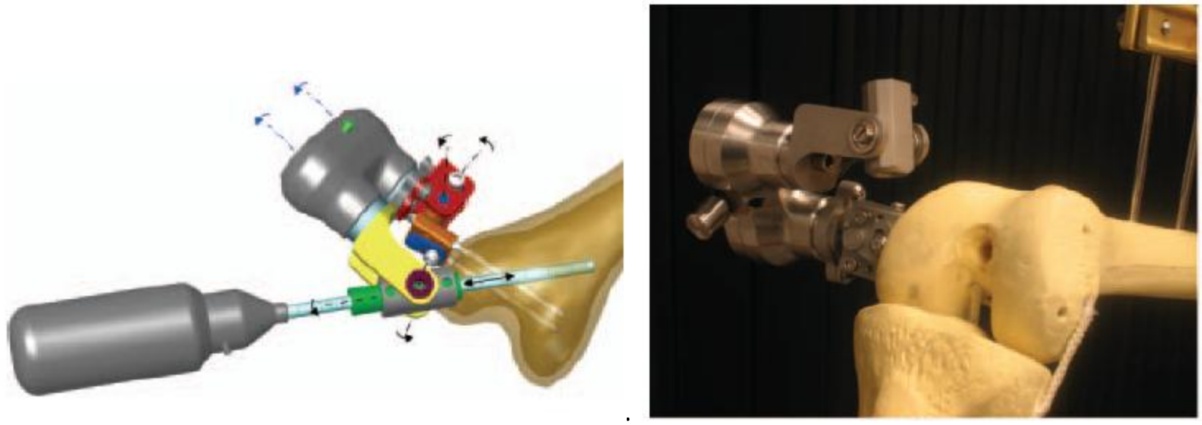

Figure 3.11 Praxiteles surgical robot {11}

3.2.5. Patient Specific Jigs

Patient specific jigs are disposable plastic parts that fit to the surface of the tibia and femur. They include holes that are used to place the pins that the cutting guides fix to. Unlike other navigation systems, all surgical planning is performed preoperatively, requiring the surgeon to only expose the knee and perform the resection during the operation. In addition, no mechanical alignment jigs must be assembled and the intramedullary canals may remain intact. Because in this case correct jig alignment depends on a close fit to the cartilage surface, jigs are designed to fit select areas so that the jig may only fit in one, correct position. After virtually fitting the jig to the bone, the jig creation system places alignment screw holes in the jig according to the virtual resection so that mechanical alignment jigs and intraoperative surgical navigation systems are not needed [28].

Intraoperatively, a surgeon uses a patient specific jig by exposing the knee then placing it on the surface of the bone and checks for snugness of fit. If it is acceptable, bicortical fixation pins are drilled into the guide holes of the jig and the jig is then removed. Patient specific jigs may include slots so that the jig itself is the cutting guide but this is not common. The cutting guides may then be fixed to the guide pins and the resection may continue as planned.

Chapter 4

Automatic Segmentation and Analysis

Because the proposed cutting guide is unpowered, motors and an intraoperative navigation system may not be used to control the cutting tool along the desired pathway. Conformation to the patient anatomy is achieved by moving the cutting guide along rigid tracks, whose shape is derived from patient anatomy. In this way, a complex robotic system is not necessary to guide the cutting tool. For the patient specific tracks to be generated, the bone and cartilage geometry of the distal femur must be reconstructed digitally so that their features may be analyzed to create the cutting tool. The required femur with cartilage model is obtained through one of three modalities: CT, X-ray, or MRI. Digital analysis of the femur is conducted through a statistical bone atlas combined with the proprietary software package Implant Design and Analysis Suit (IDAS) to obtain the raw feature data (contours) of the femur and cartilage [1]. This raw data is further refined to obtain the completed cutting tool.

4.1. Bone and Cartilage Model

The patient bone and cartilage model is reconstructed by first imaging their leg with CT, bi planar X-ray, or MRI. CT and MRI are volumetric imaging techniques which yield a set of image slices (DICOM files) along the long axis of leg. The bone model is then extracted from these slices in a process called segmentation, whereby the area of interest is outlined in each slice and saved through manual or automatic methods [11]. After smoothing the raw model, the final patient bone model is obtained. While both methods are volumetric, only MRI may capture the patient cartilage directly, resulting in a bone model with cartilage. CT may not be used to image cartilage as cartilage has a similar attenuation rate as the surrounding soft tissue, resulting in cartilage that is not separable from the surrounding soft tissue.

To generate a surface model of the femur utilizing bi planar X-ray, the patient is fitted with a registration brace and then bi-planar X-rays are taken. To create the surface model of the patient bone from bi planar x-rays, the x-ray images and an average bone from a principal component based statistical bone atlas are placed in a 3d scene. An initial pose is then provided by the user and the average bone shape, translation, and rotation are optimized through a genetic algorithm and proprietary 2d-3d scoring metric [29].After convergence is reached, the resultant surface model generated from the atlas model is accepted as representative of the patient geometry. As with CT, additional processing is required to estimate the patient cartilage. This work is beyond the scope of this thesis.

X-ray and CT modalities require an estimated cartilage model to be applied to the distal femur surface. This mean cartilage model is derived from cartilage tissue segmented from MRI data. After the surface model of the patient femur has been created, the cartilage model is scaled to fit the specific bone then applied to the distal femur. After cartilage is added to the bone models AP profiles and ML contours may then be generated.

4.2. Contour generation

After the segmented bone with cartilage model is obtained, it is imported into a statistical bone atlas combined with IDAS. The purpose of a statistical bone atlas is mainly to deform a base, or average bone model into the shape of a patient bone model in an ordered way so that global, or overall, shape differences can be compared across populations. The purpose of IDAS is to automatically calculate bone landmarks for any bone within the atlas such as the TEA, the mediolateral contours, and the profiles of the medial condyle, lateral condyle, and sulcus [30].

Within IDAS, the TEA is defined as the vector connecting the most medial and lateral points, or vertices, of the epicondyles of the femur model. The medial and lateral profiles Figure 4.1 are generated by a plane passing through the most anterior, distal, and posterior points of the condyles of the femur model with cartilage. The intersection of the bone and plane was then re sampled to create a profile consisting of 50 equidistant points. The sulcus profile Figure 4.1 is calculated by rotating a plane about the TEA in increments of 10 degrees. The points where the plane intersects the bone surface are captured, creating contours in the mediolateral (ML) direction Figure 4.2. For each contour, the lowest point of the ML contour defines the sulcus [10,30].

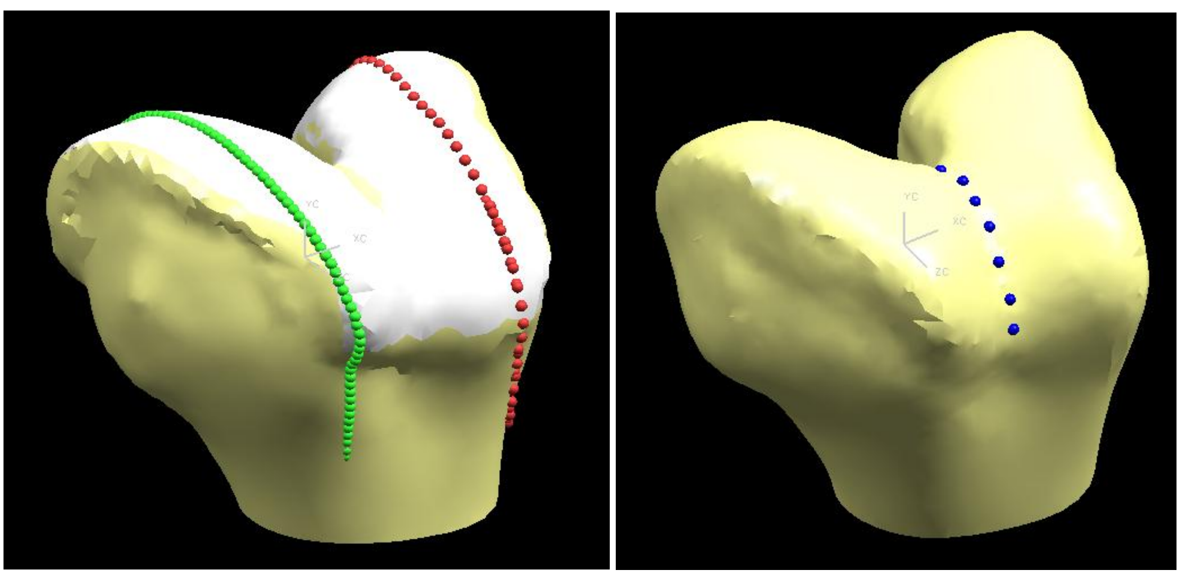

Figure 4.1 Medial (green), lateral (red), and sulcus (blue) profiles

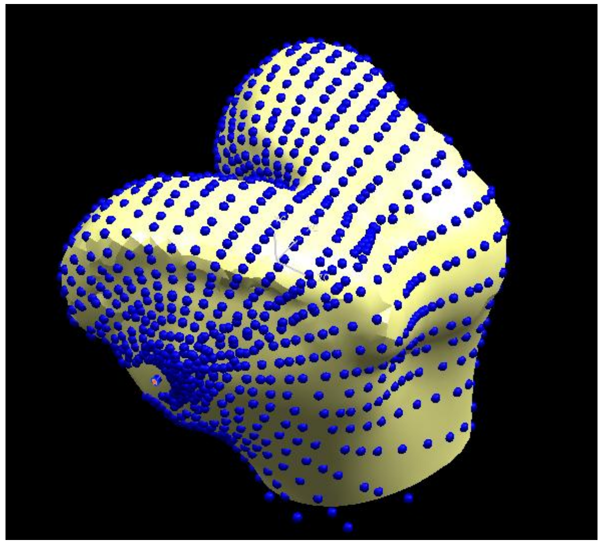

Figure 4.2 mediolateral contours rotated about the TEA

4.3. Cubic Spline Approximation

Cubic splines have found use in fitting functions to discrete data points. They are useful in this work as a way to create a continuous, smooth control path for the cutting tool from the discrete points generated by IDAS. Specifically, as a way to fit a best fit curve to multiple mediolateral contours aligned in a single plane. Because the desired curve is a best fit of multiple contours, it is not desired or possible for the spline to pass through all control points. Because of this, an approximating cubic smoothing spline, rather than interpolating cubic spline is used. Cubic splines are composed of control points connected by piecewise cubic polynomials, with one polynomial linking each successive pair of control points. A cubic polynomial has the form of

$f(x) = d + cx + bx^2 + ax^3$

and is the lowest order polynomial that may have an inflection point. While higher order polynomials, such as 5^{th} or 6^{th}, may be used to approximate a best fit curve, they are not desirable as compared to a cubic spline approximation because high order polynomials are affected by oscillations known as Runge's phenomenon at the ends of their intervals [31].

Given the N IDAS derived control points in x-y space, and the interval $x_0 < x_1 < x_2 < \ldots x_n$, there exists a spline function $f(x)$ consisting of N-1 cubic polynomials with $S_{k,0}$, $S_{k,1}$,$S_{k,2}$,$S_{k,3}$ as coefficients of the form,

as defined in Numerical Methods Using Matlab [32], $f(x) = f_k(x) = s_{k,0} + s_{k,1}(x - x_k) + S_{k,2}(x - x_k)^2 + S_{k,3}(x - x_k)^3$ for $x \in [x_k, x_{k+1}]$ and $k = 0, 1, 2, \ldots, N-1$.

In expanded form this spline is represented as

$$f(x) = \begin{cases} s_{0,0} + \ s_{0,1}(x - x_0) + s_{0,2}(x - x_0)^2 + s_{0,3}(x - x_0)^3 \text{ if } x_0 < x < x_1 \\ s_{1,0} + \ s_{1,1}(x - x_1) + s_{1,2}(x - x_1)^2 + s_{1,3}(x - x_1)^3 \text{ if } x_1 < x < x_2 \\ s_{2,0} + \ s_{2,1}(x - x_2) + s_{2,2}(x - x_2)^2 + s_{2,3}(x - x_2)^3 \text{ if } x_2 < x < x_3 \\ \cdot \\ \cdot \\ s_{N-1,0} + \ s_{N-1,1}(x - x_2) + s_{N-1,2}(x - x_2)^2 + s_{N-1,3}(x - x_2)^3 \text{ if } x_{N-1} < x < x_N \end{cases}$$

Given the cubic function *f*(*x*) along the interval [x_0,x_N], the resulting piecewise curve *Y* = *f*(*x*) and its first and second derivatives are all continuous along the interval [x_0,x_N]. Because *f'*(*x*) and *f''*(*x*) are continuous, the graph of Y = *f*(*x*) has smooth corners and the radius of curvature is known at each point [33].

The final form of the smoothing spline Matlab function used, csaps, returns the smoothing spline *f(x)* fit to the IDAS derived data set of N points and allows the value of the spline to be assessed at discrete values along the interval [x_0,x_n]. This allows points along the spline to be sampled and then used to manually reconstruct the spline in the CAD program NX4 as there is no direct way to import the spline function into NX4. The smoothing spline function cspaps minimizes

$$P\sum_{j=1}^{n} w(j)\left|y(:,j)-f(x(j))\right|^2 + (1-p)\int \lambda(t)\left|D^2 f(t)\right|^2 \ dt$$

Where *n* is the number of IDAS defined control points defined as x,y coordinates, and the smoothing parameter p may range from 1-0, with 1 fitting the natural spline to the data and 0 yielding the least squares straight line fit to the data [34]. Adjusting the smoothing parameter p between 0 and 1 allows a balance to be found between the natural spline, which fits close to the data yet is unsmooth, and the least squares straight line, which is not close to the data but is smooth.

Chapter 5

Tool Path Generation and Cut Simulation

5.1. System overview

As illustrated in figure 5.1, the instrument data source may be from either CT, x-ray, or MRI modalities. The femur DICOMS are passed through an automatic segmentation processes followed by modality dependant automatic cartilage reconstruction to complete the femur with cartilage model. This is then passed to a second module, which generates the contours. These contours are then used as the inputs to the generation of the patient specific cutting tool, which is the focus of this thesis. This process is illustrated in figure 5.2.

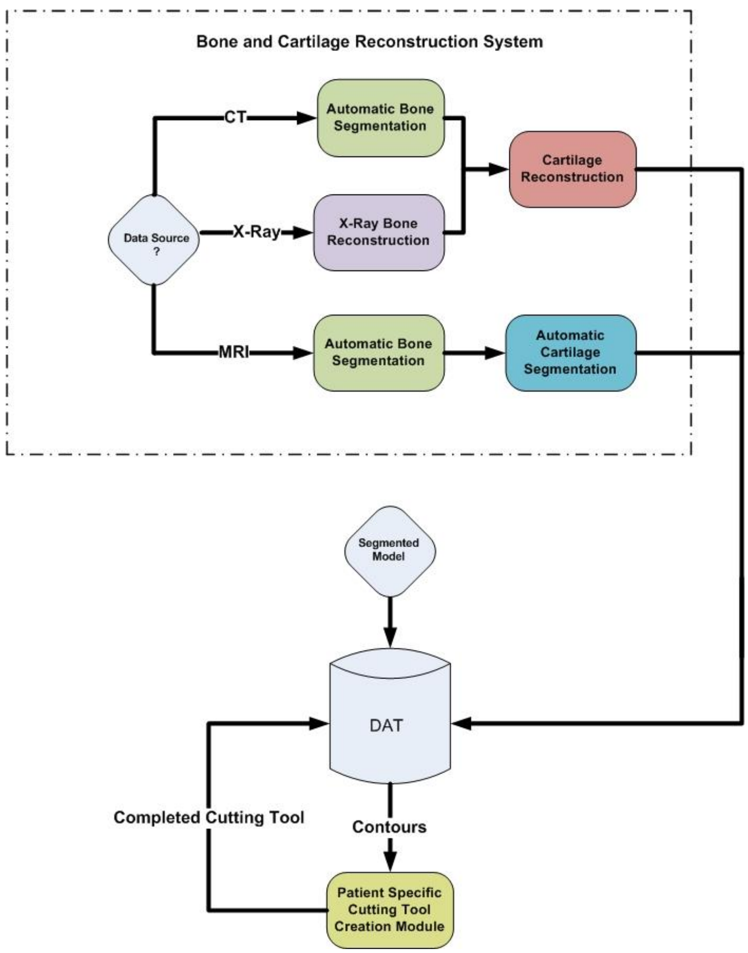

Figure 5.1 Patient specific cutting tool system overview

As shown in figure 5.2, the input contours are the contours of the femur with cartilage in the mediolateral direction and the profiles of the femur with cartilage in the anteroposterior direction. The mediolateral (ML) contours and anteroposterior (AP) profiles split into two pathways. The ML contours are passed through a curve fitting process to generate the mediolateral tool paths that the surgical drill would follow. These are then sent to the cut verification process. The AP profiles do not require this curve fitting procedure and the generated AP tool paths are sent to the cut verification process. At the cut verification process, the AP and ML tool paths are matched to their respective partner (ML tool path to AP tool path, etc) and the resulting cut of the surgical drill traveling along the tool path pair is simulated.

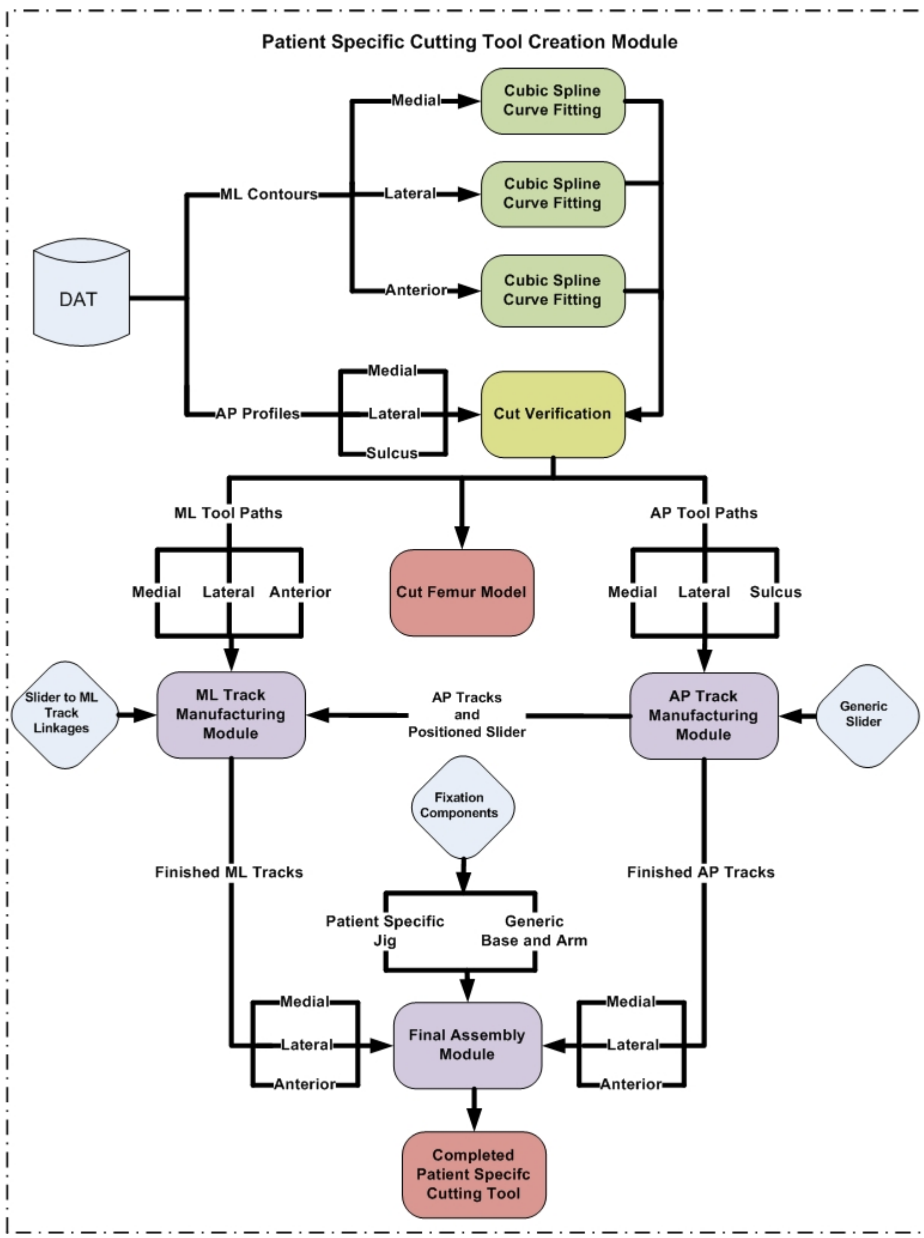

Figure 5.2 Generation process for the patient specific cutting tool

5.2. Modeling Space

Unigraphics NX 4 was used for CAD model creation and resection simulation. It is a parametric CAD package capable of solids modeling. All models are positioned with respect to a global coordinate system, which is maintained throughout the modeling process. Solids are created by specifying a datum plane or model face as the sketch plane. A two dimension sketch of the solid model profile is drafted, constrained, and then extruded. In addition, two dimensional sketches can be swept along a line, creating a sheet that can be used to simulate the path of a cutting tool Figure 5.3. This is similar in principle to current virtual resection techniques and allows any resection to be accurately simulated figure 5.4 assuming the cutting tool is rigidly restrained to its intended path. The femur model was imported into NX4 with a 1 to 1 scale factor and dimensions of cm, preserving the native model scale.

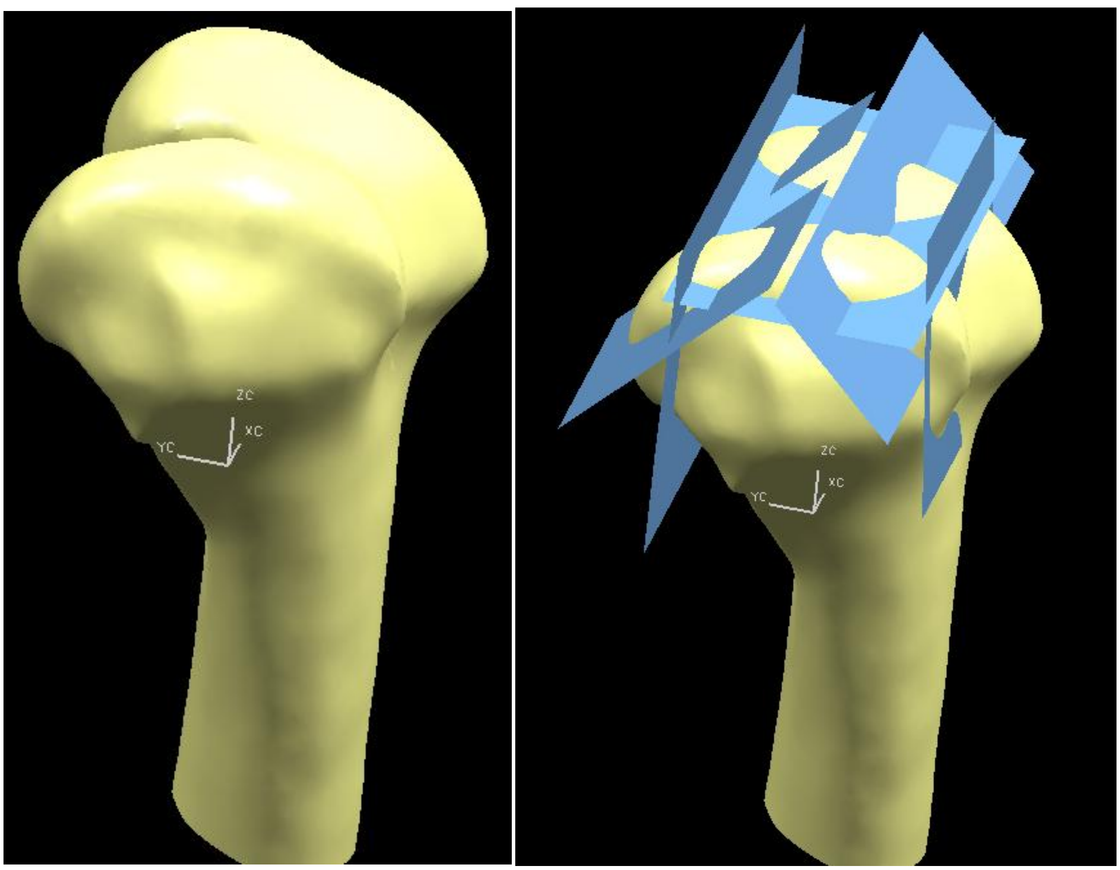

Figure 5.3 Femur model and simulated oscillating saw tool paths for a five planar resection

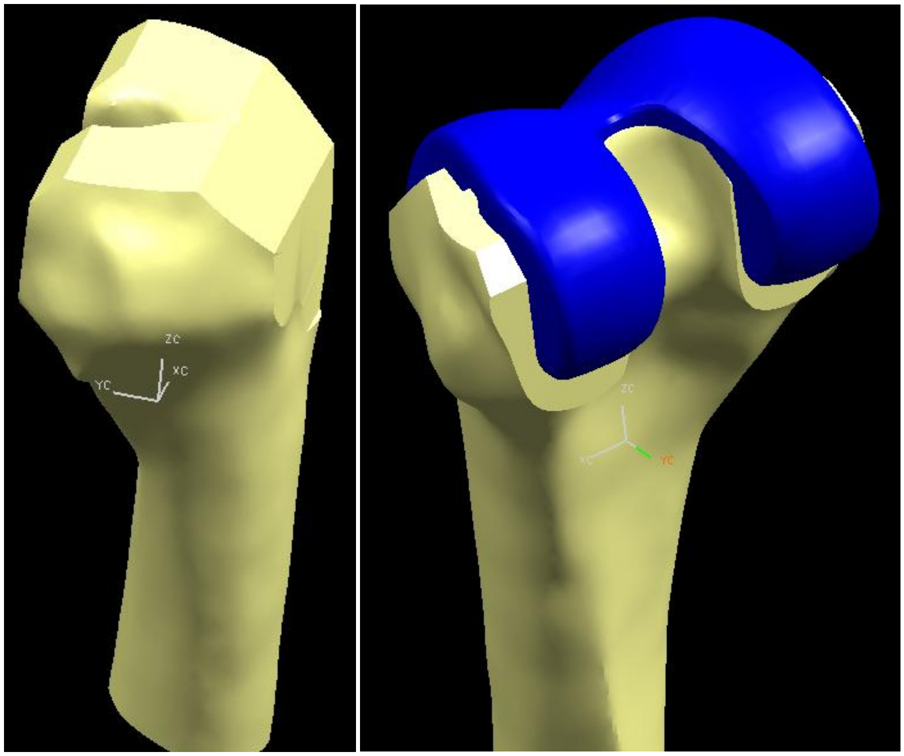

Figure 5.4 Simulated five resection planes of a traditional TKA and fitted implant

5.3. Mediolateral Tool Path

The mediolateral tool paths are defined by the IDAS derived mediolateral contours. The tool paths guide the surgical drill bit across the distal femur surface in the mediolateral direction. The tool paths are created by selecting the relevant mediolateral contours from the entire contour set, refining this data to allow a spline based contour approximation, which then creates the final mediolateral tool path sets Figure 5.5.

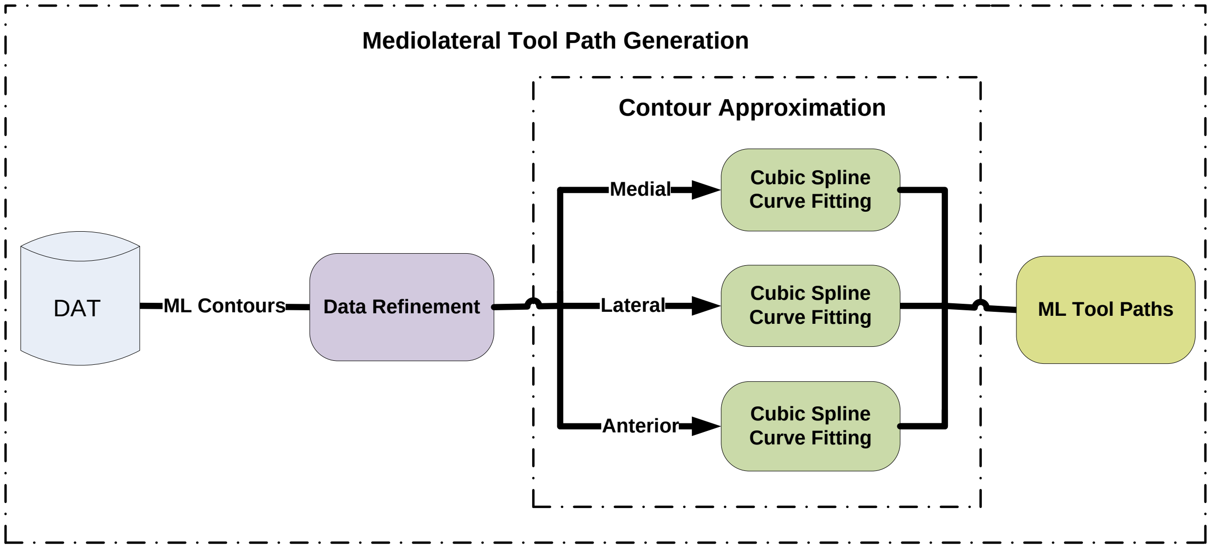

Figure 5.5 Process steps for creating the mediolateral tool paths

It was determined through iterative tool path simulations, explained in the following chapter, that one mediolateral tool path could acceptably resect the medial condyle, while two mediolateral tool paths were required to resect the lateral condyle. This is due to the geometry of the medial condyle being more rounded or ball shaped from the anterior to posterior, and the anterior of the lateral condyle being swept more anteriorly than the medial condyle. The lateral condyle requires one mediolateral tool path to resurface the distal and posterior regions and one mediolateral tool path to resurface the anterior region. Because the geometry of the medial and lateral condyles is dissimilar, the tool paths are not interchangeable between condyles.

5.3.1. Data Refinement

From the entire contour set Figure 5.6, three mediolateral contours each were chosen to define the pathways for the mediolateral and anterior sections of the distal femur. Further, these were bisected into the medial and lateral contours, and lateral anterior contour. It was found that no medial anterior contour was needed and so was therefore omitted. Only three contours were required for each because additional control points do not necessarily result in a better approximating fit. As shown in Figure 5.7, the inclusion of points below the lowest point of the intercondylar groove, shown in pink, decreases the quality of the resulting pathway because it would shift the pathway below the lowest point of the sulcus. If the cutting tool were in this position and swept foreword, it would gouge into the intercondylar groove. Points below that of the lowest point of the intercondylar groove were not included Figure 5.7.

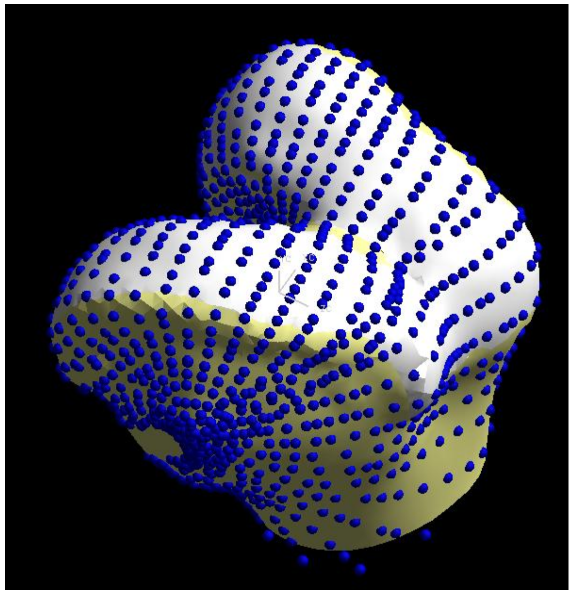

Figure 5.6 ML contours rotated about the TEA

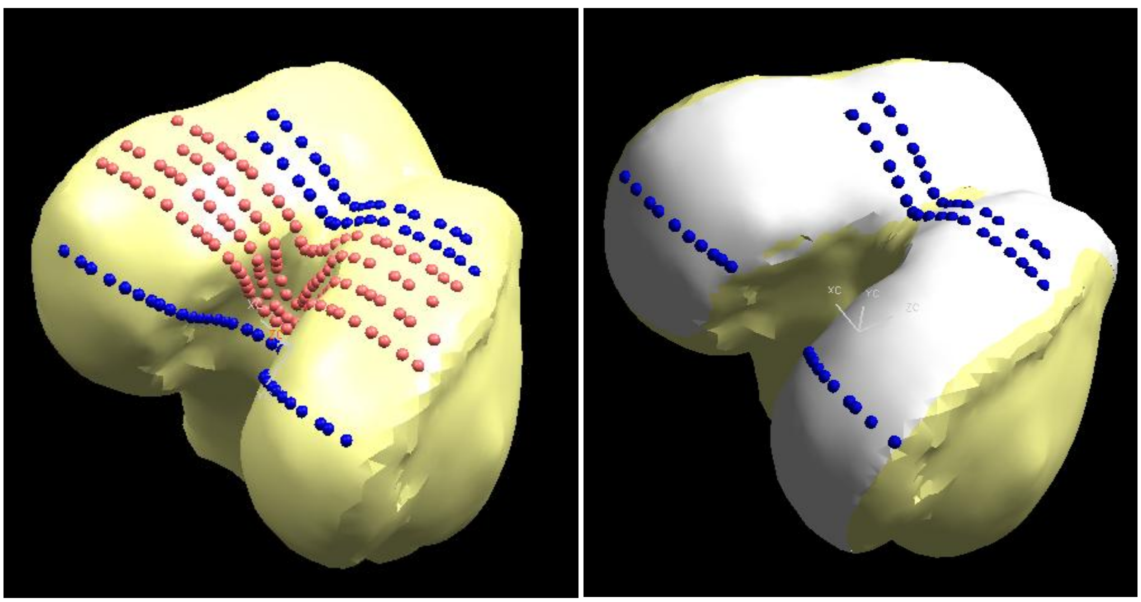

Figure 5.7 Selected (blue) and omitted (pink) mediolateral contours

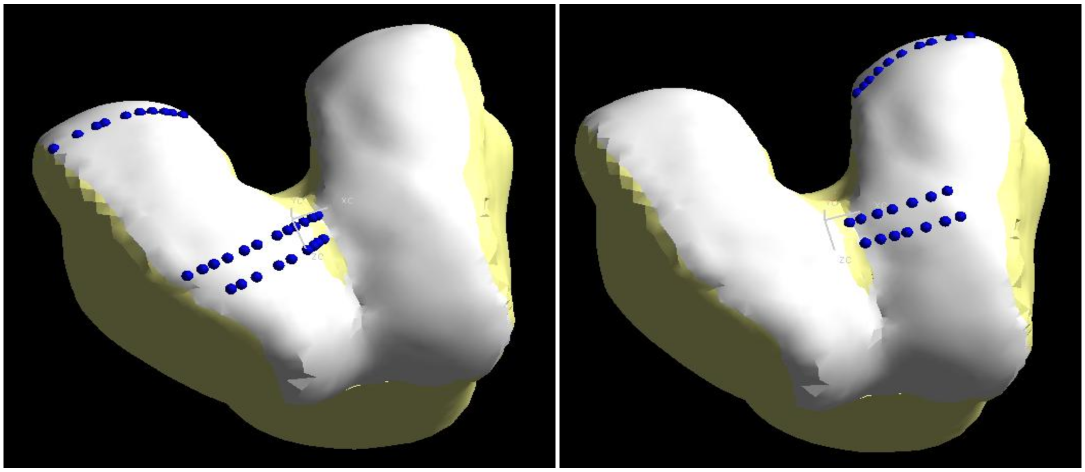

Figure 5.8 Contours defining the medial and lateral cutting pathway

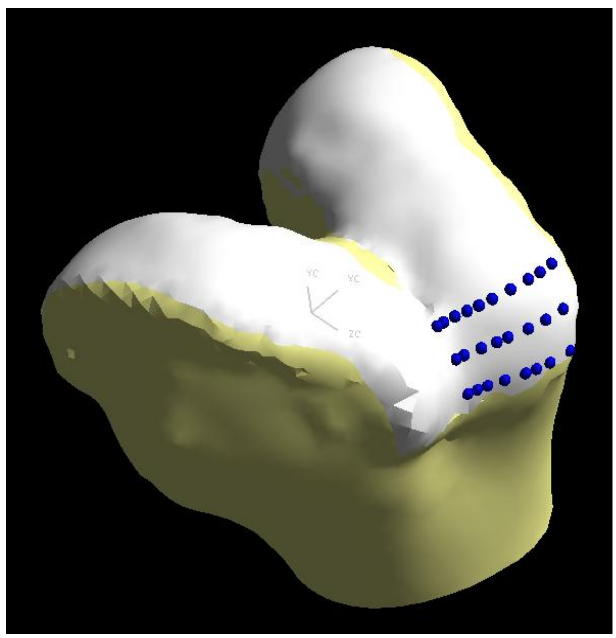

Figure 5.9 Contours defining the anterior mediolateral cutting pathway

To fit a two dimensional cubic spline to the three dimensional contours given (figures 5.8 and 5.9), the contours were imported as STL files into NX4 and first rotated about the TEA into one plane Figure 5.10, 5.11. This allows the IDAS generated contours created in 3D space to be fit by a 2D curve.

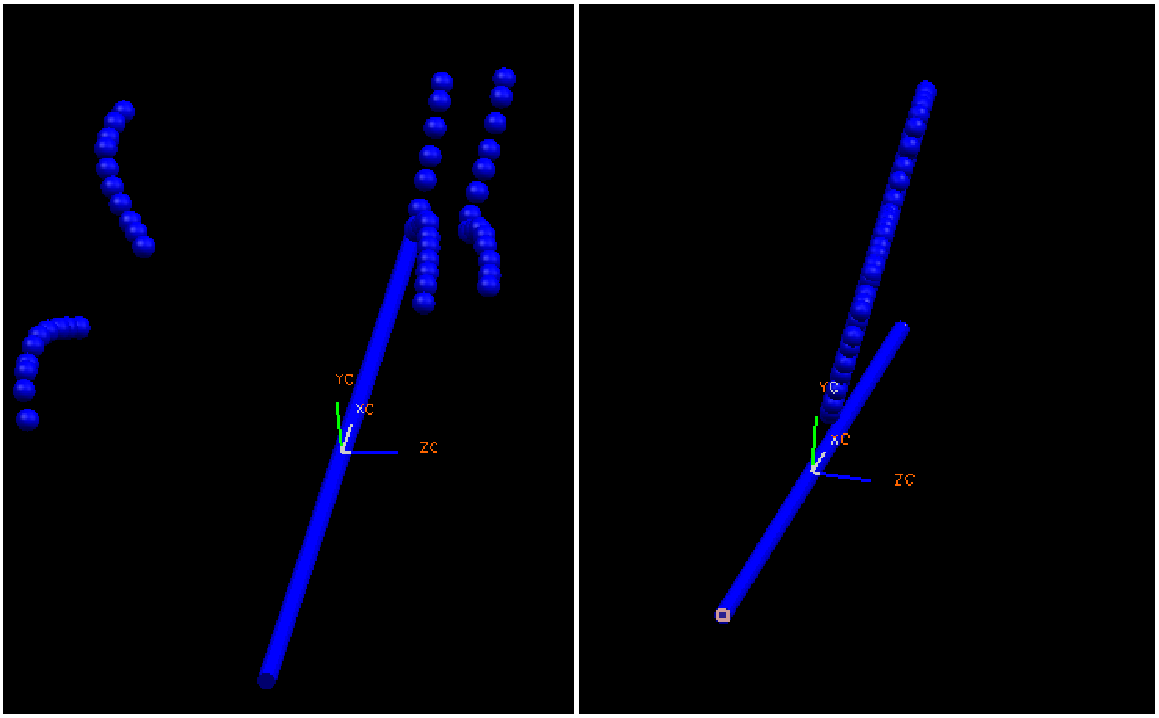

Figure 5.10 Medial and lateral contours before and after rotation about the tea into one plane

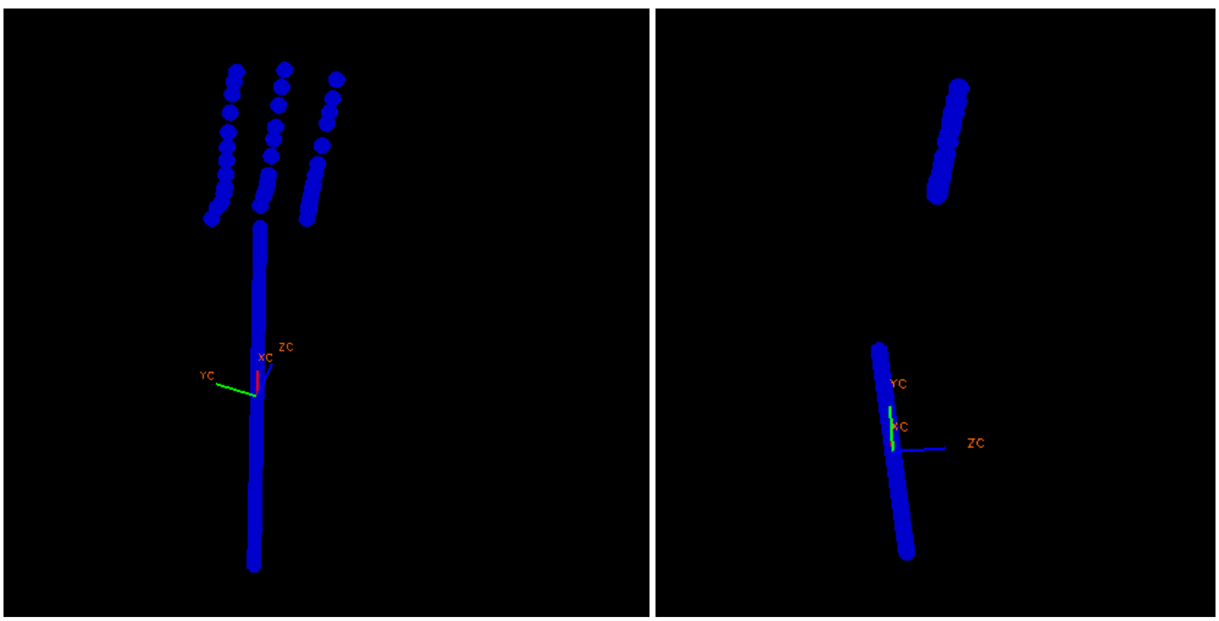

Figure 5.11 Lateral anterior contours before and after rotation about the TEA into one plane

The xy center location of each contour point was found, creating a [40x2] matrix representing the medial and lateral contours and [40x2] matrix representing the anterior lateral contour.

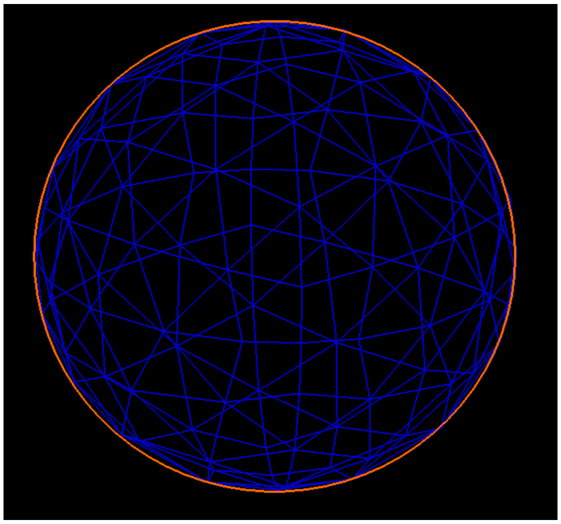

Figure 5.12 Example contour point

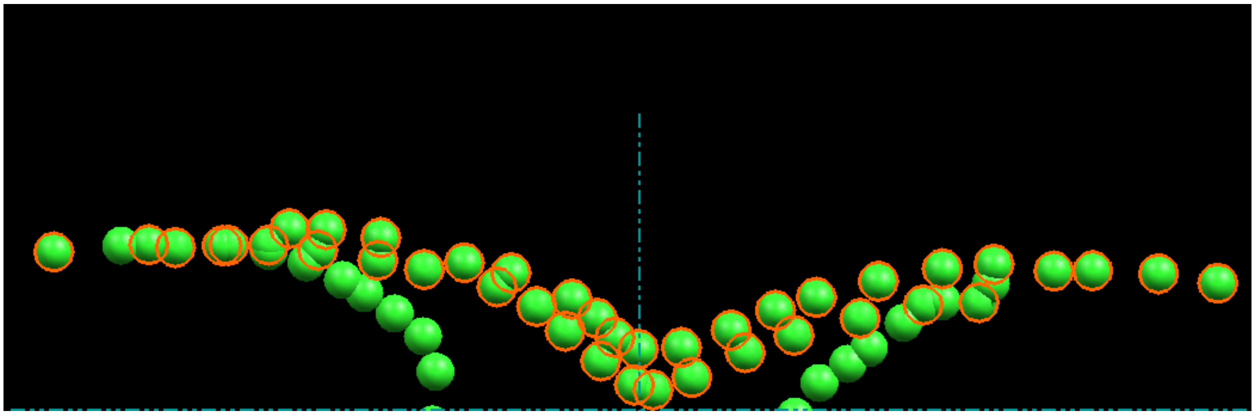

Figure 5.13 Example medial and lateralcontour point set

5.3.2. Mediolateral Contour Approximation

For both the anterior contour and medial and lateral contours, a [40x2] matrix defining the center of each point in xy space was created. A smoothing spline was then fit, with the initial smoothing parameter set to 1, allowing the natural spline to be fit to the data Figure 5.14, 5.15, 5.18,5.19. This smoothing parameter was then lowered ($p = 0.92$ for the medial and lateral contours, $p = 0.9929$ for the anterior lateral contours) until a smooth spline was obtained Figure 5.16,5.20. This was then evaluated in increments of 2 mm across the range of each contour set ($-2.5 \leq x \leq 3.1$ for the medial and lateral contours, $0 \leq x \leq 2.2$ for the lateral anterior contour). The evaluation resulted in a [29x2] matrix of xy coordinates to define the medial and lateral smoothing spline and a [12x2] matrix of xy coordinates to define the lateral anterior smoothing spline. These points were then imported into NX4 and arcs were fit to the points using a 3 point construction method to recreate the fit splines Figure 5.17, 5.21. These recreated splines represented the mediolateral tool paths, defined by the IDAS generated contours from patient geometry.

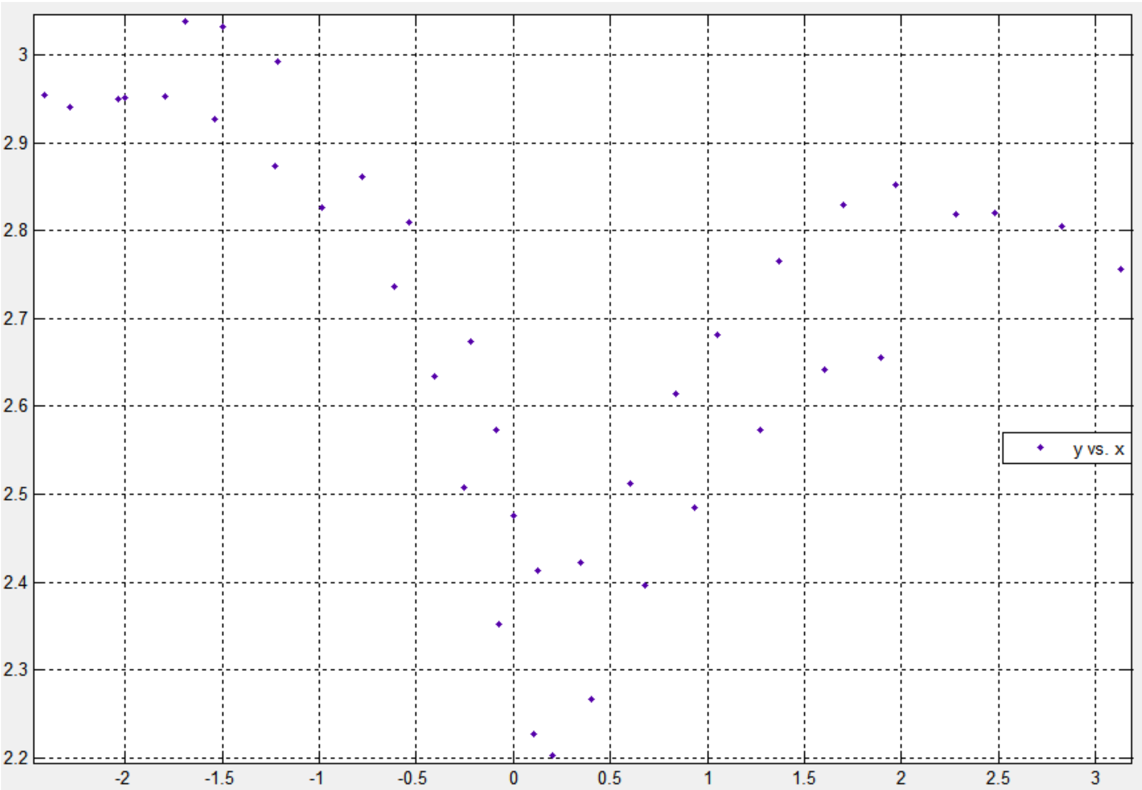

Figure 5.14 Medial and lateral contour points (cm)

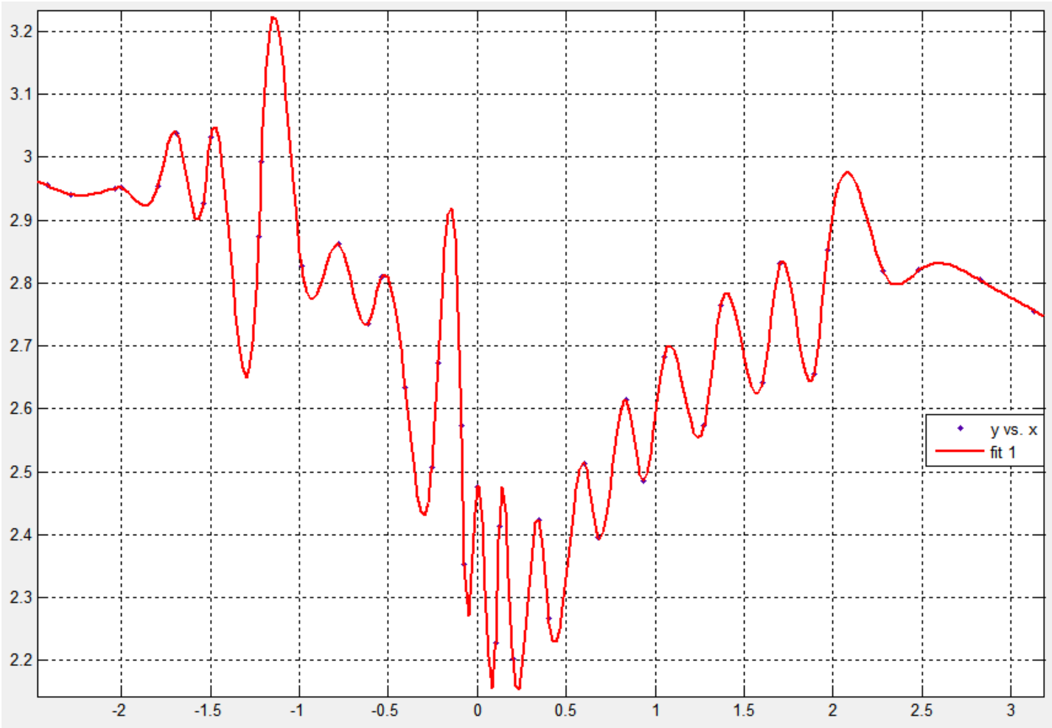

Figure 5.15 Natural unsmoothed spline fit to the medial and lateral contour points (cm)

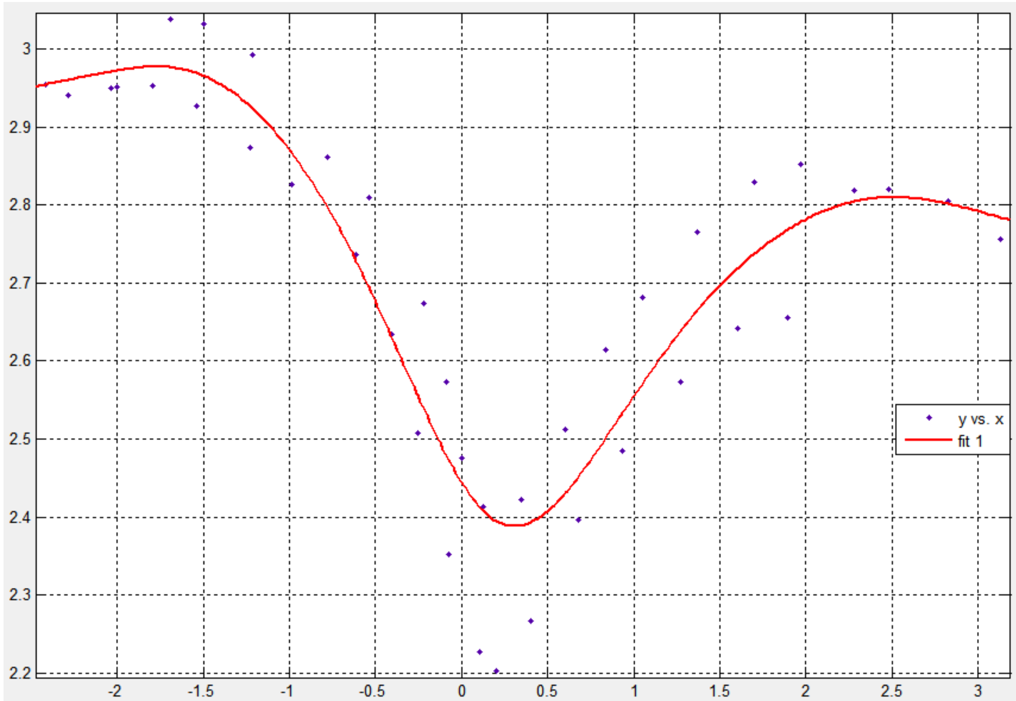

Figure 5.16 Smoothed spline fit to the medial and lateral contour points (cm), R^2 = 0.88

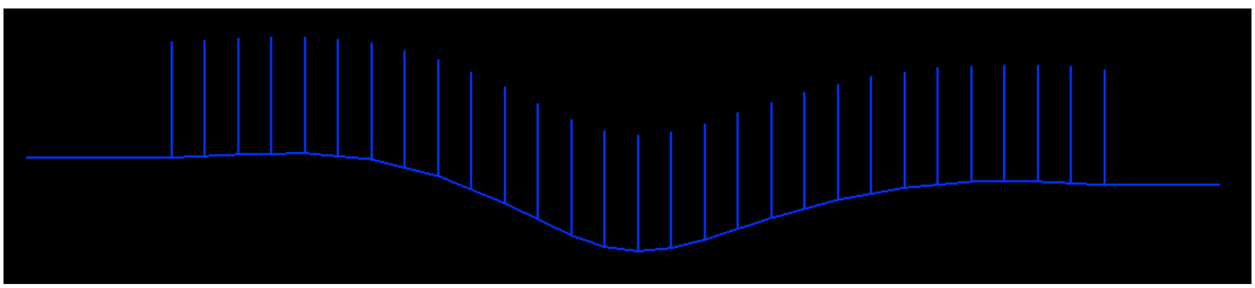

Figure 5.17 Reconstructed NX4 medial and lateral spline

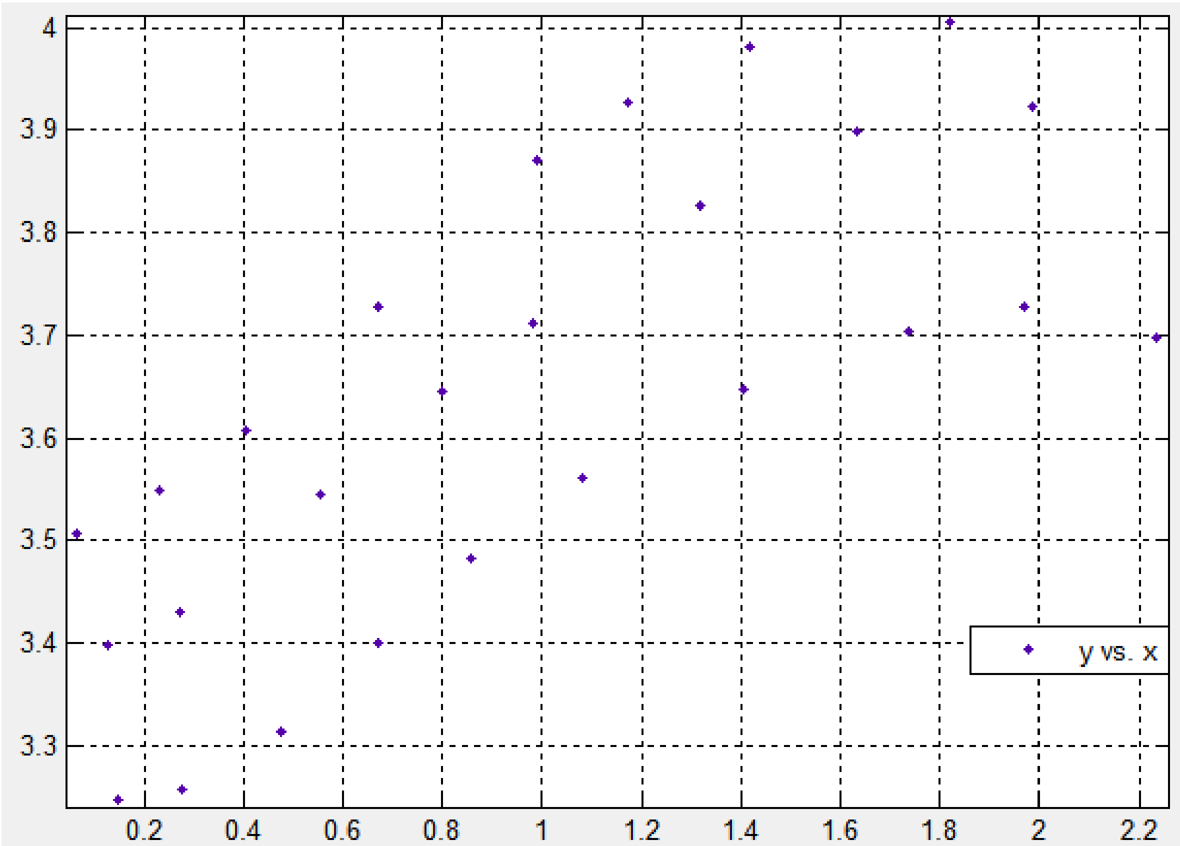

Figure 5.18 Anterior lateral contour points (cm)

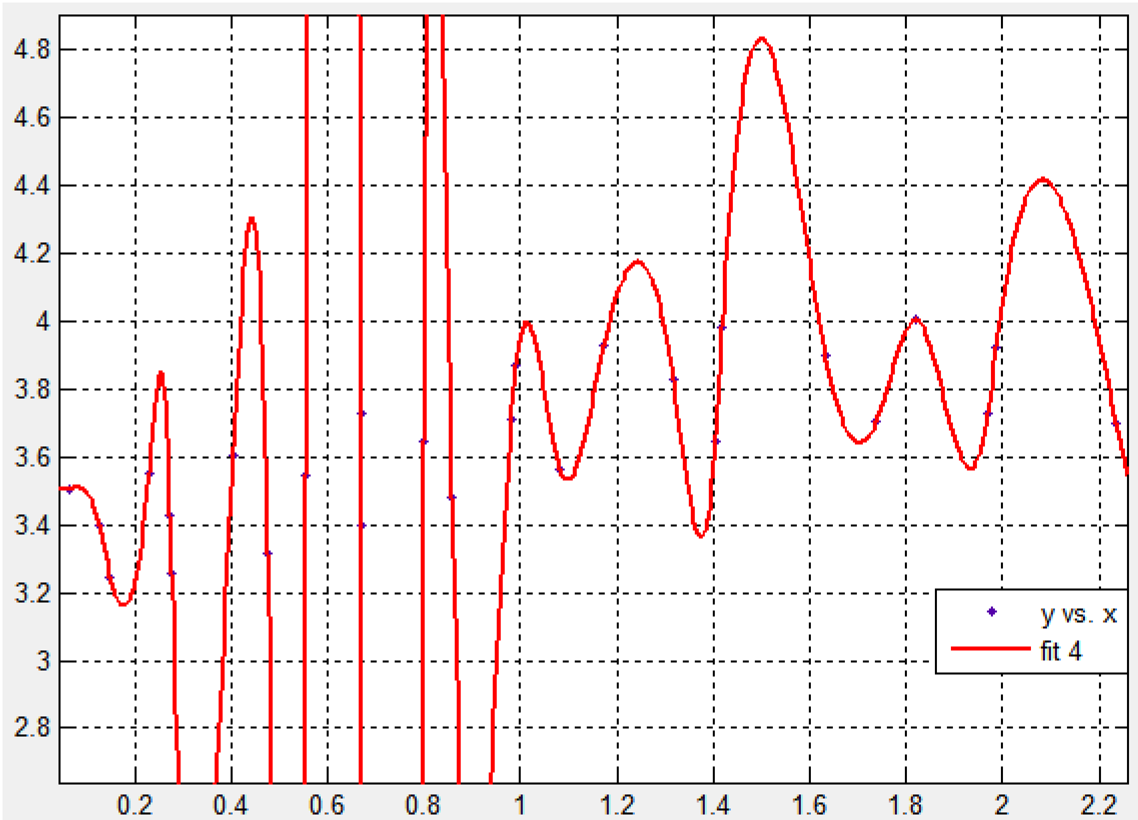

Figure 5.19 Natural unsmoothed spline fit to the anterior lateral contour points (cm)

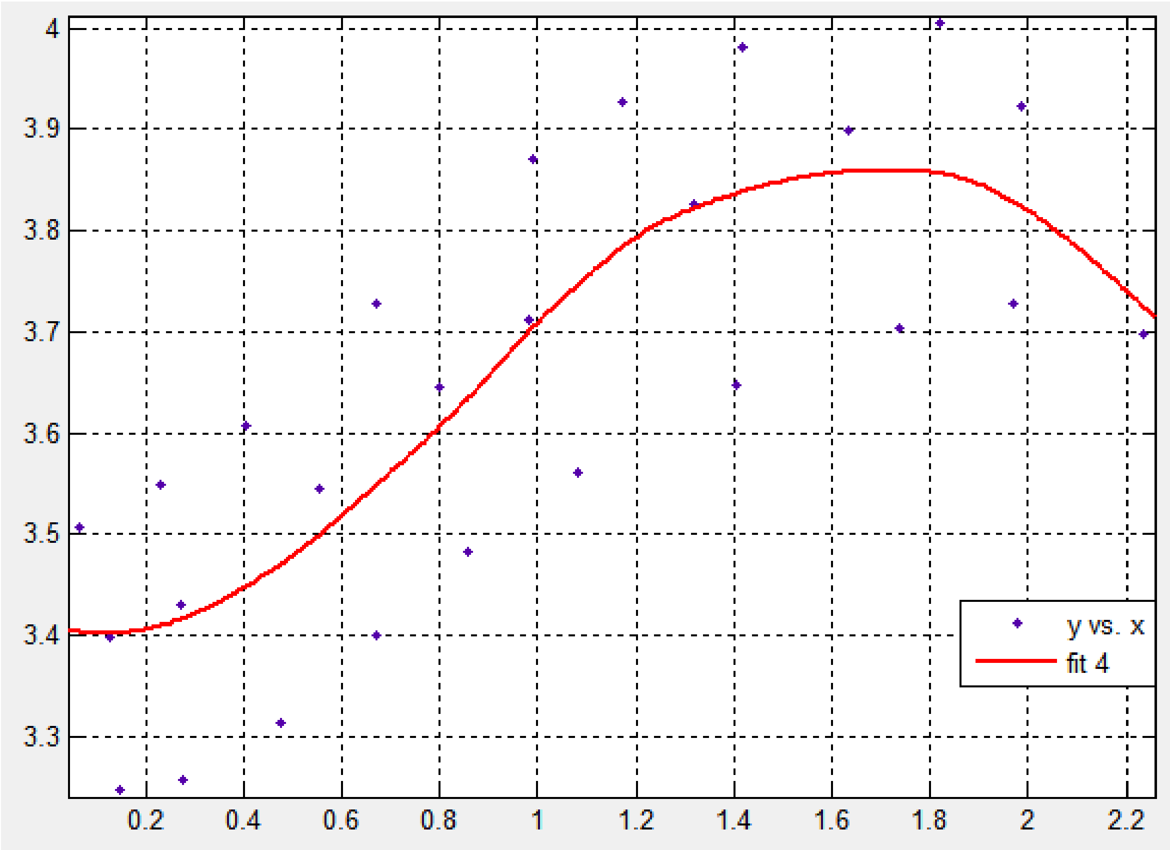

Figure 5.20 Smoothed spline fit to the medial and lateral contour points (cm), R^2 = 0.6608

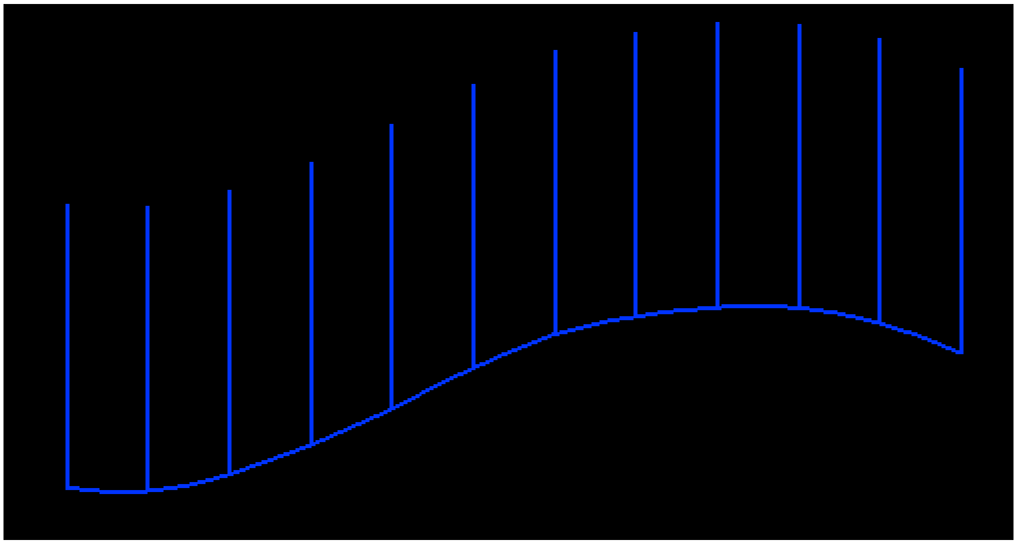

Figure 5.21 Reconstructed NX4 lateral anterior spline

5.4. Anteroposterior Tool Path

5.4.1. Data Refinement

The anteroposterior (AP) tool paths are generated from medial, lateral, and sulcus profiles Figure 5.22, created by IDAS. The points defining each profile are parameterized with the same approach as used for the mediolateral profiles. After a circle is fit to each point, the centers of each circle are then connected to its neighbors by arcs to create a continuous curve. The lateral profile required no further editing and the lateral tool path was generated from it directly. The sulcus profile was scaled through spherical linear extrapolation before obtaining the sulcus tool path. The medial profile was combined with the extrapolated sulcus profile to create the medial tool path Figure 5.23.

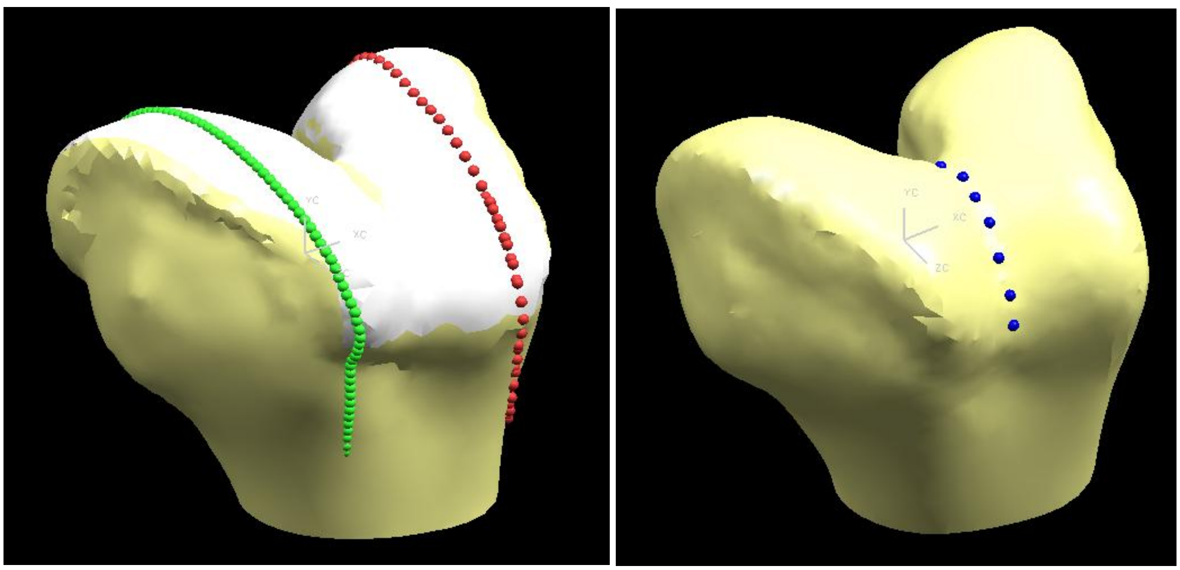

Figure 5.22 Medial (green), lateral (red), and sulcus (blue) profiles

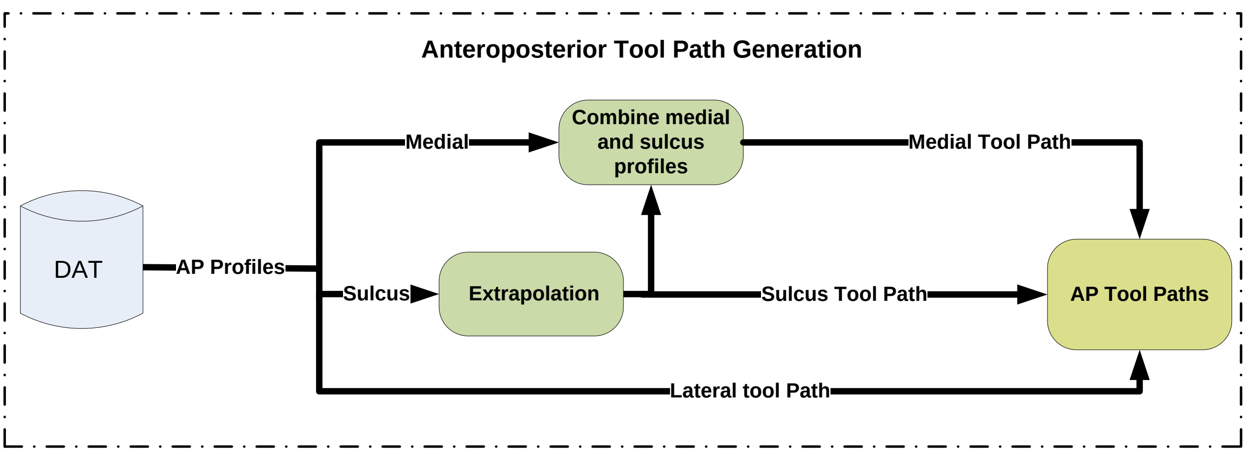

Figure 5.23 AP tool path generation

5.4.2. Medial Tool Path

The medial anteroposterior tool path is defined by both the medial profile and the sulcus profile. It guides the medial mediolateral tool path around the medial condyle. From the anterior of the femur to the most posterior point of the sulcus it is defined by the sulcus profile Figure 5.24. From the most posterior point of the sulcus and around the condyles it is defined by the medial profile Figure 5.24. The medial profile alone could not be used solely for the medial anteroposterior tool path because sweeping the medial ML tool path anteriorly along a path defined by the medial profile resulted in an unsatisfactory resection of the anterior femur. By merging the medial and sulcus profiles together Figure 5.27 to define the medial cutting tool path an acceptable posterior and anterior resection of the medial side was obtained. The sulcus profile was combined smoothly to the posterior medial profile through linear spherical extrapolation, accomplished by extrapolating the sulcus curvature outward to intersect with the posterior medial profile curvature. This was accomplished by first fitting arcs to the centers of the circles fit to the sulcus profile points. An intersecting line was then drawn from the most posterior sulcus point to the most anterior end point of pathway defined by the posterior medial profile. Rays with their lengths equal to this intersecting line were then drawn at perpendiculars from the arcs fit to the sulcus profile. The extrapolated curve maintained the shape of the sulcus curvature Figure 5.26.

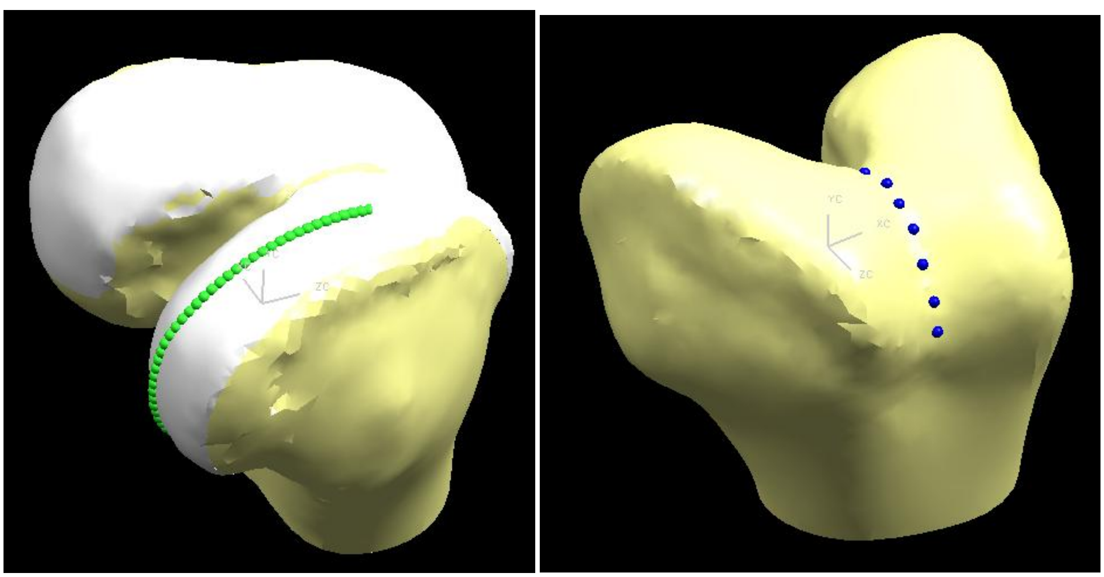

Figure 5.24 Medial and sulcus profiles defining the medial AP track

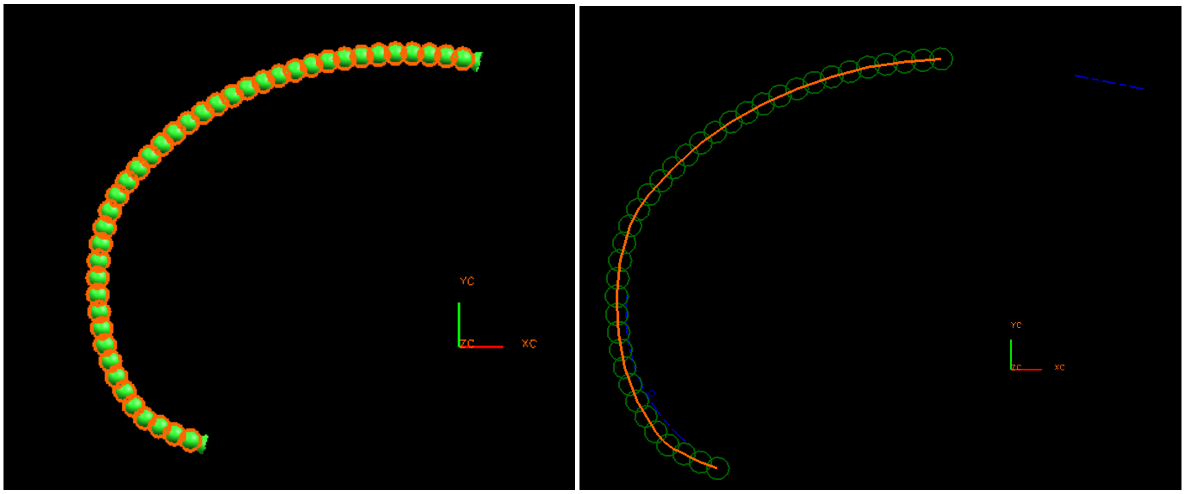

Figure 5.25 Medial profile section defining the posterior of the medial AP track

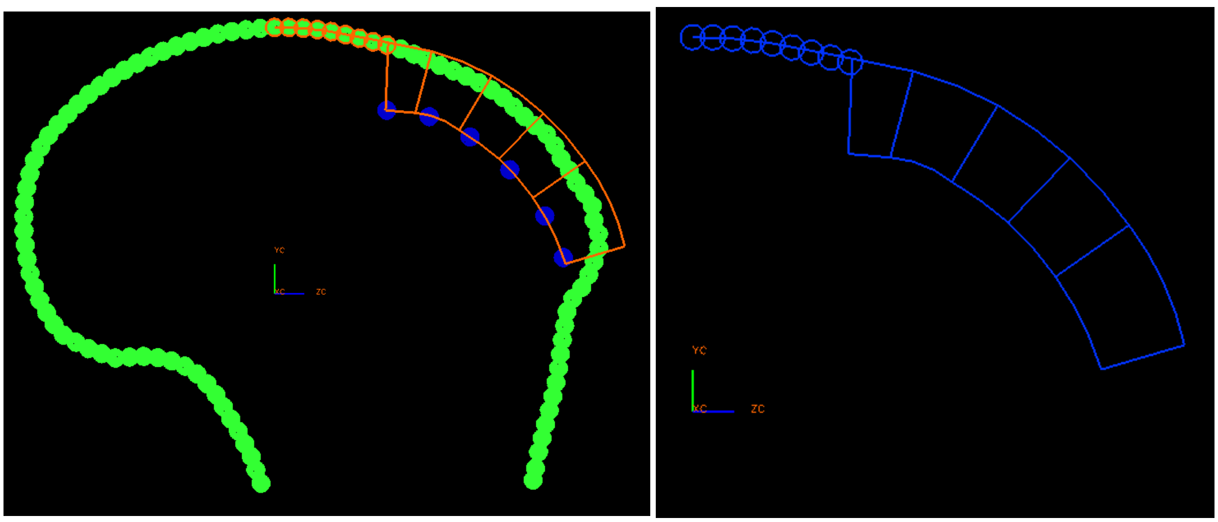

Figure 5.26 Sulcus profile (blue) defining the anterior section of the medial AP track

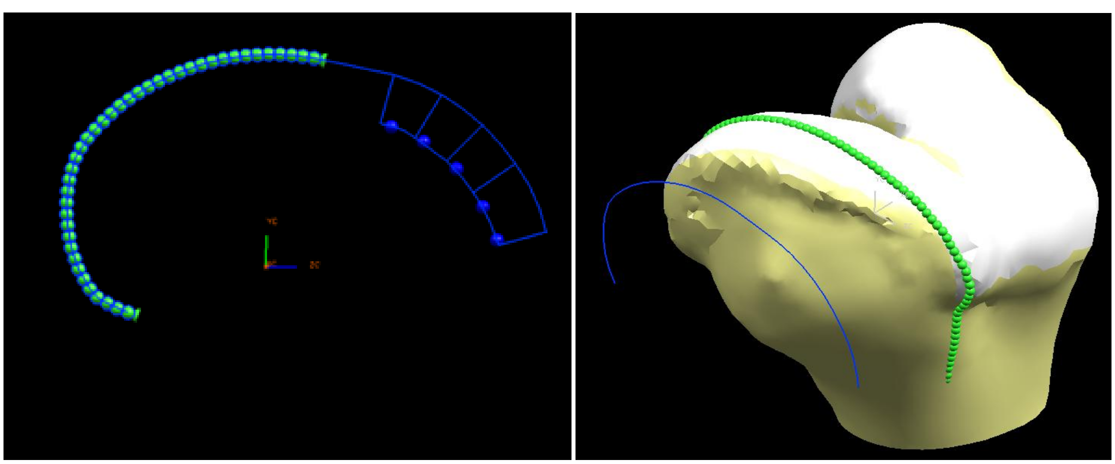

Figure 5.27 Medial AP tool path

5.4.3. Lateral Tool Path

The lateral tool path is defined by the lateral profile as shown. It guides the lateral mediolateral tool path around the lateral condyle.

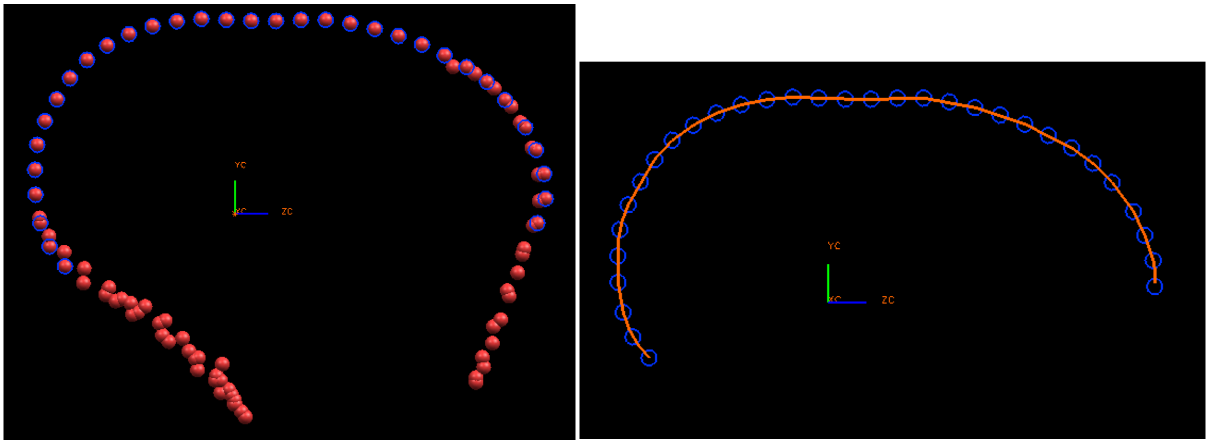

Figure 5.28 Lateral AP tool path

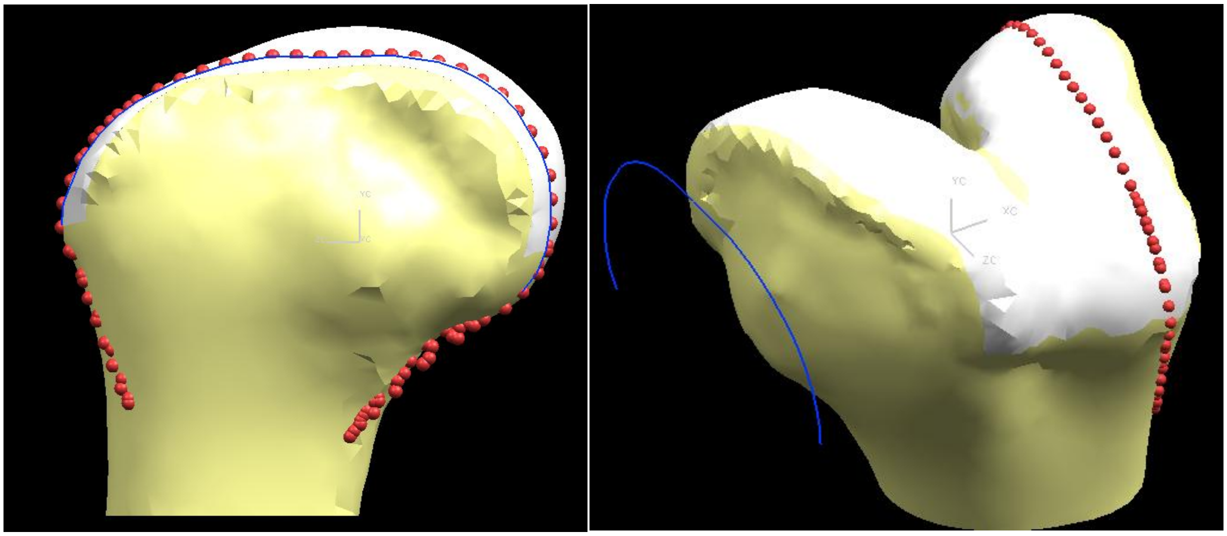

Figure 5.29 Lateral AP tool path

5.4.4. Sulcus Tool Path

The sulcus tool path is defined by the sulcus profile. It guides the anterior mediolateral tool path around the lateral condyle. The fit sulcus curve was extrapolated outward through spherical linear interpolation so that when linked to the anterior mediolateral track, the anterior lateral surface could be processed without being obstructed by the medial condyle.

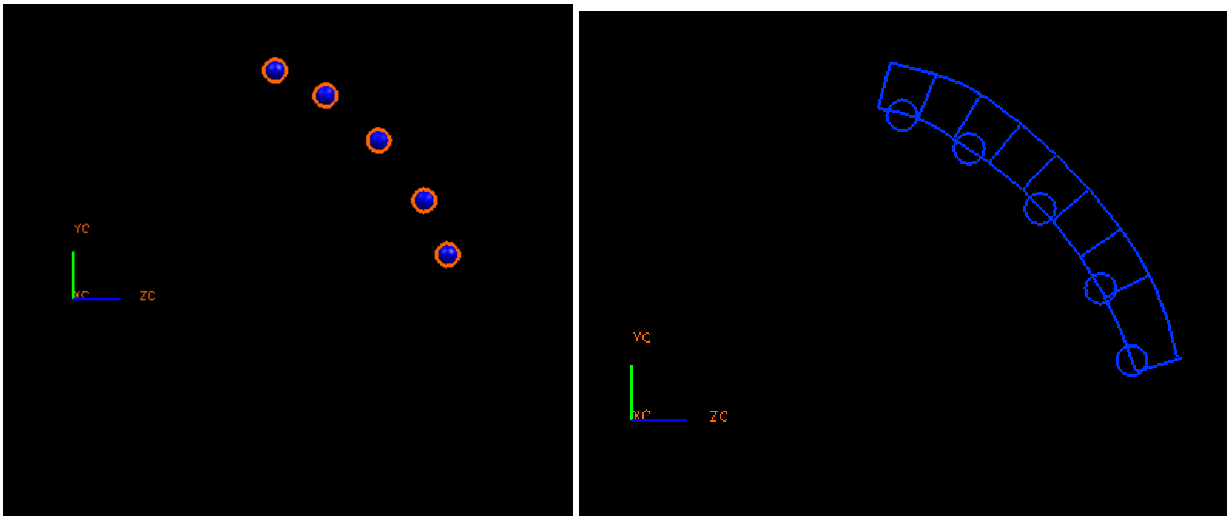

Figure 5.30 Anterior AP tool path creation

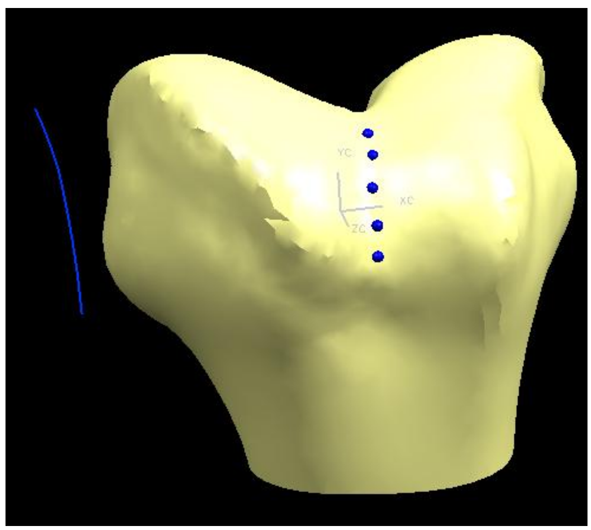

Figure 5.31 Anterior AP tool path

5.5. Cut Simulation

The anteroposterior and mediolateral tool paths combined define the range of motion that the surgical drill will travel. NX4 was used to create a cut simulation by sweeping the mediolateral tool paths along their respective anteroposterior tool paths. The resulting sheets represented the path that the tip of the drill would take, provided the following assumptions. First, there existed a one degree of freedom linkage between the surgical drill and mediolateral tool path that allowed the drill tip to translate along the mediolateral path without rotation about the tool path. Second, there existed a one degree of freedom linkage between the mediolateral tool path and anteroposterior tool paths that allowed the mediolateral tool path to travel along the anteroposterior tool path. The tool paths were rigid and do not deform. Lastly, the system was free from vibration of the drill or “slack” between linkages that will allow wobbling.

The goal of the simulation was to determine if the drill tip would gouge into the bone and then assess the thickness of cartilage removed. Gouges to the bone and removal of cartilage were assessed visually. If both were deemed acceptable, the tool path was accepted and the sheet that represented the path of the drill bit was developed further to create a solid cutting body that was then saved as an STL body. One cutting body was created for each of the three resections, medial, lateral posterior and lateral anterior, and the resected femur was simulated through a Boolean subtraction process in Rapidform 2006 where the cutting body was subtracted from the femur with cartilage model. Finally, the total cartilage removed was simulated by subtracting through a Boolean operation the femur with cartilage model from the resected femur model, yielding only the cartilage removed by the resection.

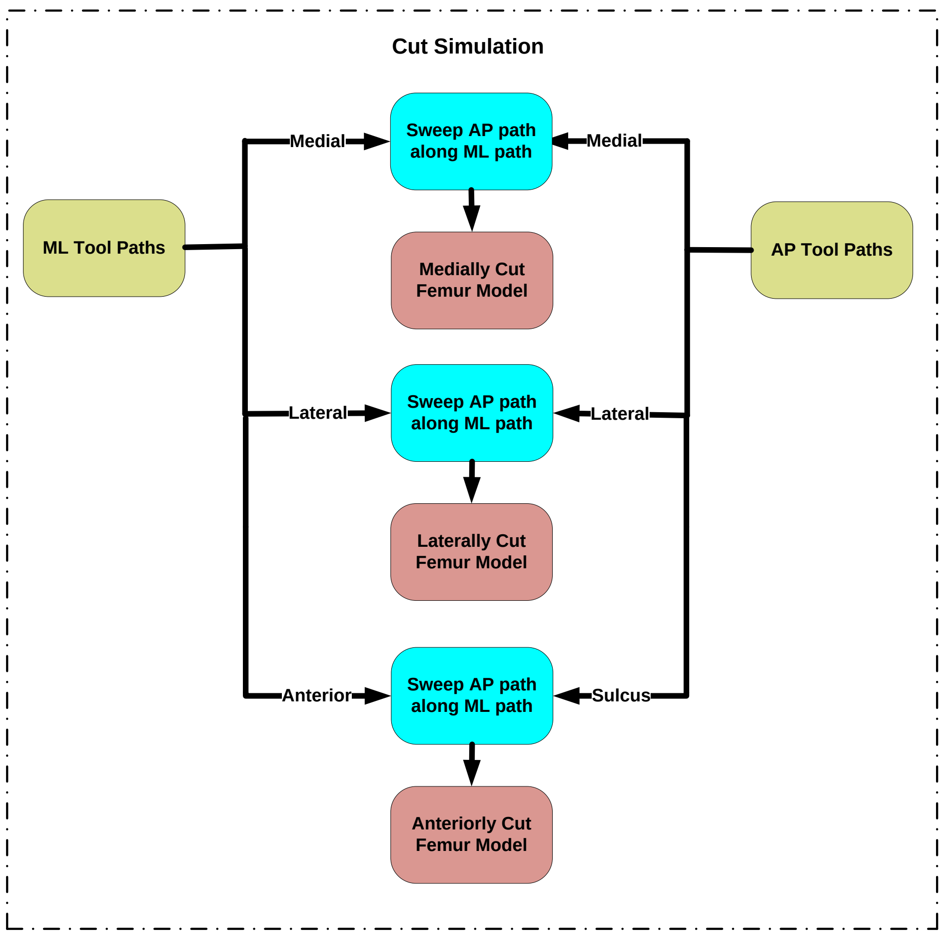

Figure 5.32 Diagram for tool path cut simulation

5.5.1. Medial Unilateral Resection Simulation

A femur model without cartilage, a cartilage model, the medial anteroposterior tool path and medial mediolateral tool path were imported into NX4. The cutting depth was set to the minimum cartilage thickness and the medial mediolateral tool path was then swept along the medial anteroposterior tool path. Some grazing of the distal femur surface occurred but it was deemed superficial and ignored. Decreasing the cutting depth to avoid this grazing would result in an overall decrease in cartilage removed overall. Therefore, it was assumed that some grazing was allowable to ensure more cartilage removed overall.

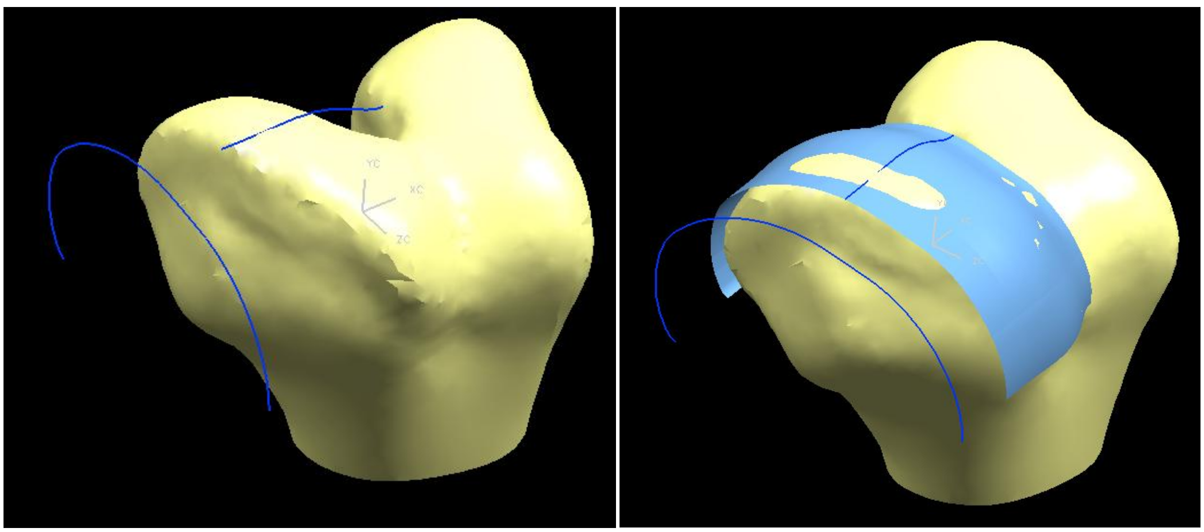

Figure 5.33 Medial AP and ML tool paths and cutting path over the bone model

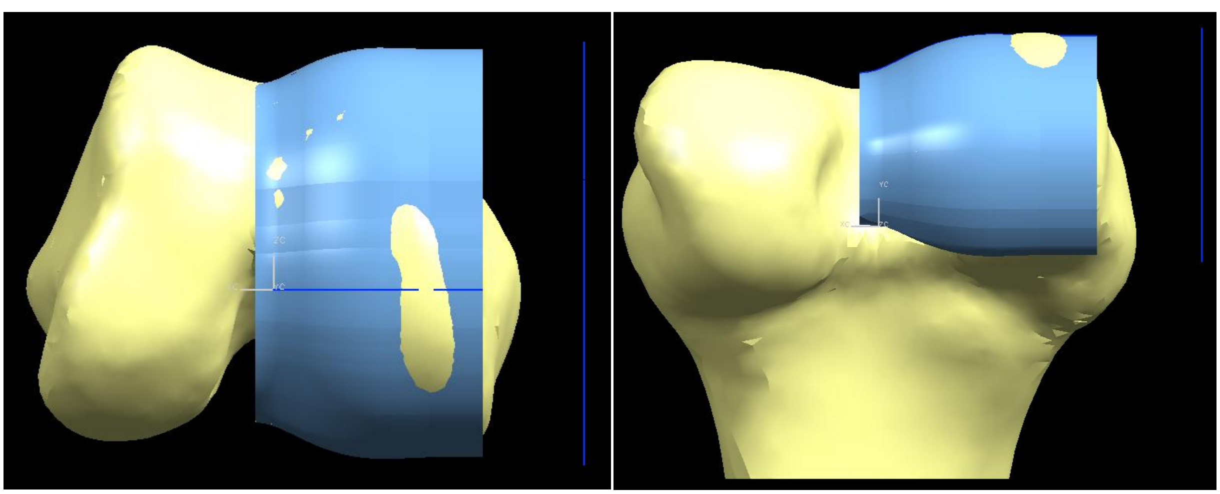

Figure 5.34 Distal and posterior views of the medial cutting path over the bone model

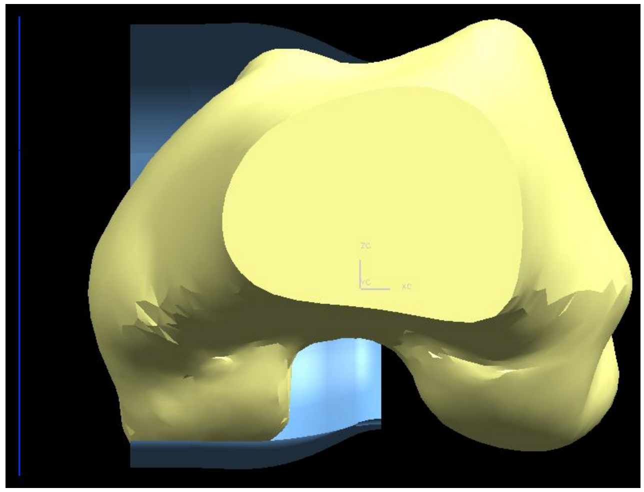

Figure 5.35 Axial view of the medial cutting path over the bone model

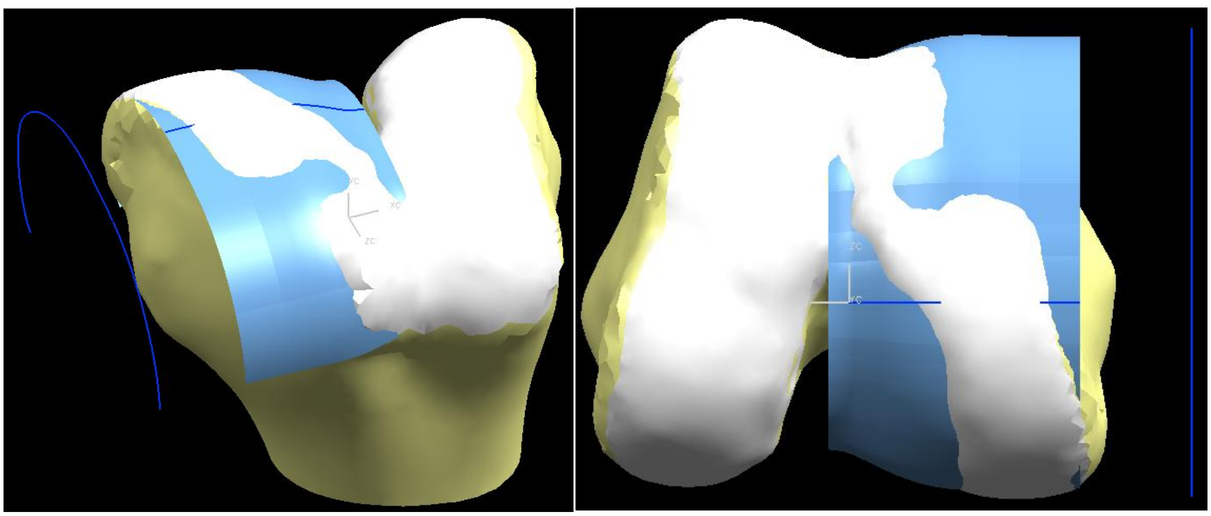

Figure 5.36 Perspective and distal views of the medial cutting path over the cartilage model

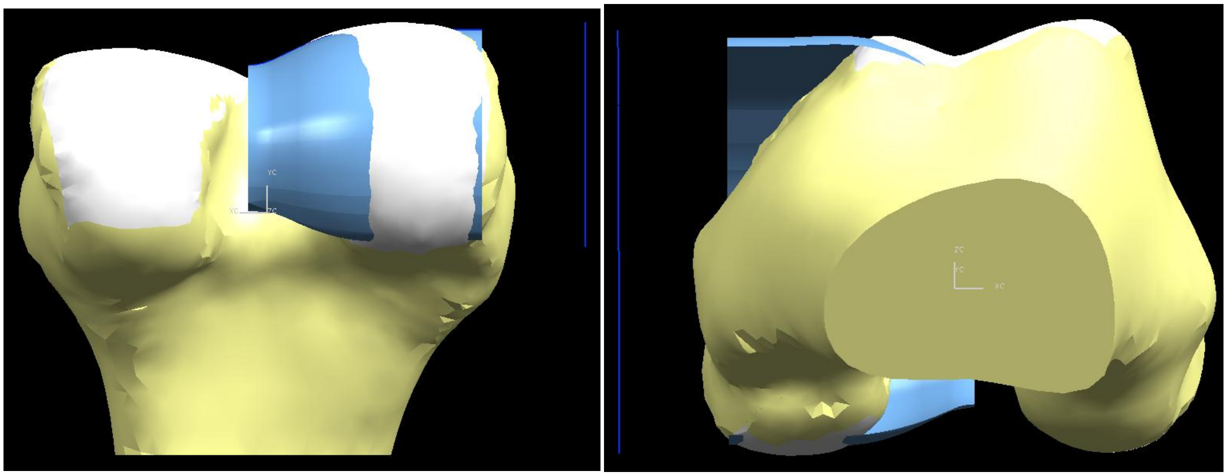

Figure 5.37 Posterior and axial views of the medial cutting path over the cartilage model

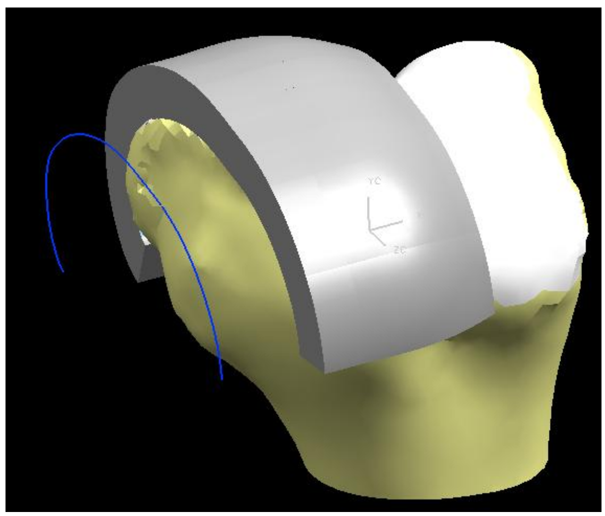

Figure 5.38 Medial cutting body

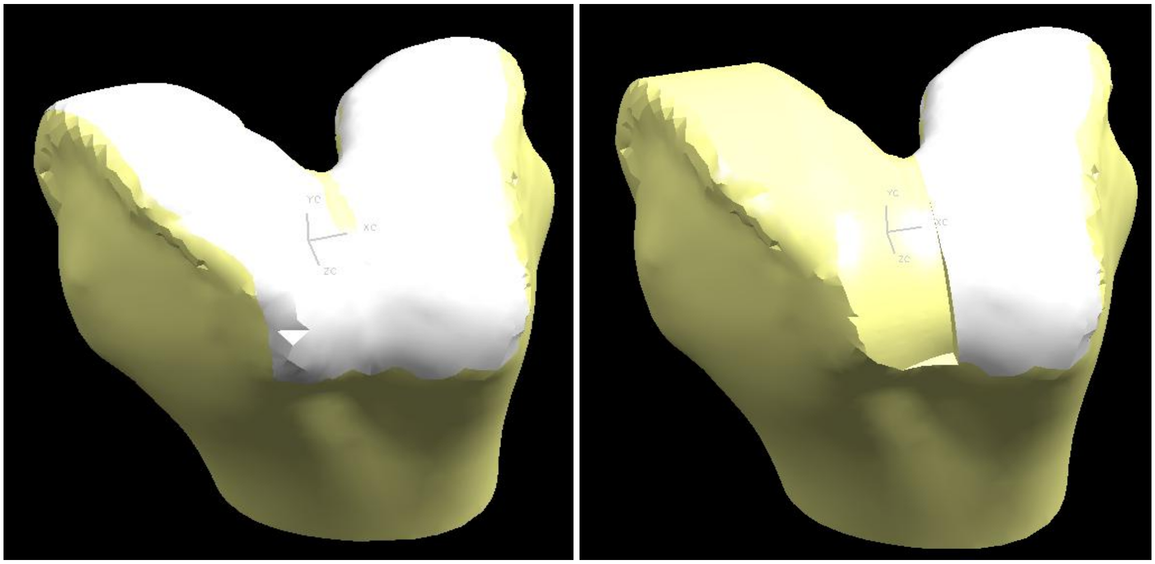

Figure 5.39 Femur model with cartilage anterior before and after simulated medial resection

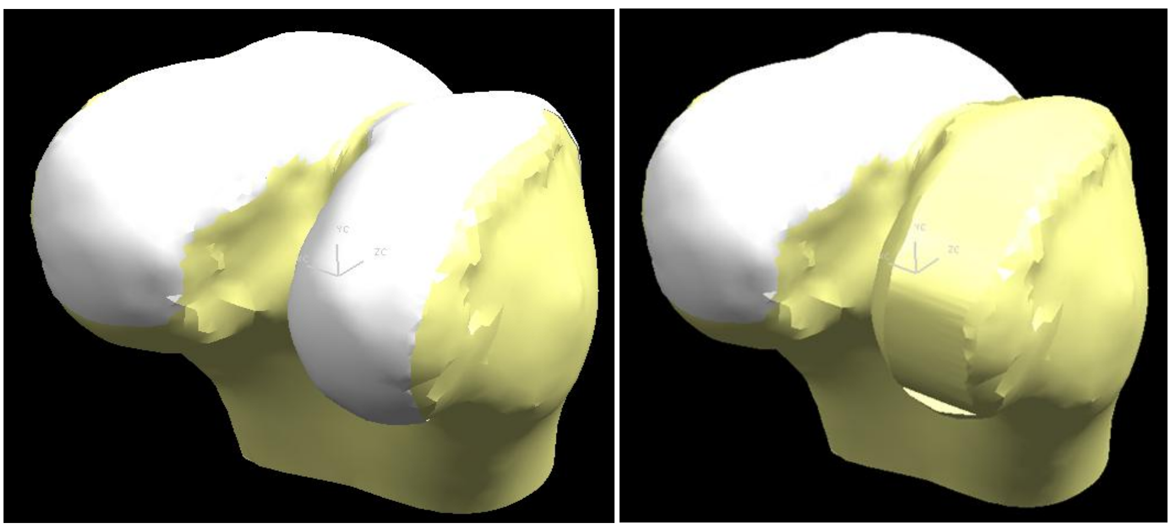

Figure 5.40 Femur model with cartilage posterior before and after simulated medial resection

5.5.2. Lateral Resection Simulation

A femur model without cartilage, a cartilage model, the lateral anteroposterior tool path and lateral mediolateral tool path were imported into NX4. The cutting depth was set to the minimum cartilage thickness and the lateral mediolateral tool path was swept along the lateral anteroposterior tool path. Some grazing of the anterior femur surface occurred but it was unavoidable without decreasing the cutting depth and cartilage removed.

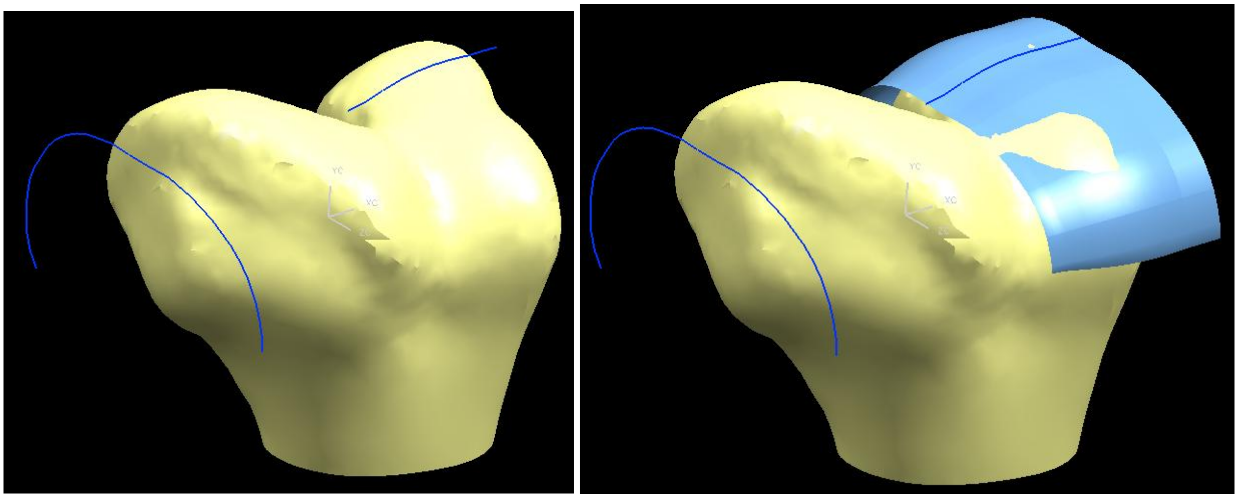

Figure 5.41 Lateral AP and ML tool paths and cutting path over the bone model

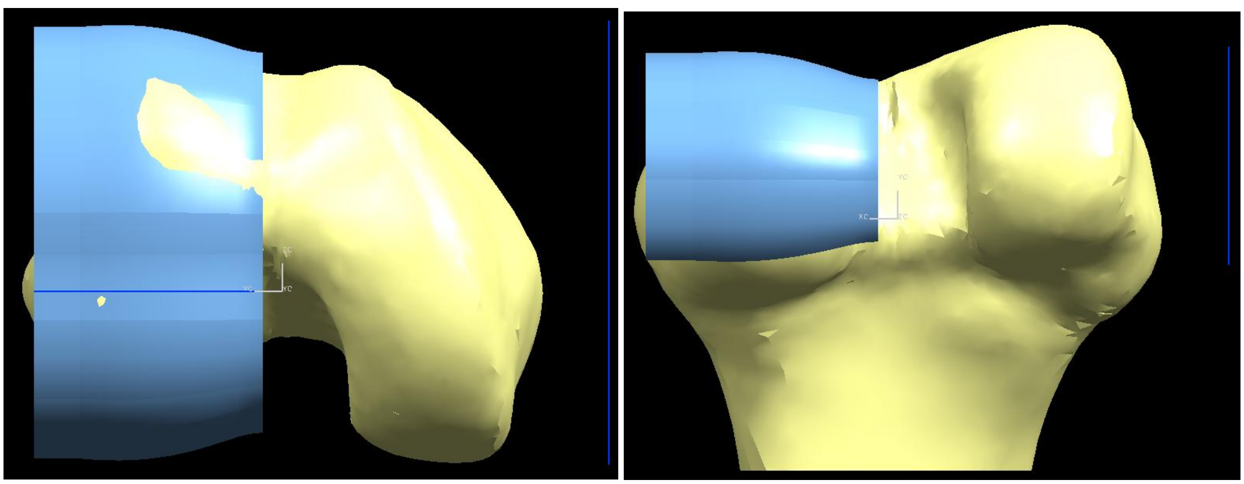

Figure 5.42 Distal and posterior views of the lateral cutting path over the bone model

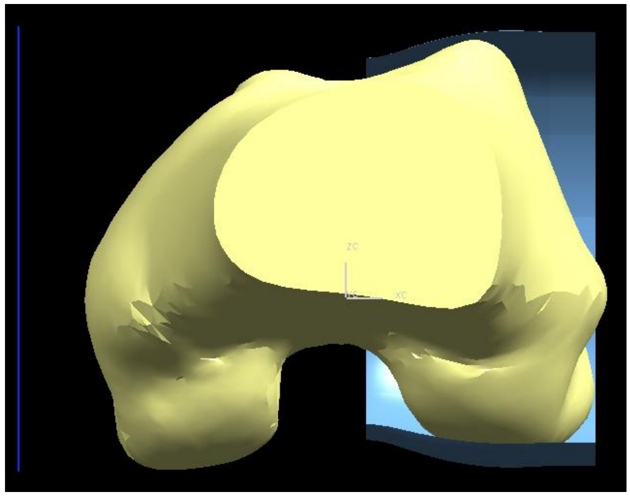

Figure 5.43 Axial view of the lateral cutting path over the bone model

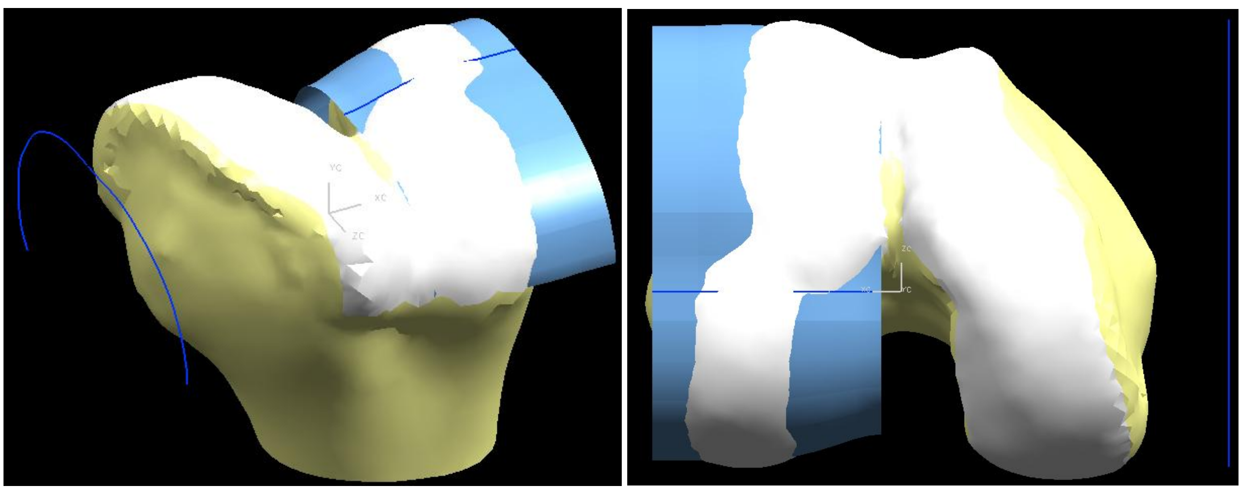

Figure 5.44 Perspective and distal views of the lateral cutting path over the cartilage model

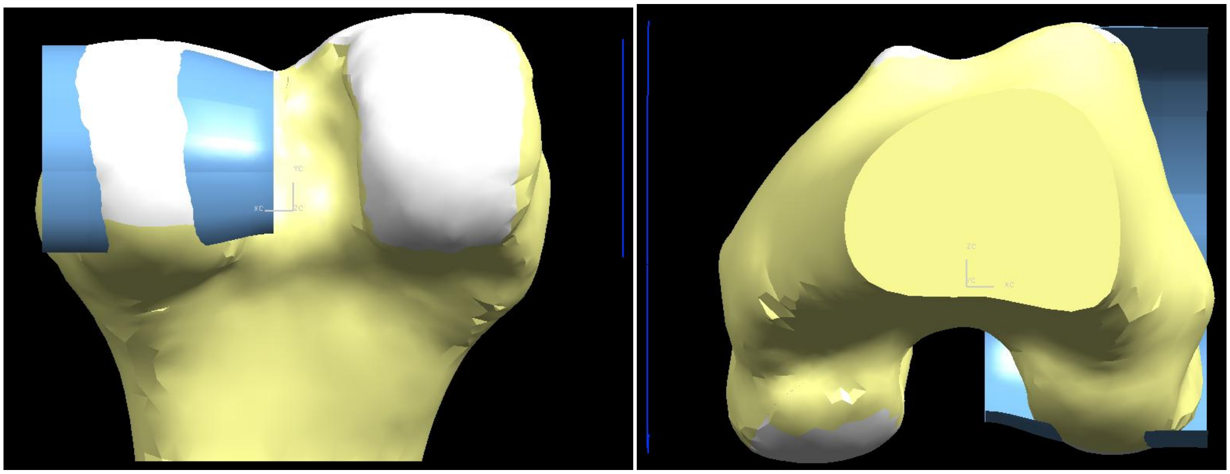

Figure 5.45 Posterior and axial views of the lateral cutting path over the cartilage model

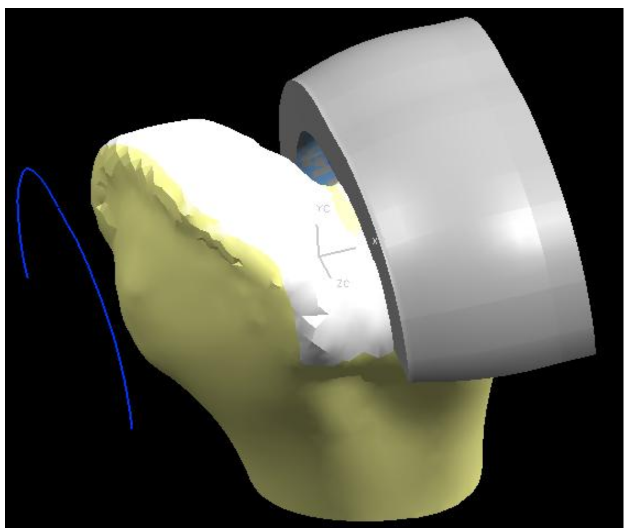

Figure 5.46 Lateral cutting body

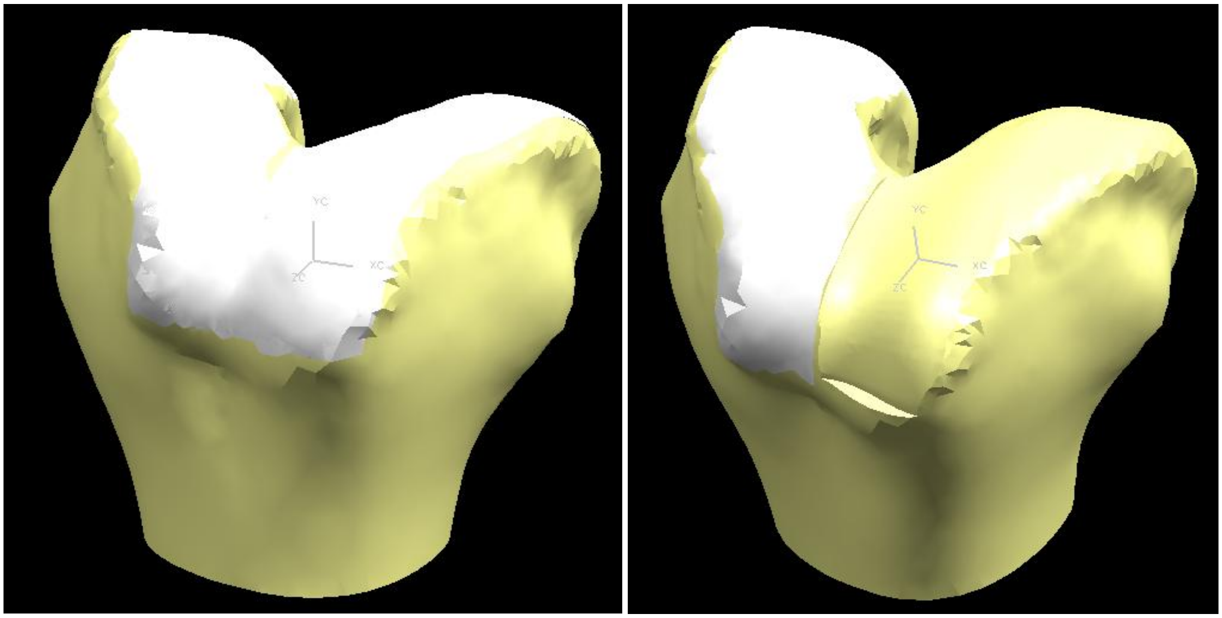

Figure 5.47 Femur model with cartilage anterior before and after simulated lateral resection

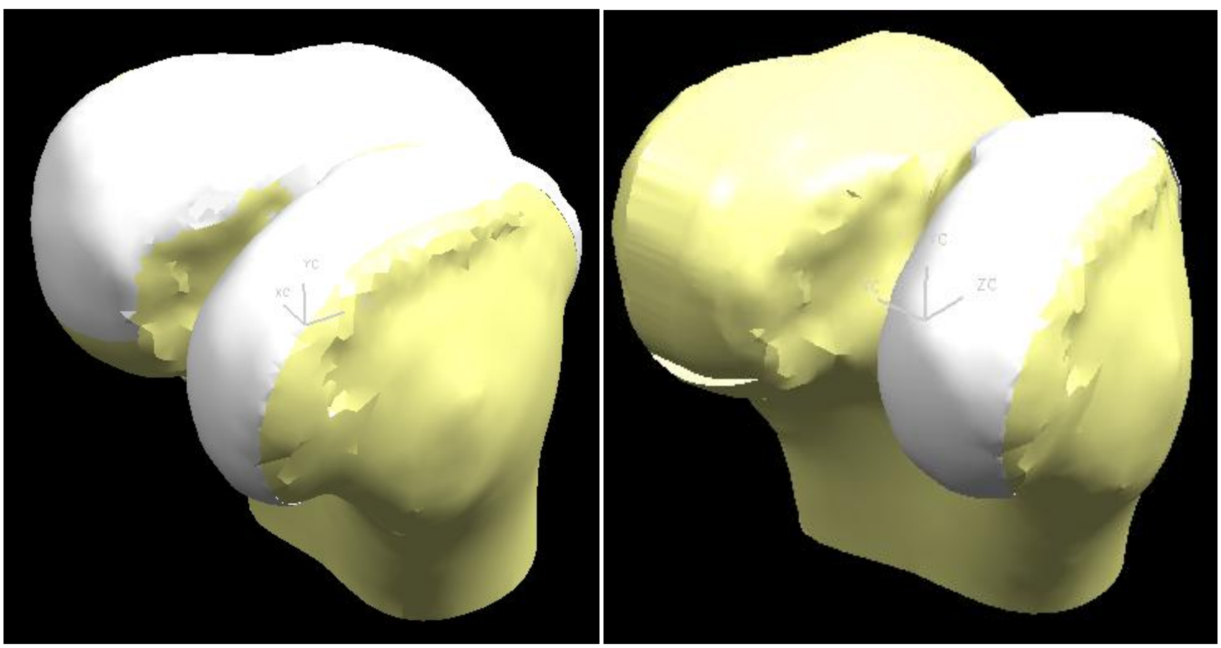

Figure 5.48 Femur model with cartilage posterior before and after simulated lateral resection

5.5.3. Anterior Resection Simulation

A femur model without cartilage, a cartilage model, the sulcus anteroposterior tool path and anterior mediolateral tool path were imported into NX4. The anterior mediolateral tool path was translated to the minimum cartilage thickness then swept along the sulcus anteroposterior tool path.

Unacceptable gouging of the anterior occurred Figure 5.49 and the lateral anterior mediolateral tool path was further refined as shown Figures 5.50. The section of the curve with the steepest slope was extended by drawing line a tangent to it.

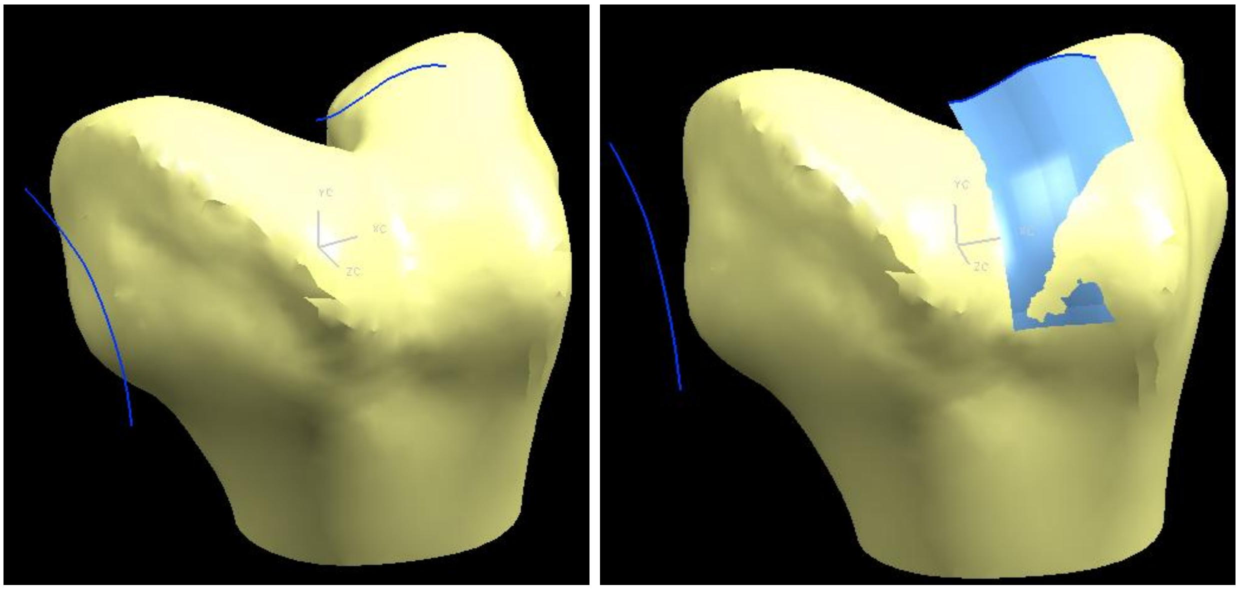

Figure 5.49 Unedited anterior AP and ML tool paths and cutting path over the bone model

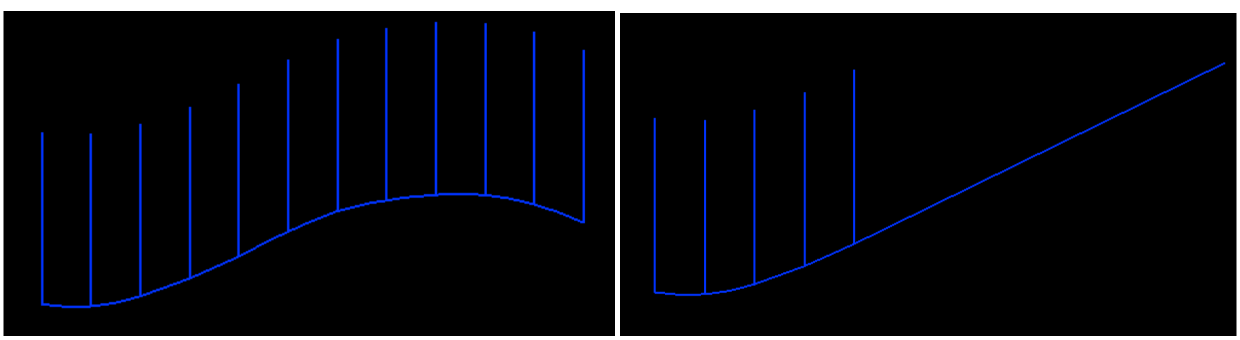

Figure 5.50 Anterior ML tool path before (left) and after (right) editing

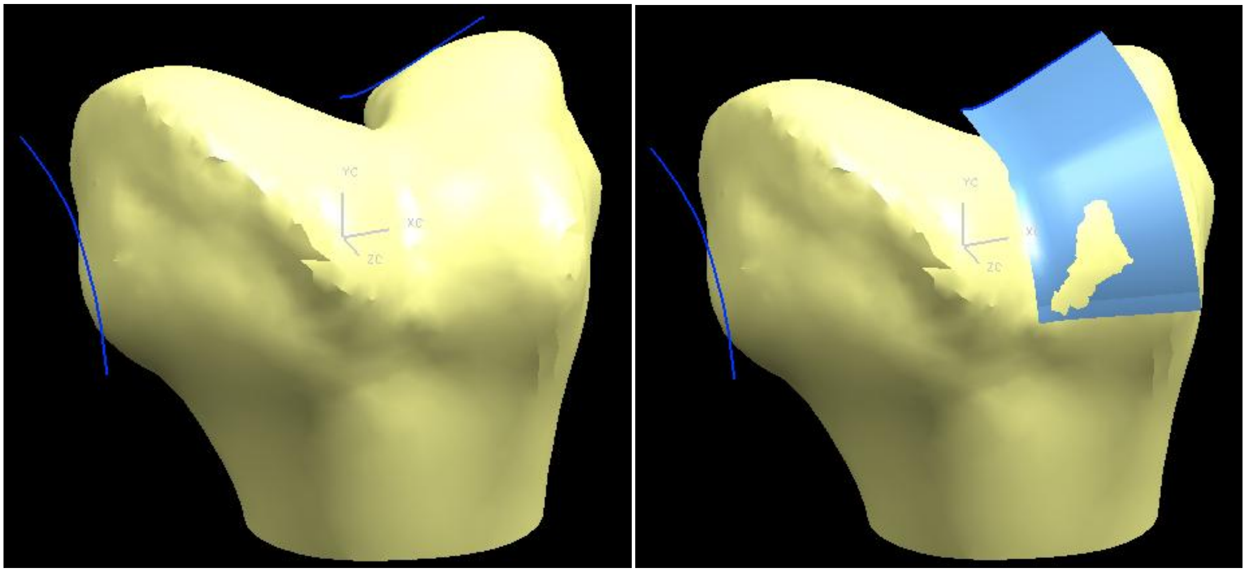

Figure 5.51 Edited anterior AP and ML tool paths and cutting path over the bone model

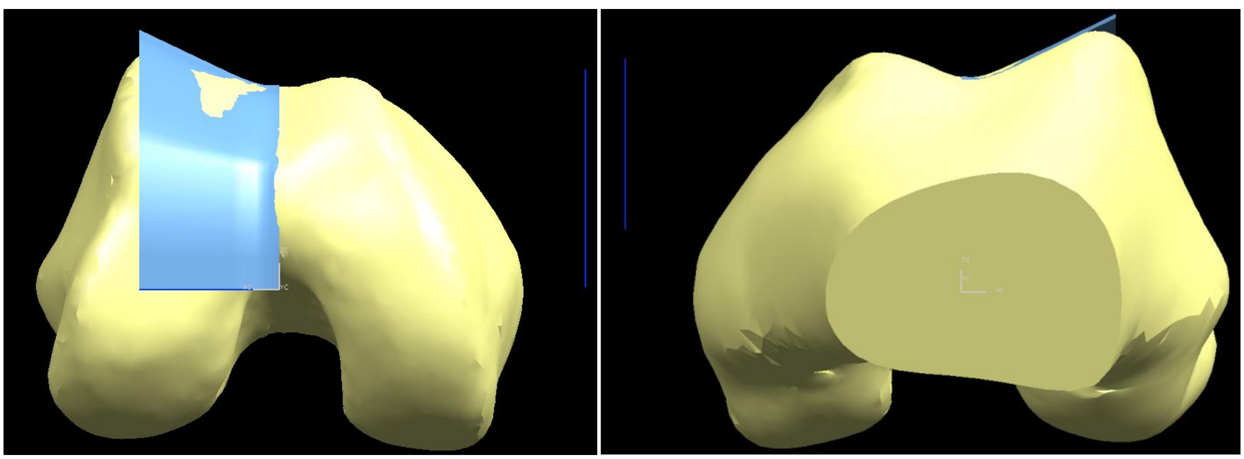

Figure 5.52 Distal and axial views of the anterior cutting path over the bone model

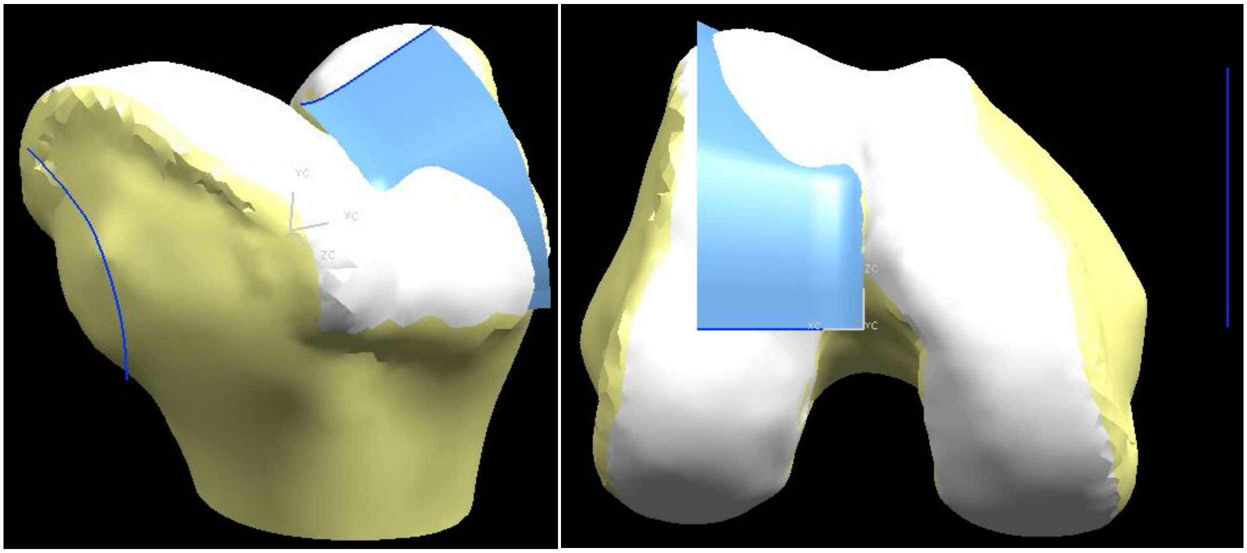

Figure 5.53 Perspective and distal views of the lateral cutting path over the cartilage model

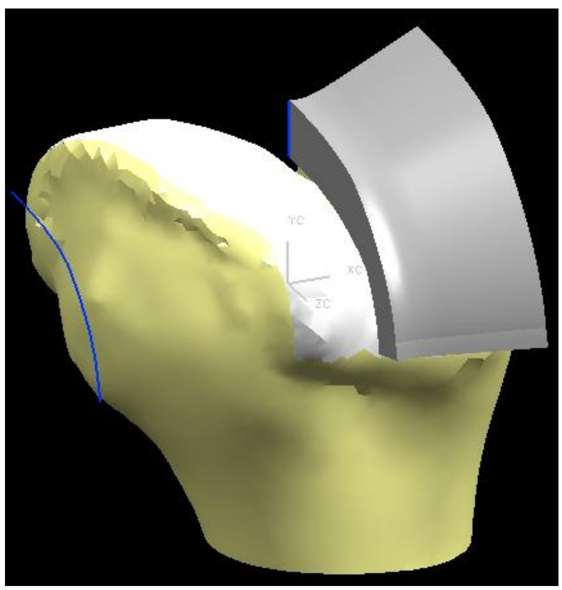

Figure 5.54 Anterior cutting body

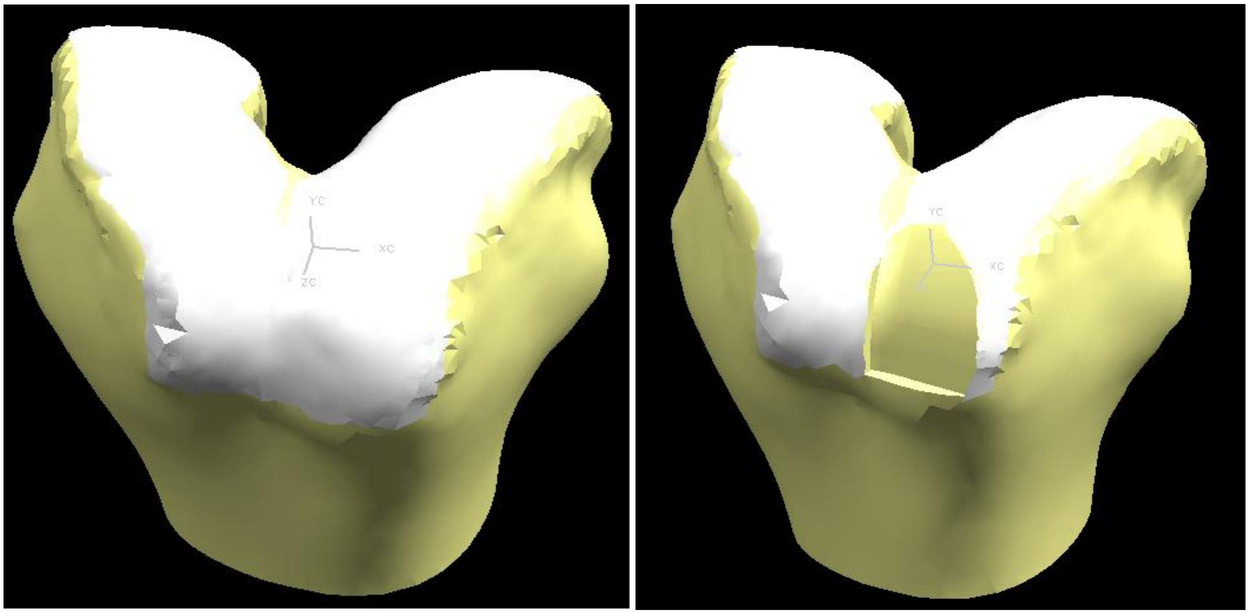

Figure 5.55 Femur model with cartilage anterior before and after simulated anterior resection

5.5.4. Lateral Unilateral and Total Resection Simulation

The medial and lateral unilateral and total resections were simulated. The medial resection, the results of which already shown, required only the medial mediolateral and anteroposterior tool paths. The lateral resection required the lateral mediolateral and anteroposterior tool paths to be applied followed by the anterior mediolateral and sulcus anteroposterior tool paths. The total resection required all three tool path pairs to be applied successively.

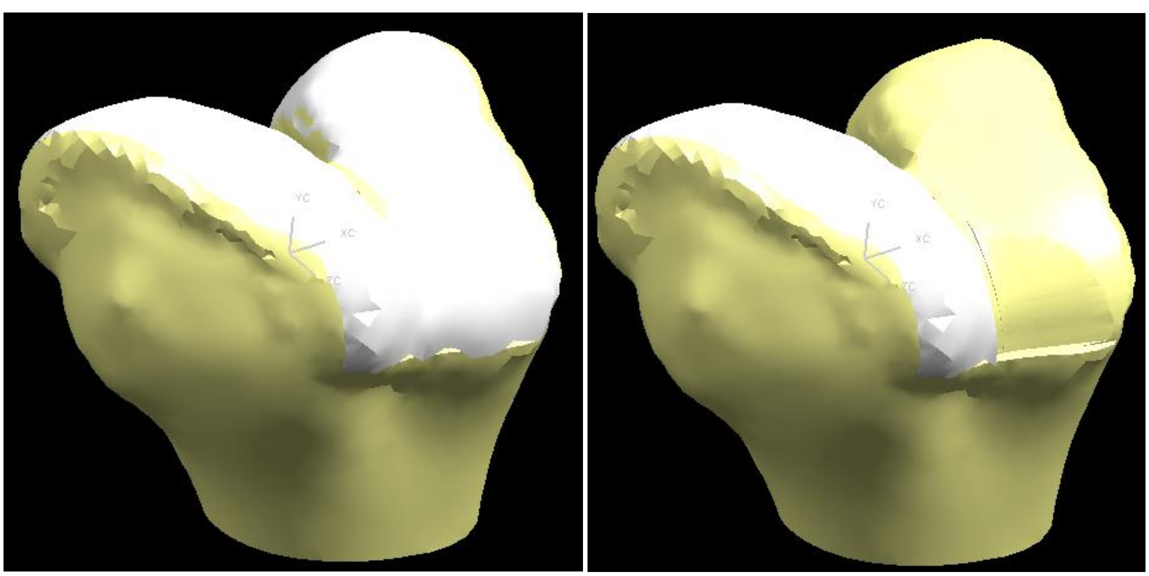

Figure 5.56 Femur model with cartilage anterior before and after simulated lateral and anterior resection

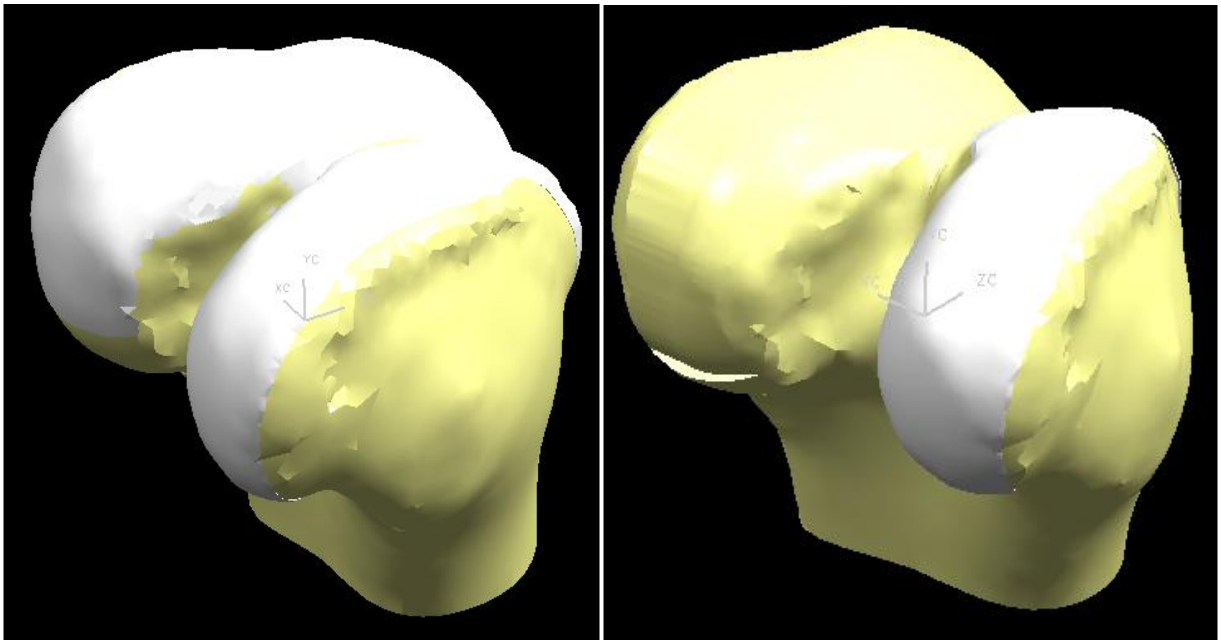

Figure 5.57 Femur model with cartilage posterior before and after simulated lateral and anterior resection

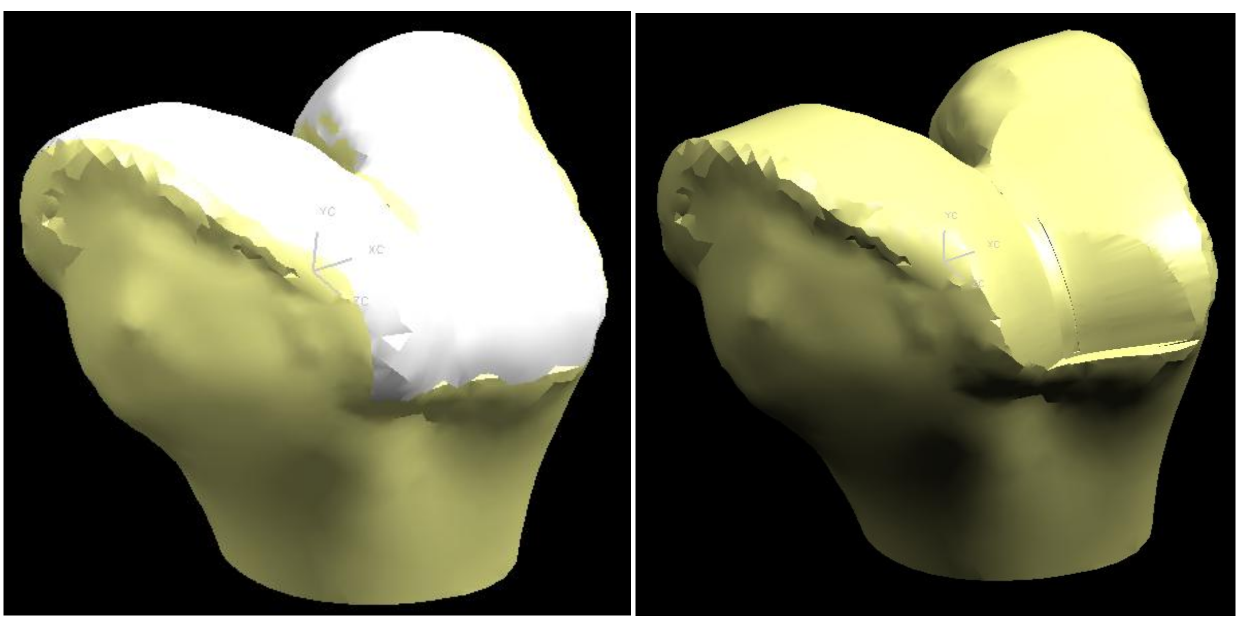

Figure 5.58 Femur model with cartilage anterior before and after simulated total resection

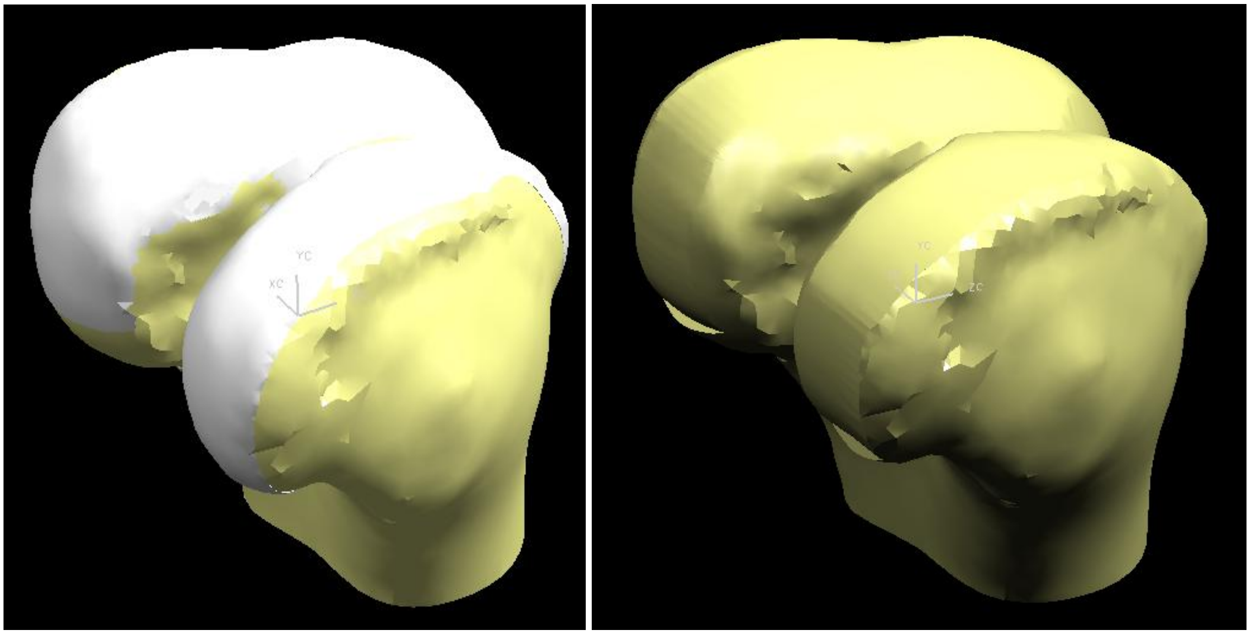

Figure 5.59 Femur model with cartilage posterior before and after simulated total resection

5.6. Cartilage Thickness Analysis

The total processed femur and cartilage STL models were imported into Amira 3.0. To quantitatively assess the thickness of cartilage removed, a distance analysis between the outer surface of the cartilage to the outer surface of the processed femur was performed with the upper limits of 2 mm and 3.5 mm to illustrate the full thickness range. The missing portion of the medial cartilage is due to a recession on the medial side. This area must be resurfaced manually by the surgeon as increasing the cutting depth to address this specific area would result in gouging the bone throughout. The mean cartilage thickness removed was 0.38 mm with a maximum of 3.6 mm.

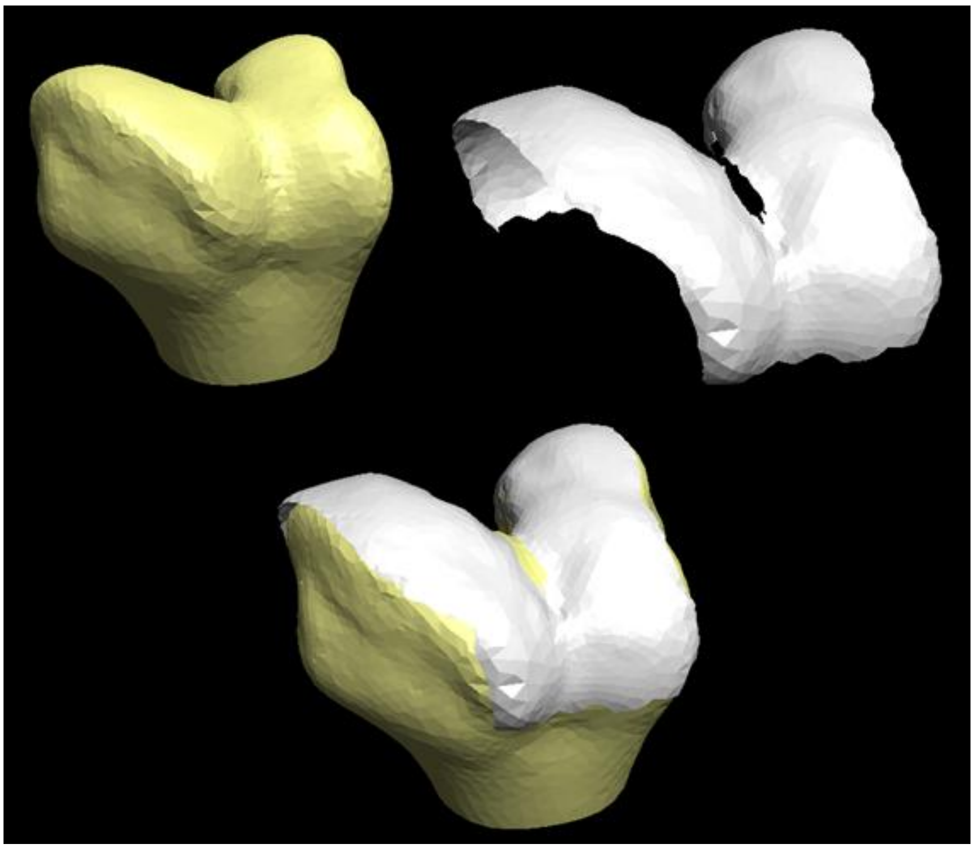

Figure 5.60 Femur model without cartilage (top left), cartilage model (top right), and femur model with cartilage (bottom left).

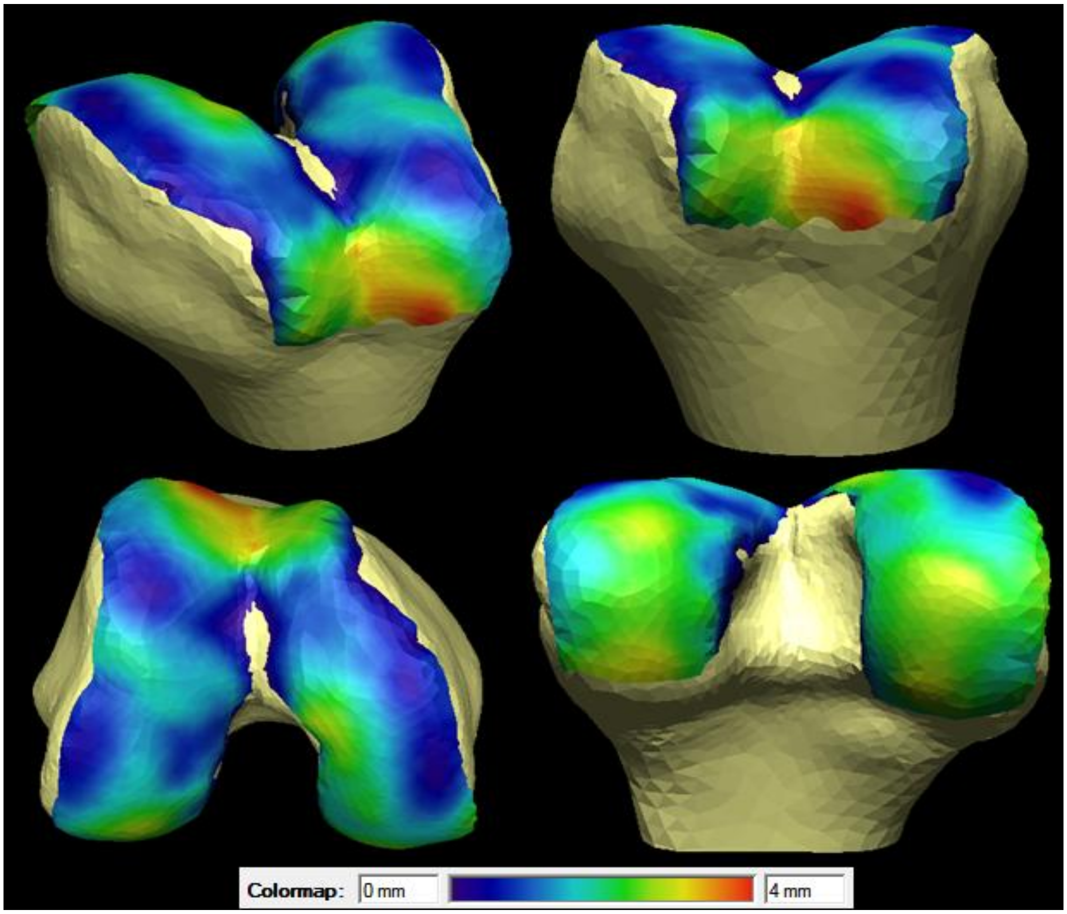

Figure 5.61 Distance map of cartilage thickness (range 0 – 4 mm)

Mean thickness	1.46 mm
RMS	1.69 mm
Maximum thickness	3.96 mm

Table 5.1 Thickness of distal femur cartilage before simulated resection

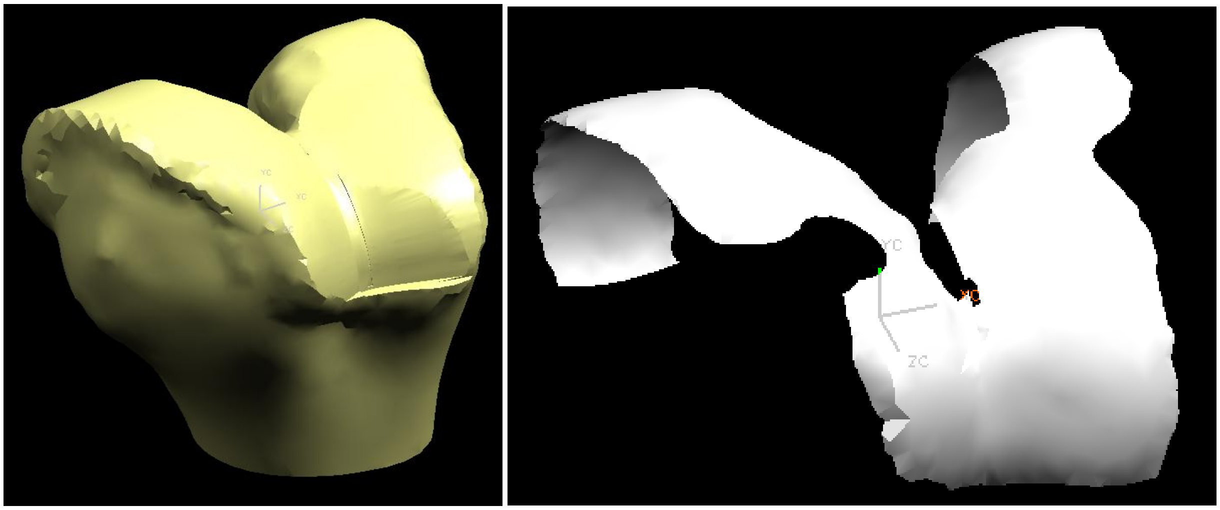

Figure 5.62 Processed femur model and removed cartilage

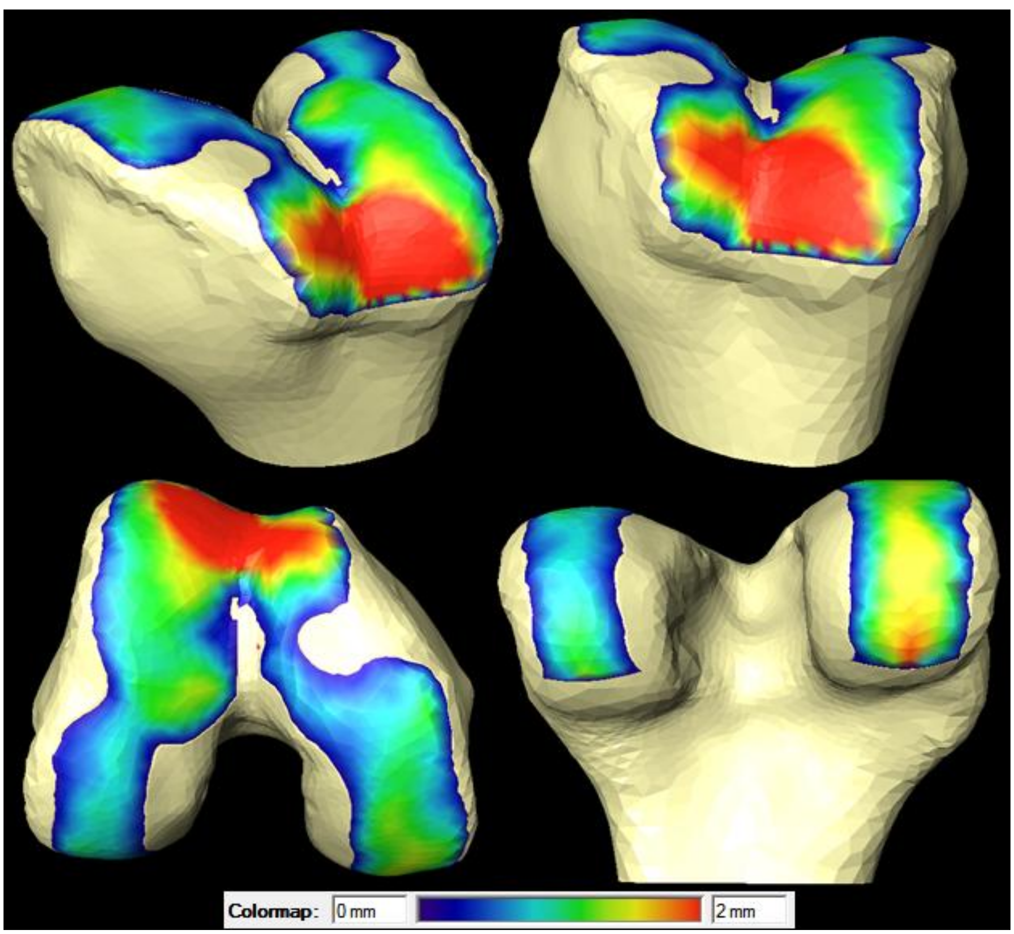

Figure 5.63 Distance map of removed cartilage thickness (range 0-2 mm)

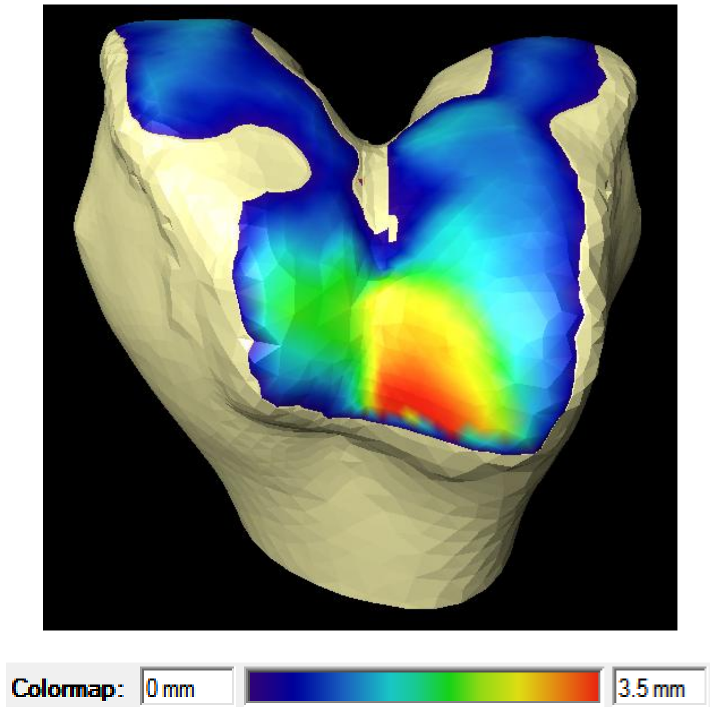

Figure 5.64 Distance map of removed cartilage thickness (range 0-3.5 mm)

Mean removed thickness	0.386 mm
RMS	0.713 mm
Maximum removed thickness	3.62 mm

Table 5.2 Thickness of removed distal femur cartilage by simulated resection

Mean remaining thickness	1.1 mm
RMS	1.4 mm
Maximum remaining thickness	3.96 mm

Table 5.3 Thickness of remaining distal femur cartilage after simulated resection

Chapter 6

Instrument Generation

To enable the required instrumentation to resect the distal femur according to the simulated resection, the instrumentation design requirements were the same as the virtual resection assumptions. In review, the mediolateral tool path and surgical drill linkage has one degree of freedom along the mediolateral path. The linkage between the anteroposterior tool path and mediolateral tool path also has one degree of freedom along the anteroposterior tool path. The tool paths are rigid and do not deform. Because the instrumentation is physical rather than virtual curves, additional requirements exist. The anteroposterior tool paths must be rigidly supported with respect to the femur and be positioned in real space in the same orientation as the modeling space.

6.1. AP Tracks and Slider Component

To allow the mediolateral pathway to travel smoothly along the anteroposterior pathway, a square track and slider type assembly was chosen Figure 6.8. A square track and slider is a common mechanical design which allows a carriage to travel along a track yet is restrained to one degree of freedom due to the parallel faces and square corners preventing rotation. The slider served as the attachment point of the mediolateral tracks. One limitation of this design is that for a curved track, the ability of the slider to travel around a small track radius is limited by the thickness of the slider contacting the inner curve of the track. A slider that is too thick for the track will not advance into a curve with too small a curvature. A 3/8th inch square section was swept along the anteroposterior tool paths with an extension to the posterior to facilitate a hole and bolt Figures 6.2, 6.4, 6.6. This served as a physical constraint to limit the motion of the slider to the posterior so that it would not travel beyond the area of the simulation. A similar hole and bolt was placed at the anterior section to limit the travel of the slider in the anterior Figure 6.9. A vertical extension was added anterior to this stop point to provide a rigid fixation point to secure the anteroposterior track. The slider component was created in two halves to match the anteroposterior tracks and held together by nuts and bolts on either side so that the tightness of fit to the anteroposterior tracks could be adjusted by tightening the nuts Figure 6.8. The track contacting surface was ground to a triangular cross section to minimize its contact to a point and allow the slider to travel around smaller curvatures than possible with the larger contact area of a slider with a rectangular cross section. Each AP track was fitted with the generic slider component then the position of each fitted slider was saved, creating one specifically positioned slider per AP track.

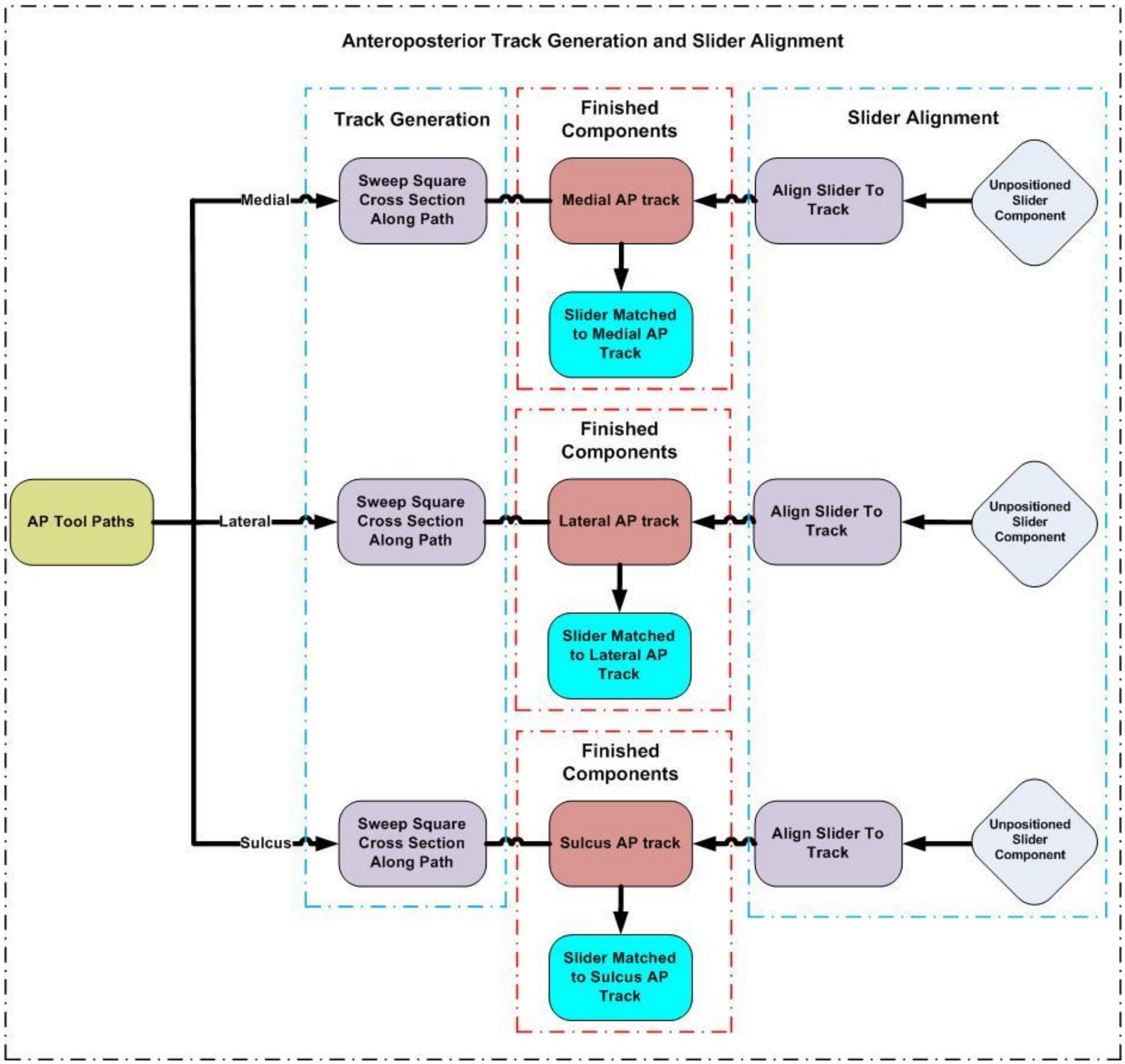

Figure 6.1 Process flow for creating the AP tracks and fitting a slider component to AP each track

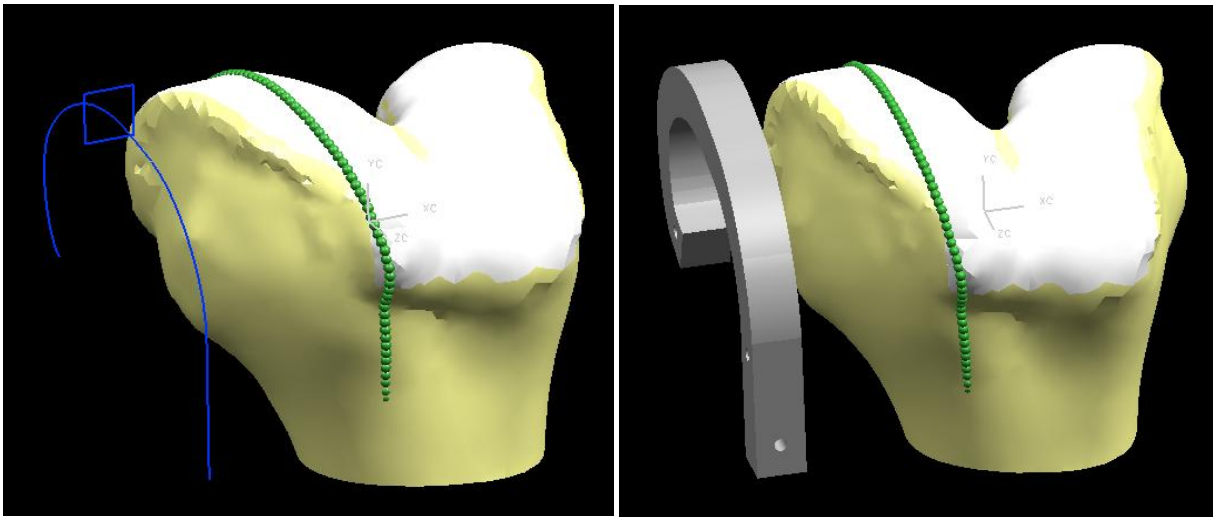

Figure 6.2 Medial anteroposterior tool path (left) and track (right) perspective view

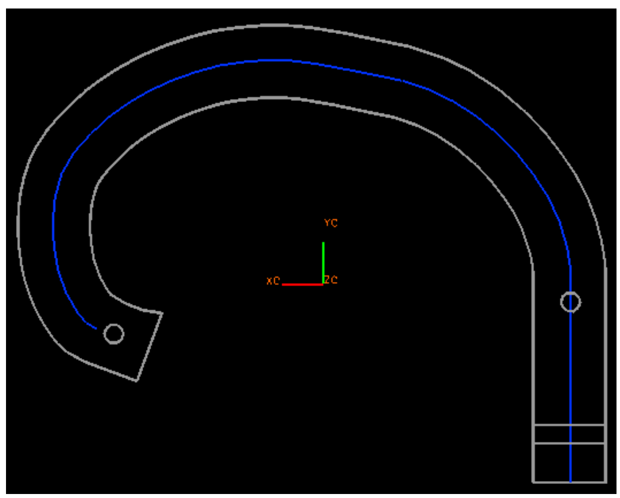

Figure 6.3 Medial anteroposterior track sagittal view

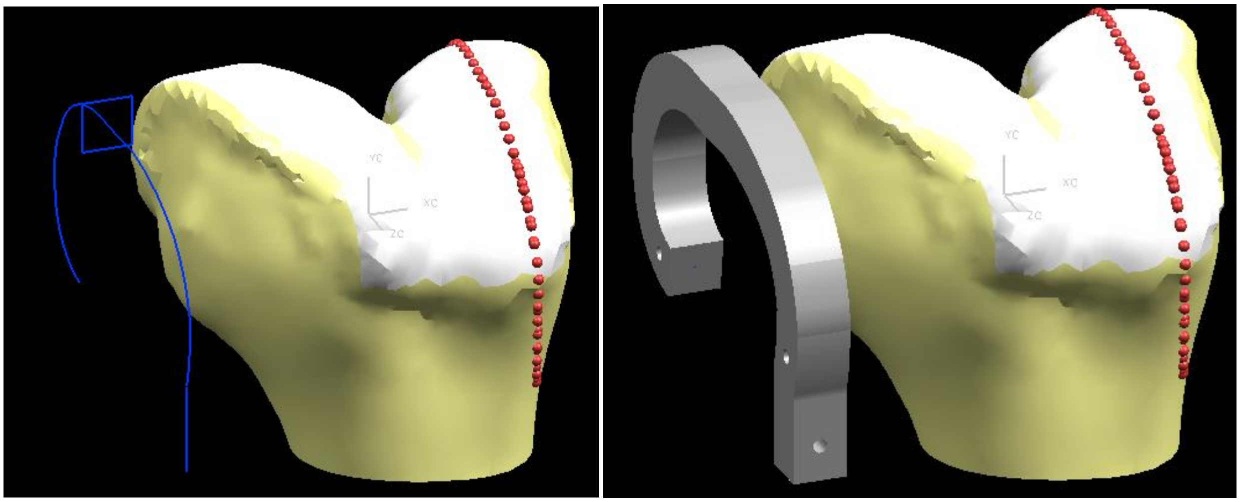

Figure 6.4 Lateral anteroposterior tool path (left) and track (right) perspective view

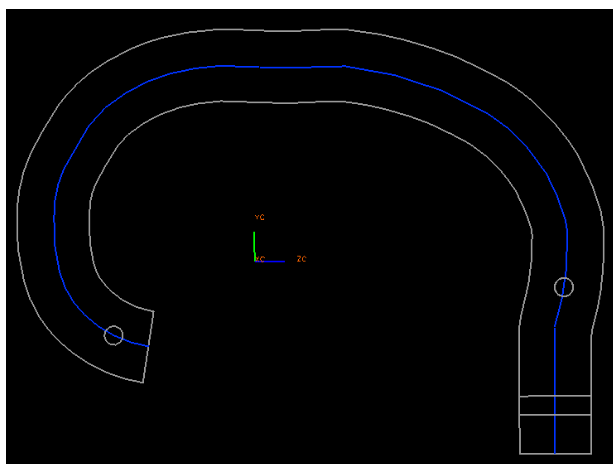

Figure 6.5 Lateral anteroposterior track sagittal view

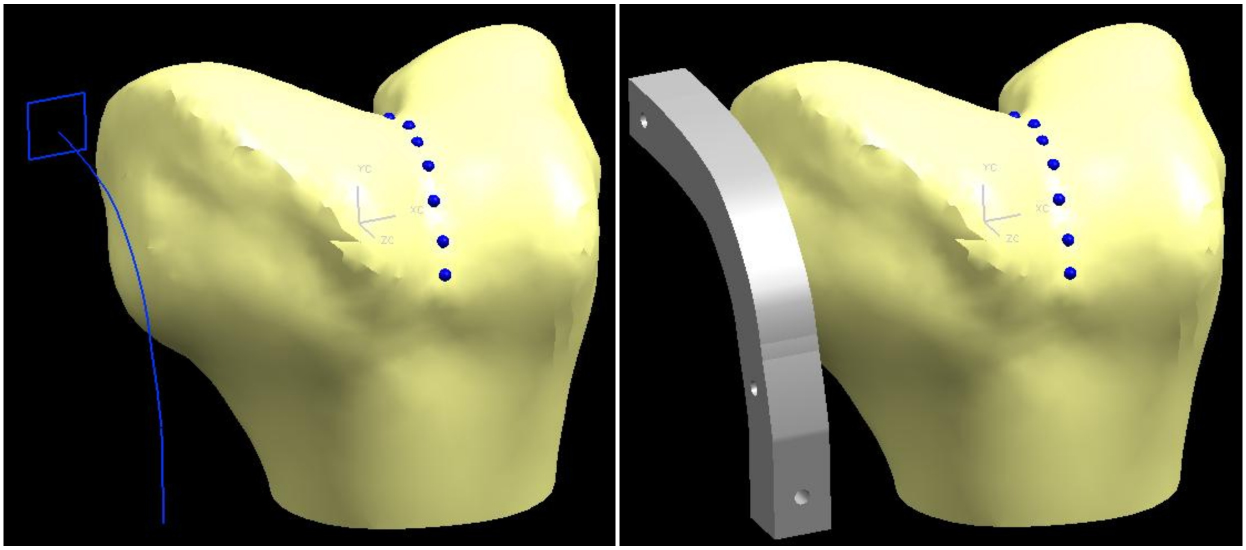

Figure 6.6 Sulcus anteroposterior tool path (left) and track (right) perspective view

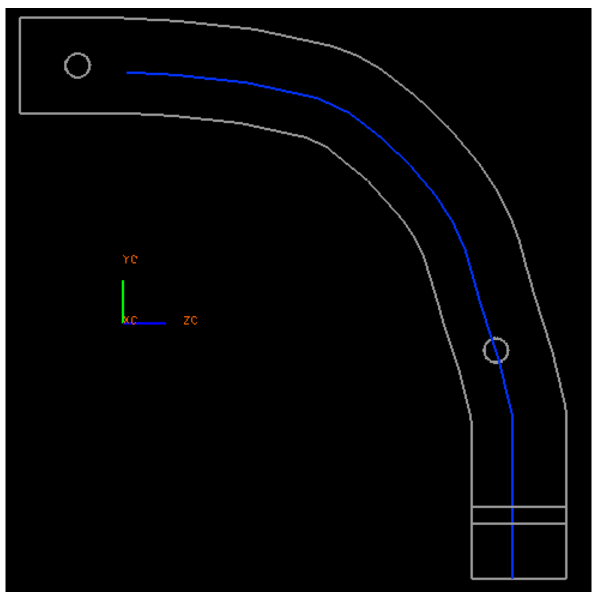

Figure 6.7 Sulcus anteroposterior track sagittal view

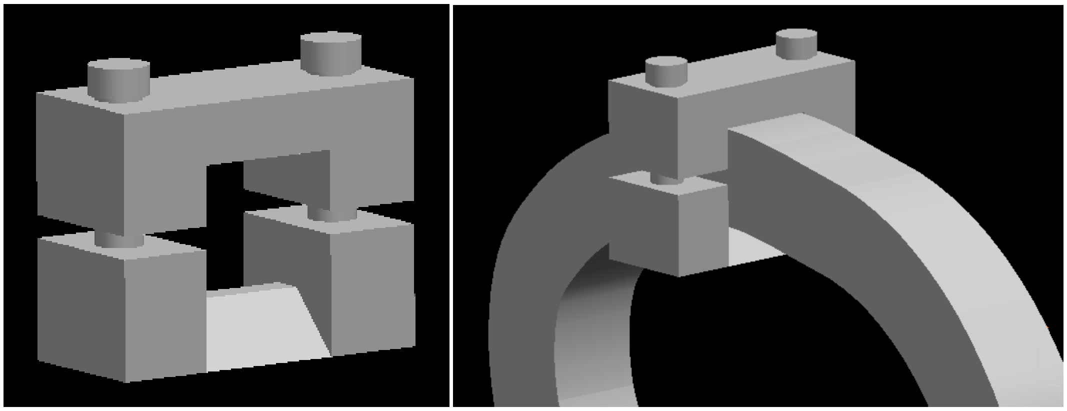

Figure 6.8 Slider component and anteroposterior fitting

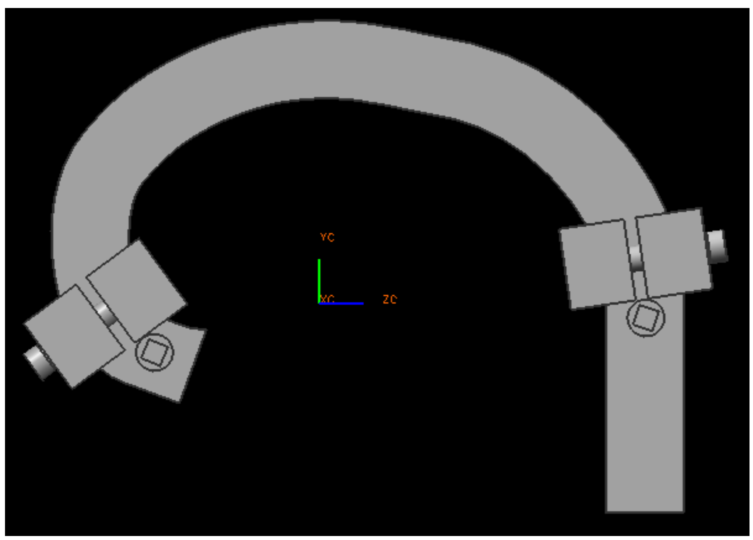

Figure 6.9 Slider component range limited by anterior and posterior bolts

6.2. AP Track Fixation

The anteroposterior tracks are generated in their correct orientation in the modeling space. To experimentally verify the cut simulation, this position must be reproduced and maintained in real space through rigid supports. The framework consisted of the iCS generated patient specific jig, a base component positioned to the bone by the jig, and a fixation arm to join the anteroposterior tracks to the jig positioned base component. Because the jig provided an unambiguous fit, the rigid components positioned by the jig were guaranteed to be in the same real space position as they were in the modeling pace.

6.2.1. Base Component

A base was created to serve as a rigid fixation point for the anteroposterior tracks. It featured two screw holes to accommodate the insertion of screws to fix the base to the bone. It also featured a square slot so that the fixation arm may be inserted and secured with a bolt. This square on square contact did not allow arm rotation and the bolt prevented arm translation. This maintained the fixation arm in the correct alignment. The base component was placed proximally in a position similar to the PiGallileo system.

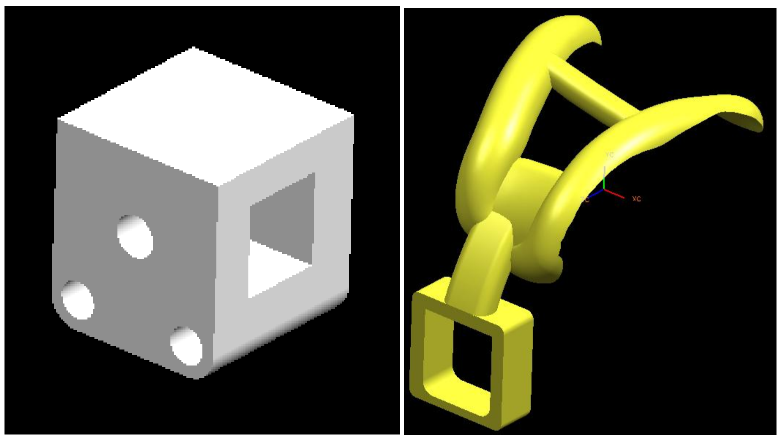

Figure 6.10 Base component and jig

6.2.2. Patient Specific Jig

The iCS jig was imported into the modeling space along with a tongue component fit to match the base component. A tongue component was created to match the base component. It featured a window to allow screws to be inserted into the base component. The tongue was adjusted to intersect with the iCS jig then both were exported as separate STL files. These were then imported into Rapidform 2006 then united through a Boolean operation, completing the jig and tongue assembly.

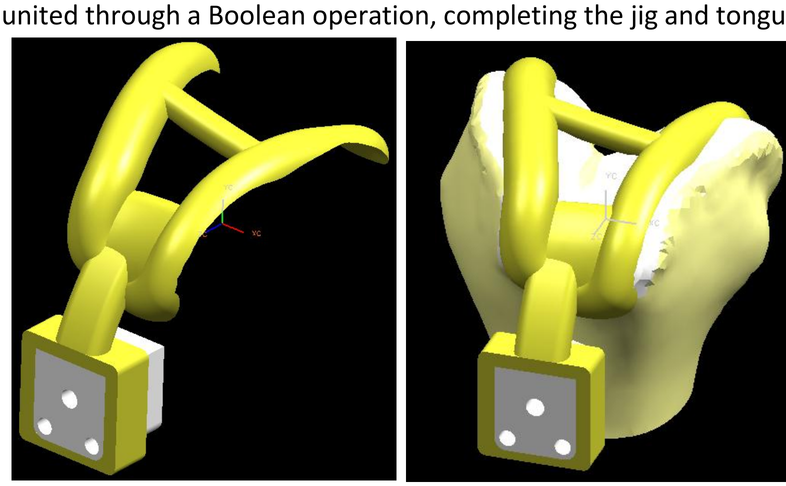

Figure 6.11 Patient specific jig and base

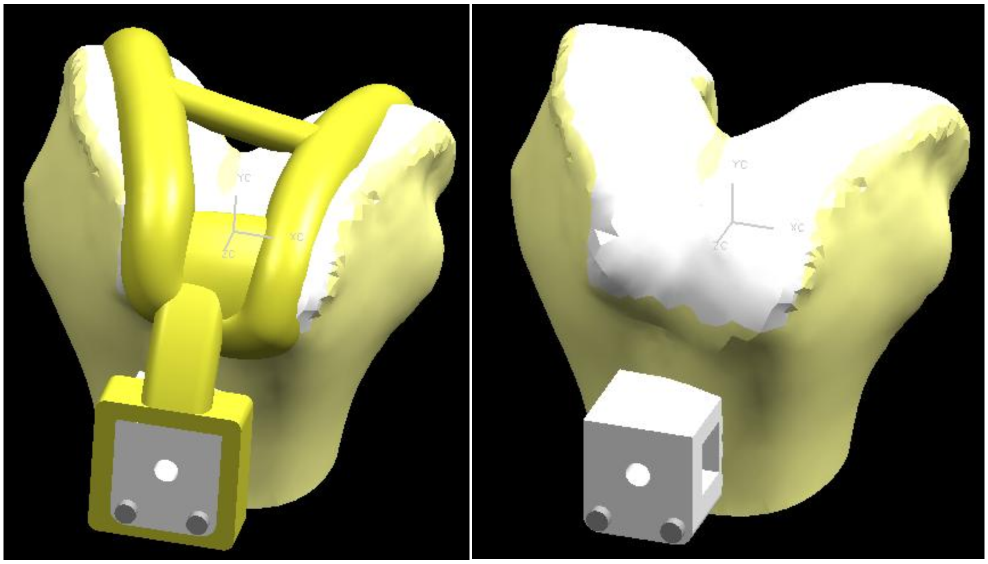

Figure 6.12 Jig and base assembly with inserted bone screws and jig removed

6.2.3. Fixation Arm

A fixation arm was created to rigidly attach the anteroposterior track to the base and provide clearance. It is inserted into the base and held in position with an M2.5 bolt. The fixation arm allows all anteroposterior tracks to be mounted from the medial side without interfering with the surrounding soft tissues. This facilitates the medial sided incision and exposure common among knee arthoplasty techniques.

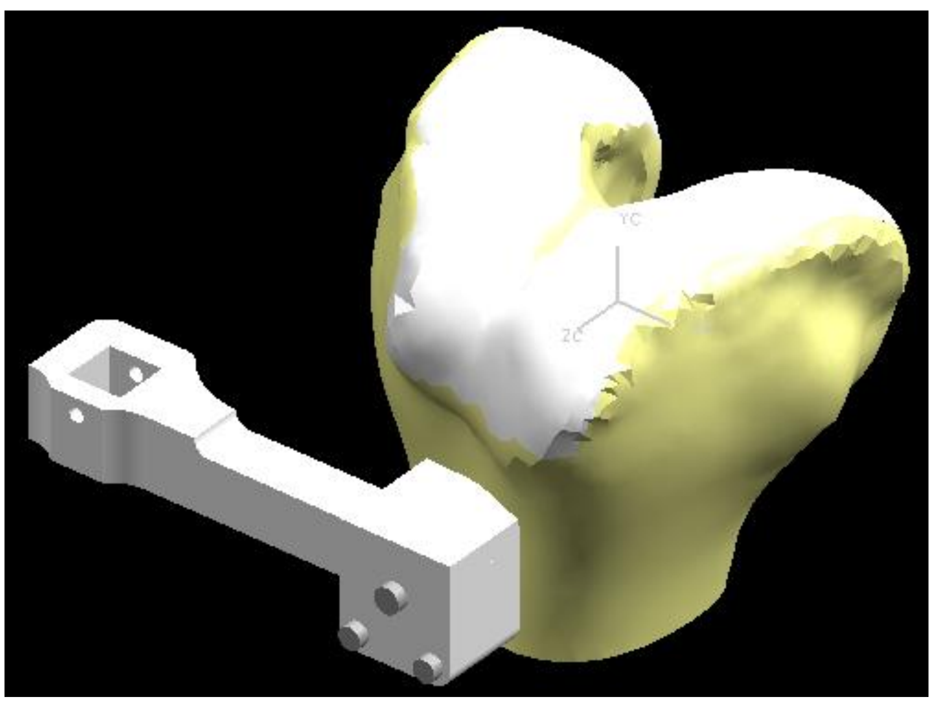

Figure 6.13 Base component with fixation arm

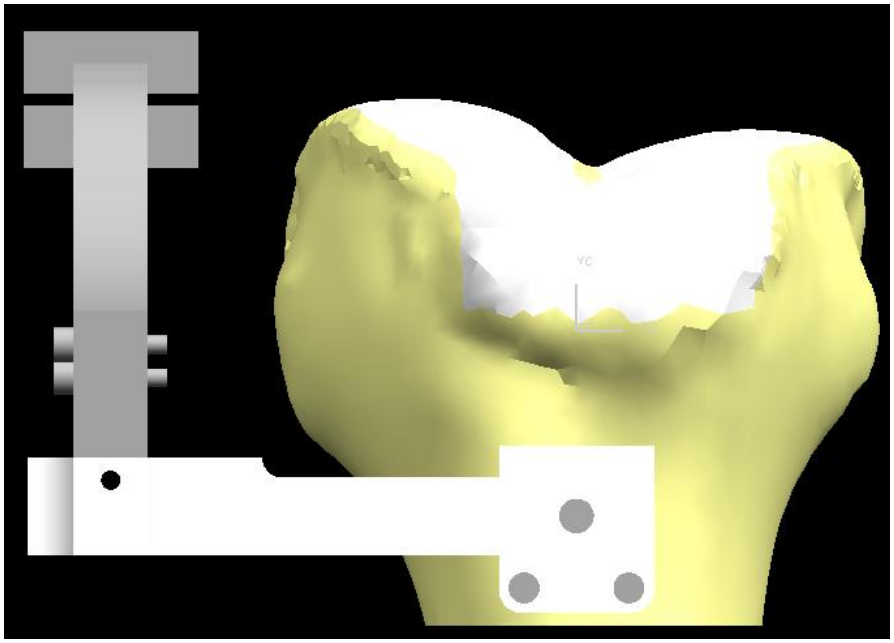

Figure 6.14 Medial AP track and slider fit to fixation arm

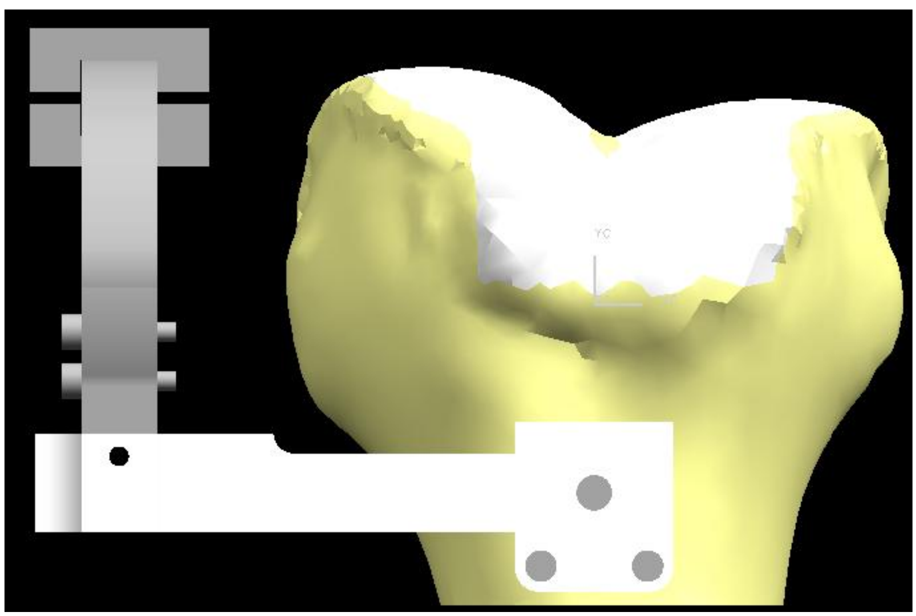

Figure 6.15 Lateral AP track and slider fit to fixation arm

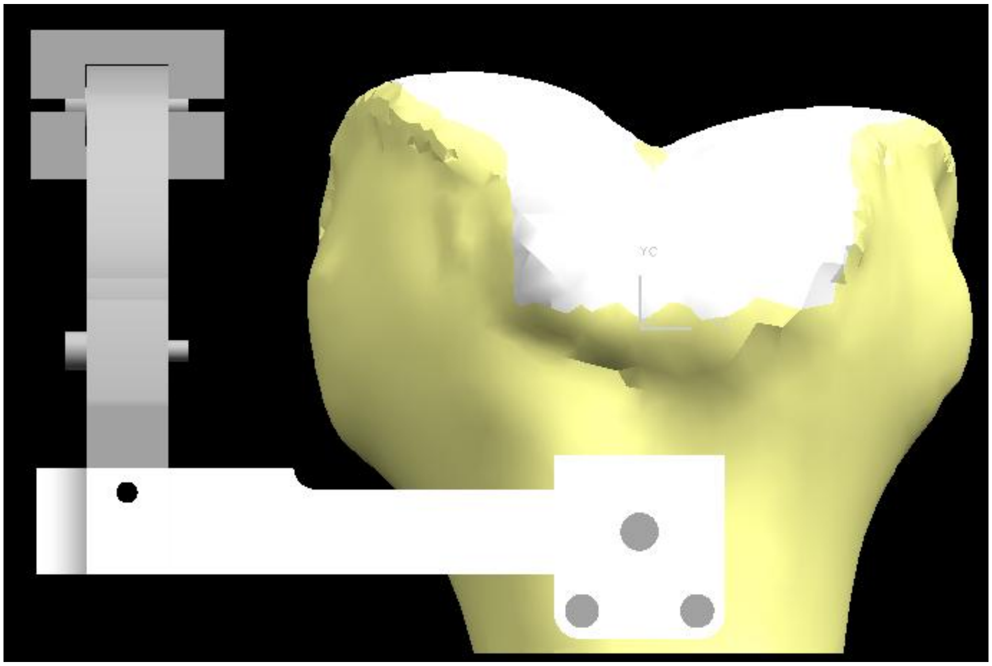

Figure 6.16 Sulcus AP track and slider fit to fixation arm

6.3. ML Track Spacer

Given the slider components previously positioned to each AP track, it is shown that there is a difference in their proximodistal position Figure 6.18. This is due to the medial, lateral, and sulcus profiles varying in the distance that they extend distally. Because of this, the mediolateral tracks will also vary in proximodistal position, causing a variation in cutting depth and deviation from the cut simulation with each anteroposterior track. A generic spacer was fit to each slider to account for this height variation and also connect each mediolateral track to its respective positioned slider Figure 6.17. Because the medial slider was positioned the most distally as compared to the other sliders, it was used as the datum for the remaining lateral and anterior fit spacers Figure 6.21. The generic spacer fit to the lateral and anterior sliders was then thickened so that the height of their top face was equal to that of the medial spacer and slider assembly Figure 6.22.

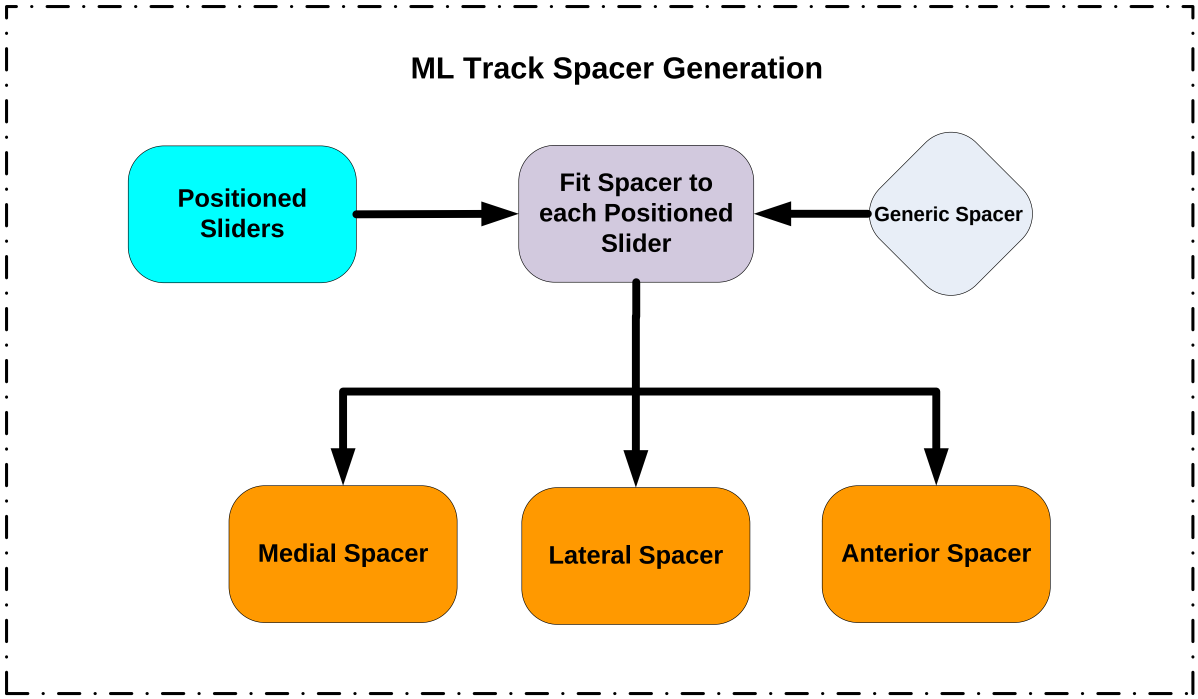

Figure 6.17 Process to fit one ML track spacer to each positioned slider

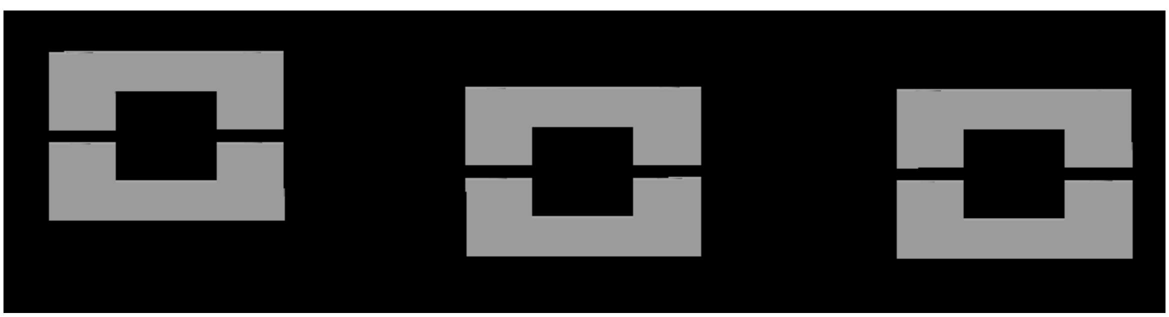

Figure 6.18 Slider height variation when fitted to the medial, lateral, and sulcus AP tracks

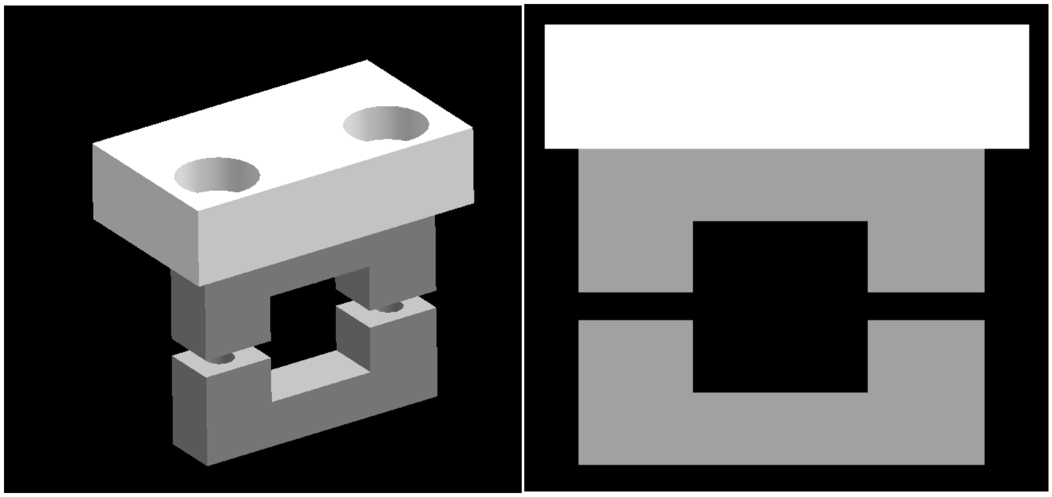

Figure 6.19 Medial slider component with spacer

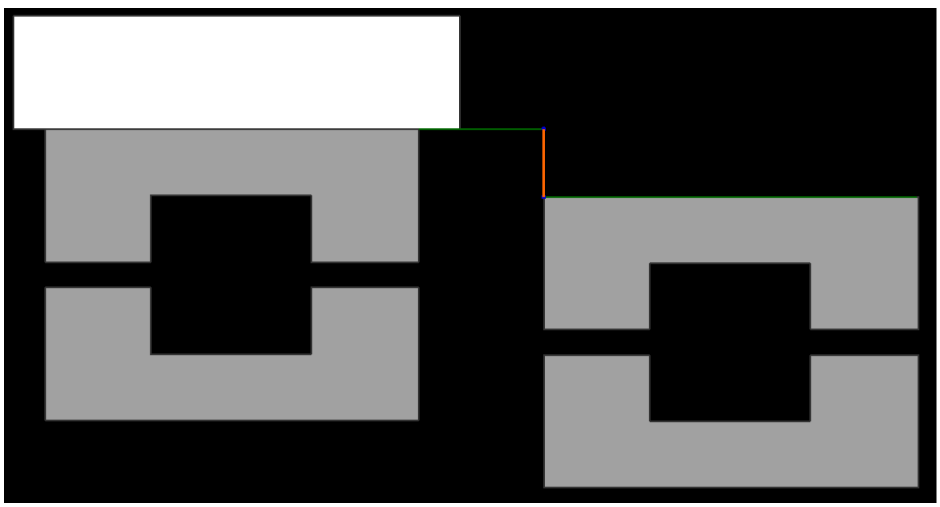

Figure 6.20 Medial slider component with spacer (right) and lateral slider (left)

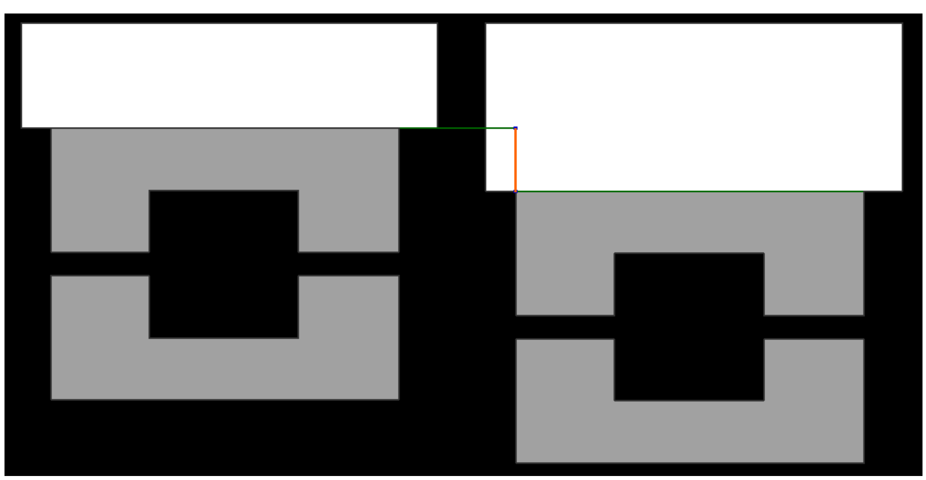

Figure 6.21 Medial slider component with spacer (left) and lateral slider with thickened spacer (right)

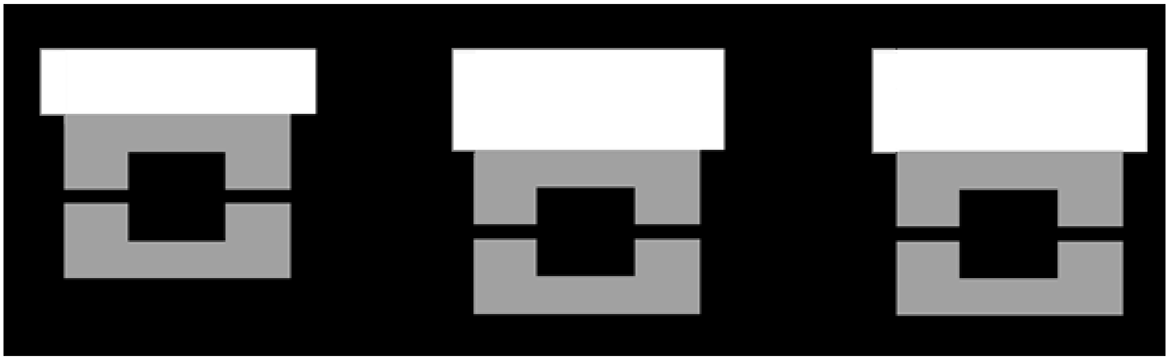

Figure 6.22 All slider components fit with plastic spacers to account for AP height variation

6.3.1. ML Track Generation

To allow a surgical drill to travel along the mediolateral pathways with one degree of freedom, the track and slider concept was reused. Using the medial slider as the datum, the distance from the top of the medial slider to the medial mediolateral tool path was determined Figure 6.24. Using this distance, each segment of the positioned mediolateral tool paths was extrapolated by drawing perpendiculars to their midpoints and endpoints Figure 6.25. Arcs were then fit to these segments defined by three points to create the extrapolated tool path Figure 6.26. A rectangular section, fit to match the cross section of the slider component, was swept along the extrapolated tool paths with an additional 1 cm of clearance to allow space for the drill to travel to the end of the track Figure 6.27. Before joining the mediolateral tracks to the spacer components, they were offset by 8 mm from the leading face of the spacer to provide clearance so that the drill bit could be placed in line with the center of the anteroposterior slider component Figure 6.28. This same extrapolation procedure was utilized to create the lateral and anterior mediolateral tracks from the lateral and anterior tool paths.

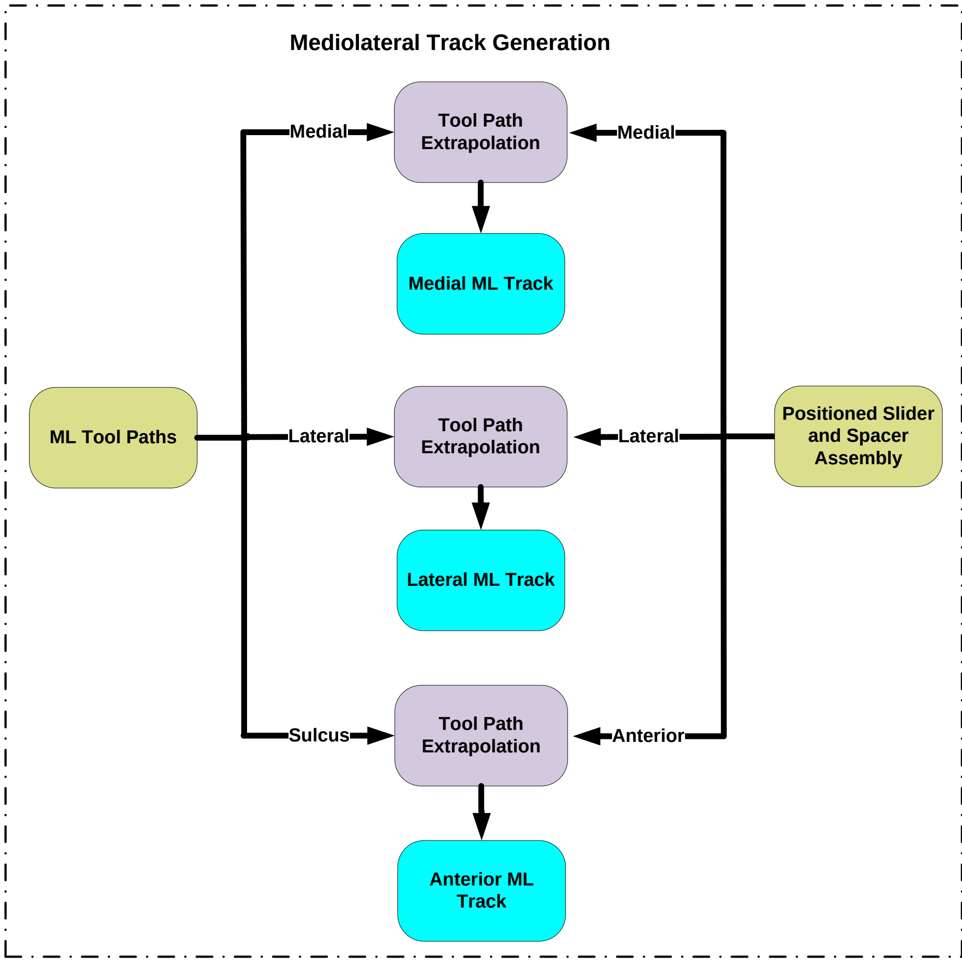

Figure 6.23 Flow diagram illustrating each ML tool path scaled to match the corresponding slider and spacer assembly

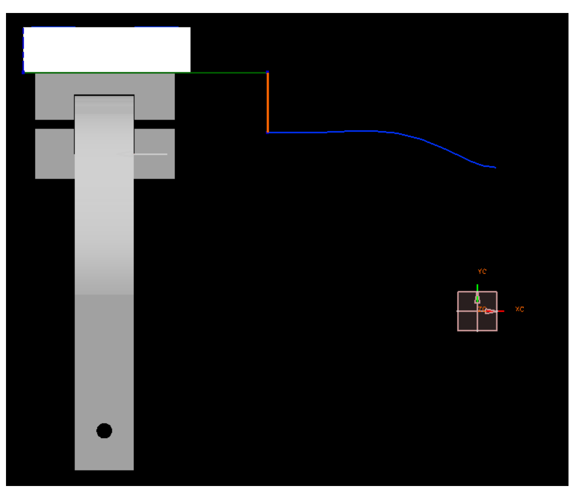

Figure 6.24 Distance from the medial tool path to the medial slider datum

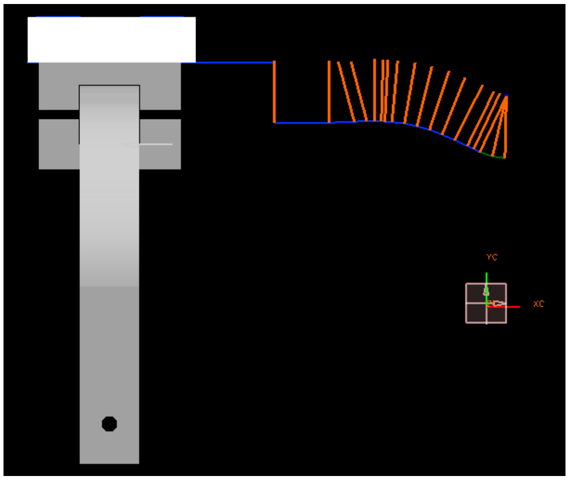

Figure 6.25 Extrapolating rays from the medial tool path

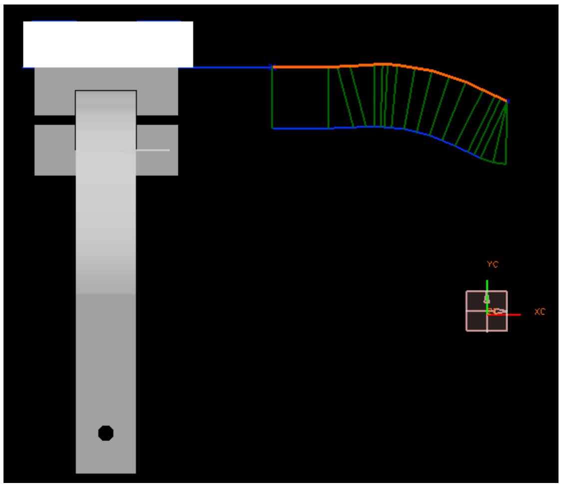

Figure 6.26 Extrapolated tool path

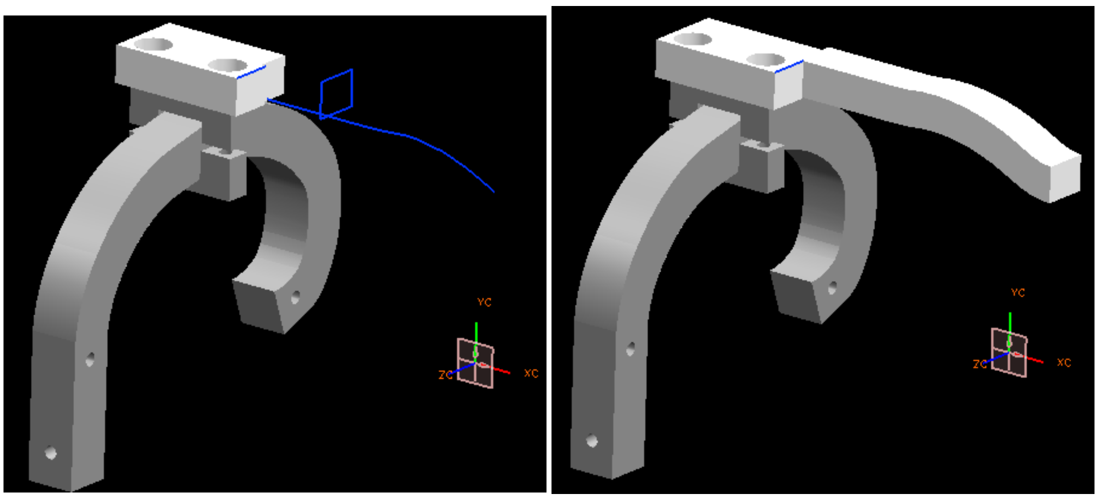

Figure 6.27 Final medial ML track

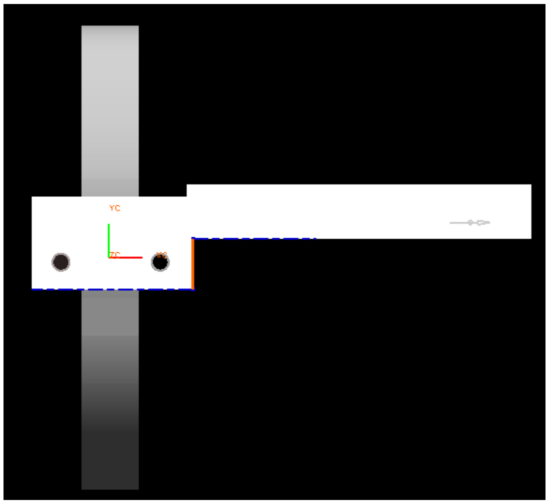

Figure 6.28 Medial ML track offset to provide drill clearance

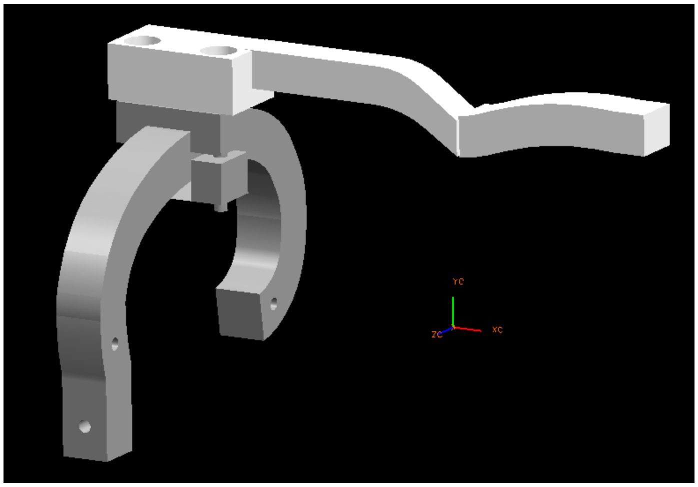

Figure 6.29 Final lateral ML track

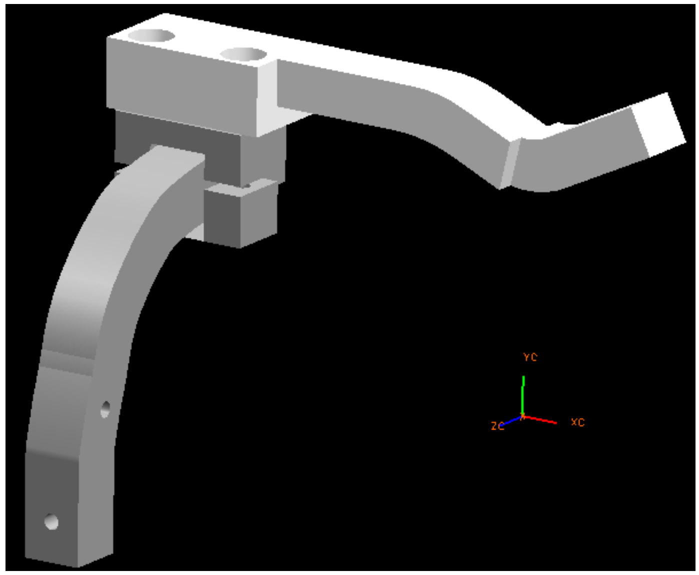

Figure 6.30 Final anterior ML track

6.4. Drill Holster

The drill provided was a Dremel D 300 rotary tool and a 3mm carbide cutter bit Figure 6.31. Measurements were taken of the Dremel and bit to define their diameters and length. These were used to construct CAD models of the drill and bit Figure 6.32. The Dremel and bit model was then placed at the determined cutting depth as measured from the medial AP slider component. In the coronal plane, the drill bit was placed at the trailing edge of the mediolateral slider component Figure 6.33. This was done so that the mediolateral position of the bit tip matched that of the mediolateral slider. In the sagittal plane, the drill bit was placed in the same plane as the center of the anteroposterior slider component Figure 6.34. This was done so that the anteroposterior position of the bit tip matched the anteroposterior position of the slider component. In this way, the drill bit tip matched the mediolateral and anteroposterior position of both slider components. A rigid holster was then constructed around the drill model and matched with bolt holes to the bolt holes of the mediolateral slider component Figure 6.35.

A positioning target was constructed around the mediolateral slider and positioned drill bit tip Figure 6.36. This was used to position the experimental drill in the same orientation as the model drill. The physical drill tip is positioned by placing it in the receptacle then securing the drill to the holster and removing the target. In this way the orientation of the drill was matched to the orientation of the model drill and bit.

Figure 6.31 Dremel 300 and 3 mm cutter bit

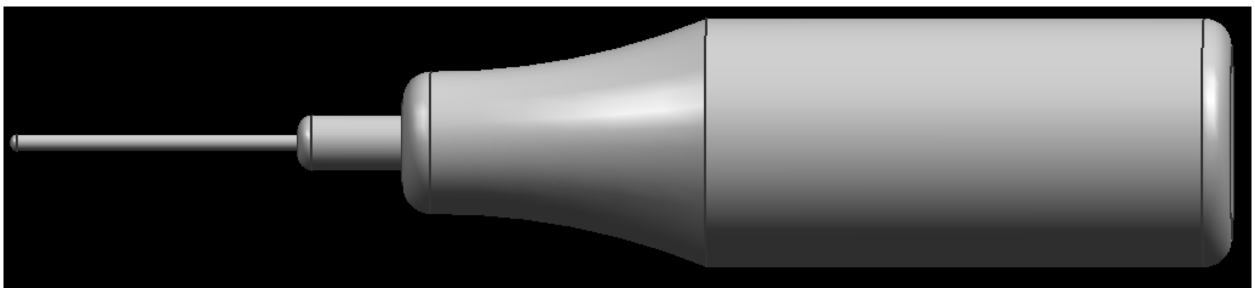

Figure 6.32 Model drill and bit

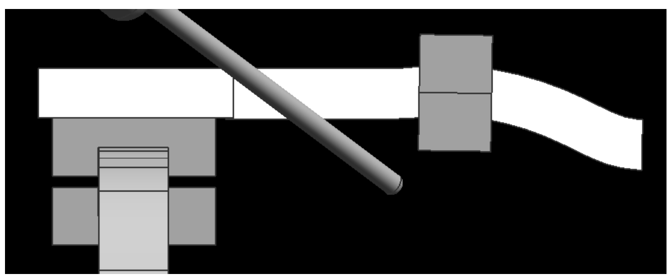

Figure 6.33 Drill bit coronal placement with respect to the ML slider

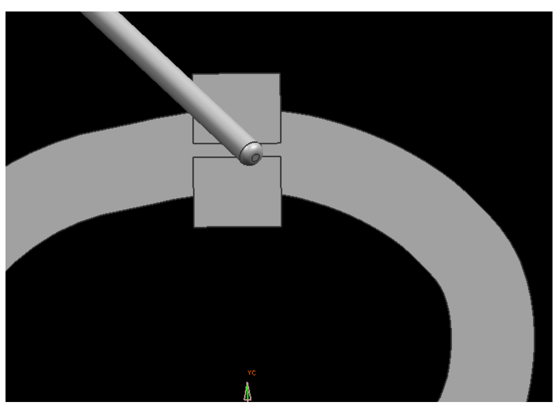

Figure 6.34 Drill bit sagittal placement with respect to the AP slider

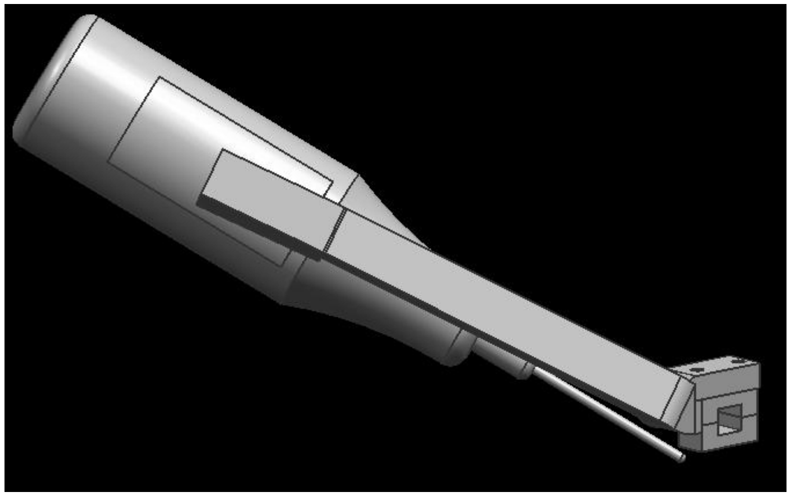

Figure 6.35 Model drill and holster

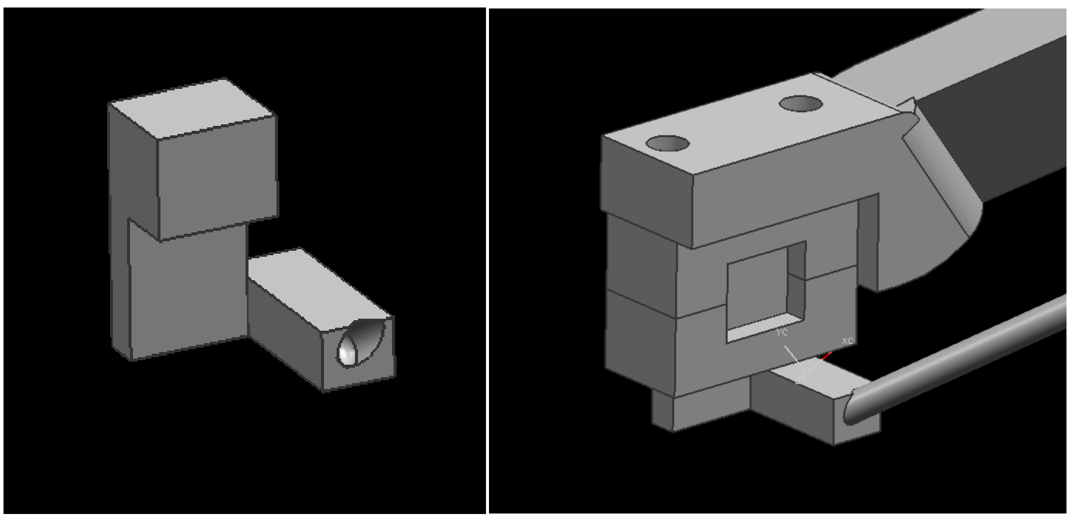

Figure 6.36 Bit positioning piece

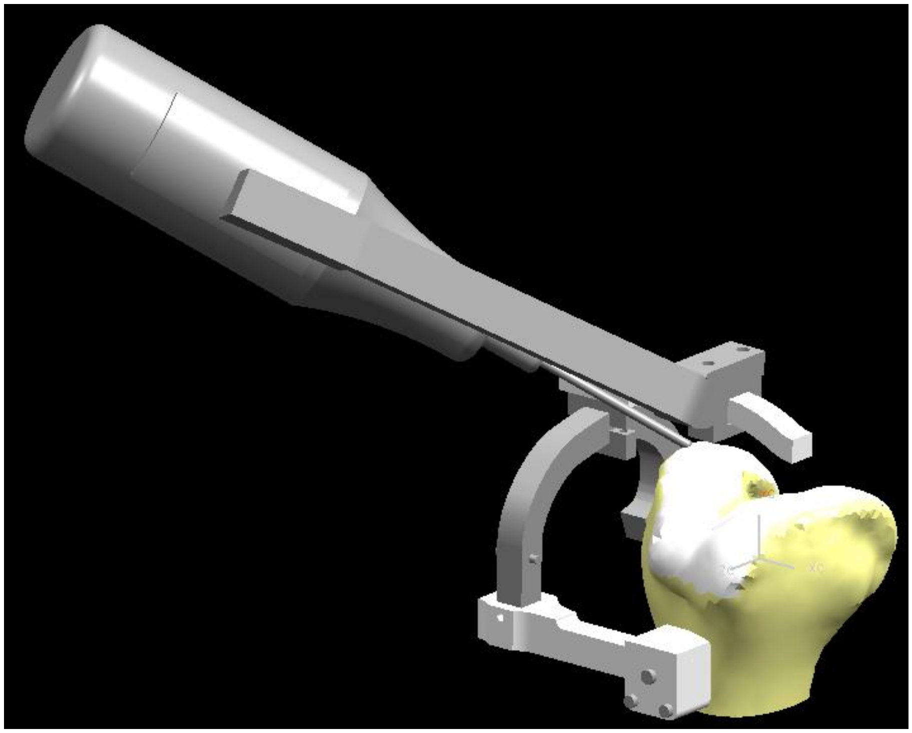

Figure 6.37 Final medial assembly

Chapter 7

Experiment and results

7.1. Manufacturing

To assess the patient specific cutting tool, the components and femur with cartilage model were manufactured. The anteroposterior tracks were manufactured through wire EDM, a CNC process which uses an electrically charged wire to cut through metal. The material selected for the anteroposterior tracks and slider was 4140 annealed steel. Steel was chosen for the anteroposterior tracks and slider component because it was determined experimentally that these components manufactured from ABS plastic were not rigid at the designed dimensions and expected loads. The wire EDM tolerances were 1/1000th of an inch and the process left a smooth surface finish of RA 32, which is similar in roughness to the top of a plastic soda cap. Also, creating the slider in two halves allowed the anteroposterior tracks and slider components to be manufactured from one plate of 4140 annealed steel in one operation, reducing manufacturing complexity.

Mechanical property	(ksi)
Tensile Strength	98
Yield Strength	61
Elastic Modulus	27,000

Table 7.1 Mechanical properties of 4140 annealed steel

A Stratysis Vantage i FDM system was used to manufacture the positioning components and mediolateral tracks from ABS plastic. The base component and patient specific jig were made through an FDM process because the irregular surfaces created from the patient anatomy are difficult to machine. The fixation arm, ML tracks, holster and targeting piece were manufactured from ABS plastic to save production cost and determine if an all steel assembly was warranted. After production, the holster was braced further with a steel support to reduce its deformation.

Mechanical property	(psi)
Tensile Strength	4300
Compression Strength	9000
Flexural Modulus	300000

Table 7.2 Mechanical properties of ABS plastic used

A base was added to the femur and cartilage model so that it could be anchored during experimentation with screws. The femur model was manufactured from zp-130 by a Z-Corp 310 3D printer. Zp-130 is a proprietary powder bound by an epoxy to create a composite.

7.2. Femur Digitization

A Monolta Vivid 910 3d digitizer was used to scan the surface of the experimental femur and create a point cloud within Rapidform 2006. The point cloud was then reconstructed to create a surface model and exported as an STL. The digitized femur model and original femur model were then imported into Amira 3.0, where the digitized femur model was aligned to the original femur model Figure 7.1. The mean surface distance between the digitized model and original model was 0.42 mm Figure 7.2.

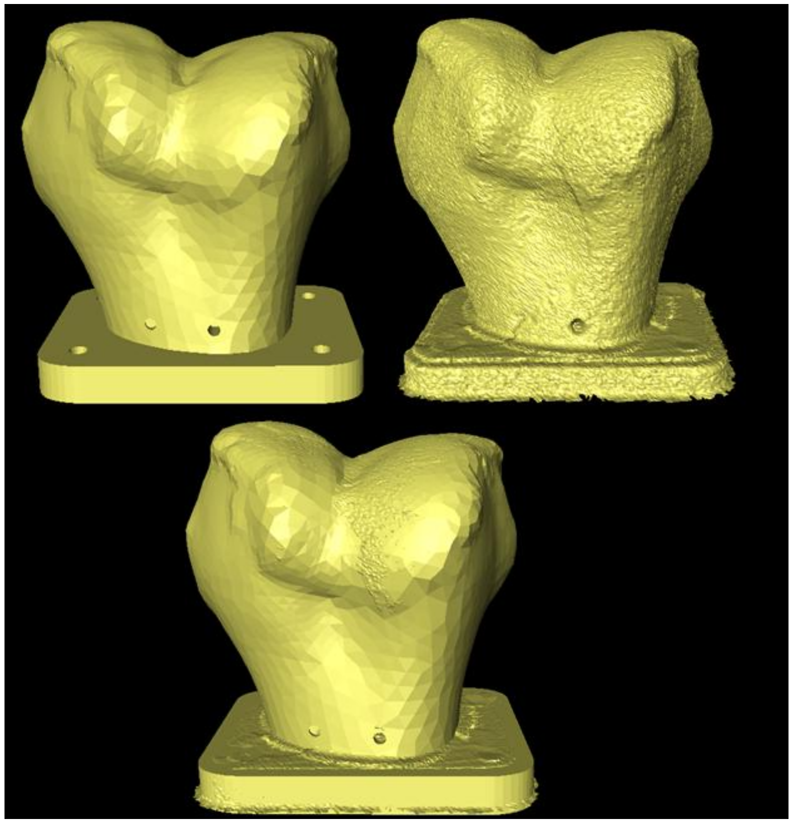

Figure 7.1. Original femur model with cartilage (top left), digitized femur model with cartilage (top right), and digitized and original models aligned together (bottom left)

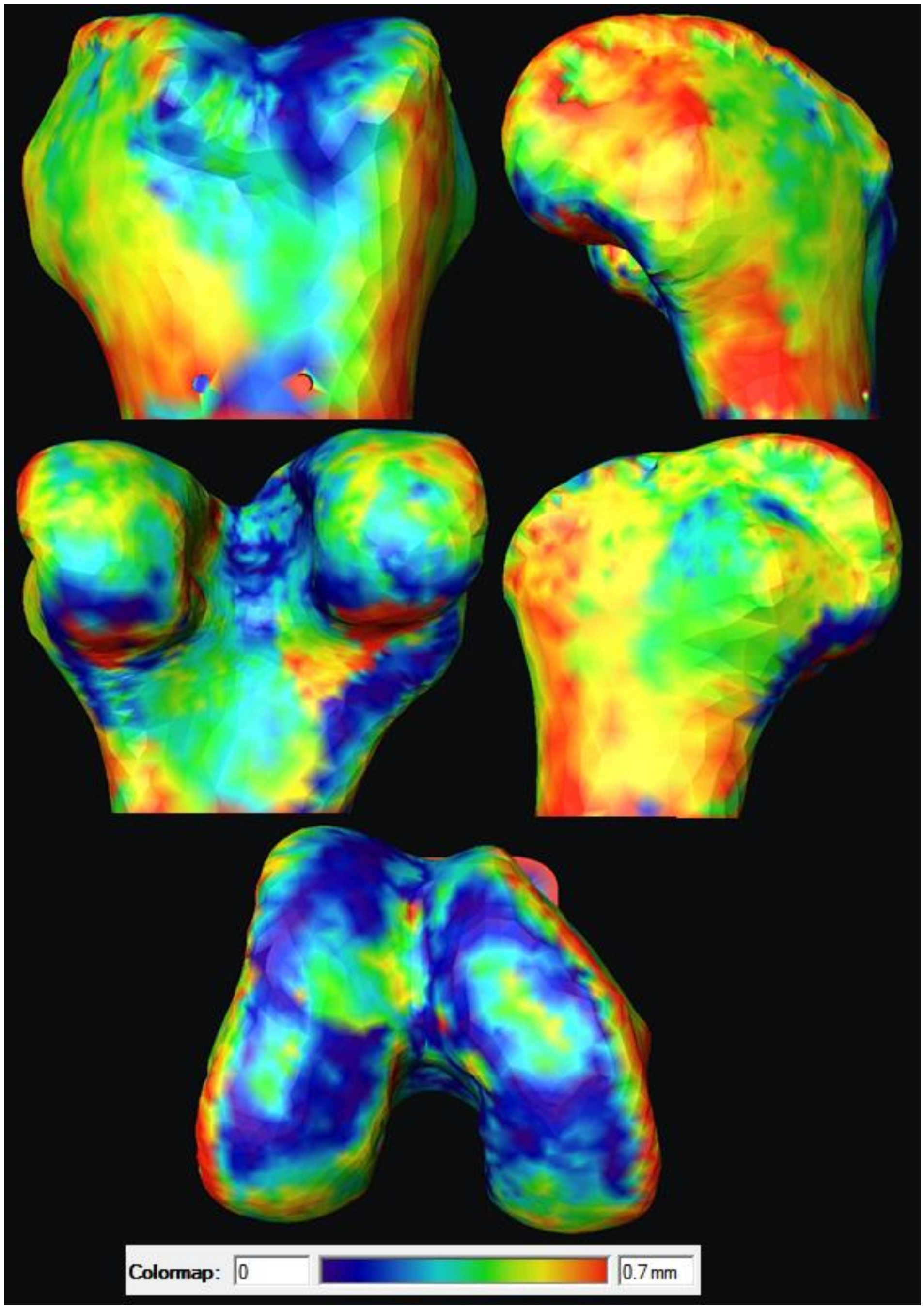

Figure 7.2. Distance map between aligned original and digitized femur models.

7.3. Experimental Procedure

The holster was matched to the slider component by inserting 1/8th inch bolts through the corresponding holes of the holster and slider component. These were then secured together with nuts. The targeting piece was then inserted into the slider. The Dremel was matched to the holster and aligned to its modeling space position by inserting the tip of the drill bit into the targeting piece and securing the Dremel to the holster with tape and zip ties. The targeting piece was then removed.

The experimental femur model was secured by screws to a wooden platform. The base component was inserted into the receptacle of the patient specific jig. The patient specific jig was placed onto the experimental femur and the quality of fit was assessed by attempting to wiggle the jig out of position. The fit of the jig was unambiguous and the base component was secured to the experimental femur with screws. The jig was then removed and the fixation arm was inserted into the slot of the base component and fixed in place with a screw. The medial, lateral, then anterior sections of the femur were processed by fitting the corresponding pair of AP and ML tracks into the slot of the fixation arm then attaching the holster and drill to the ML track. Starting from the anterior, the femur was processed by moving the drill bit along the ML track then incrementally advancing the ML track posteriorly along the AP track.

After the medial, lateral, and anterior sections were processed the base component was removed from the femur model and the femur model was removed from the wooden platform. The processed femur was then digitized with the Monolta Vivid 910 3d digitizer and a surface model was constructed with Rapidform 2006 and saved as an STL file. The digitized femur model was then aligned to the simulated femur model. The mean surface distance between the digitized model and simulated model was 0.58 mm.

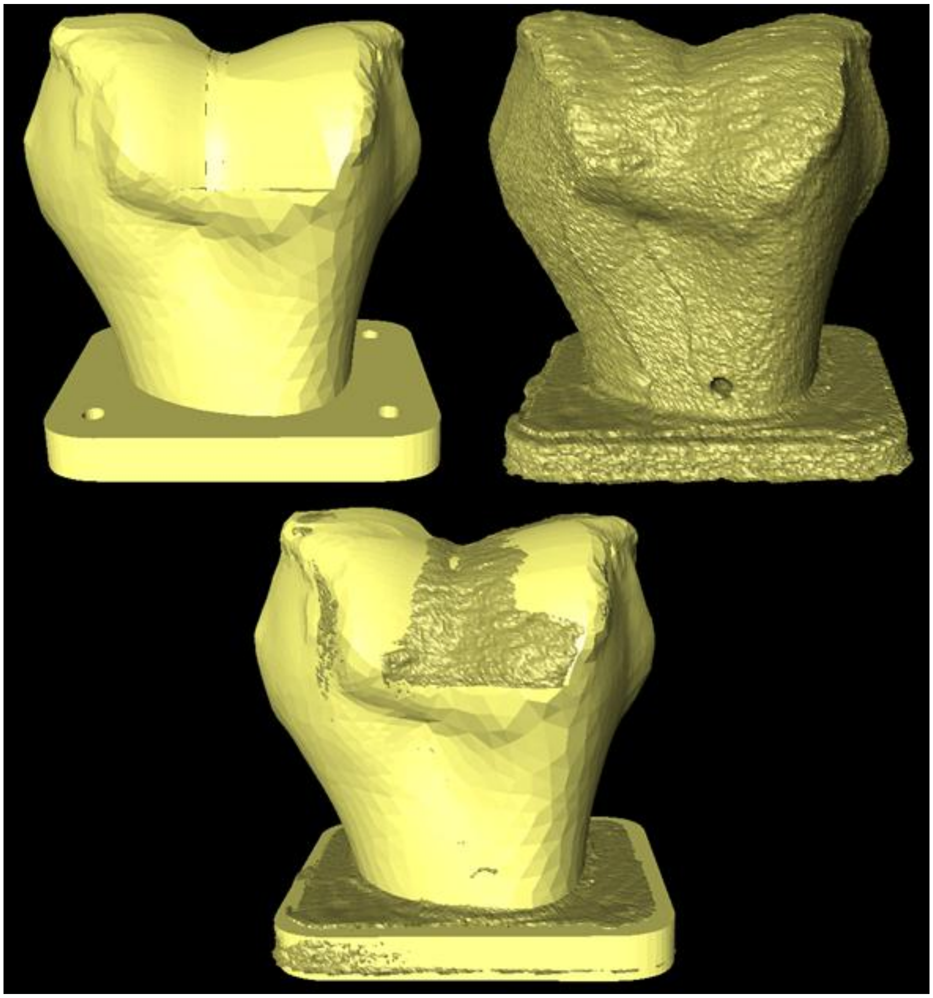

Figure 7.3. Simulated femur model after cartilage removal (top left), Digitized experimental femur model after cartilage removal (top right), and experimental and simulated models aligned together (bottom left)

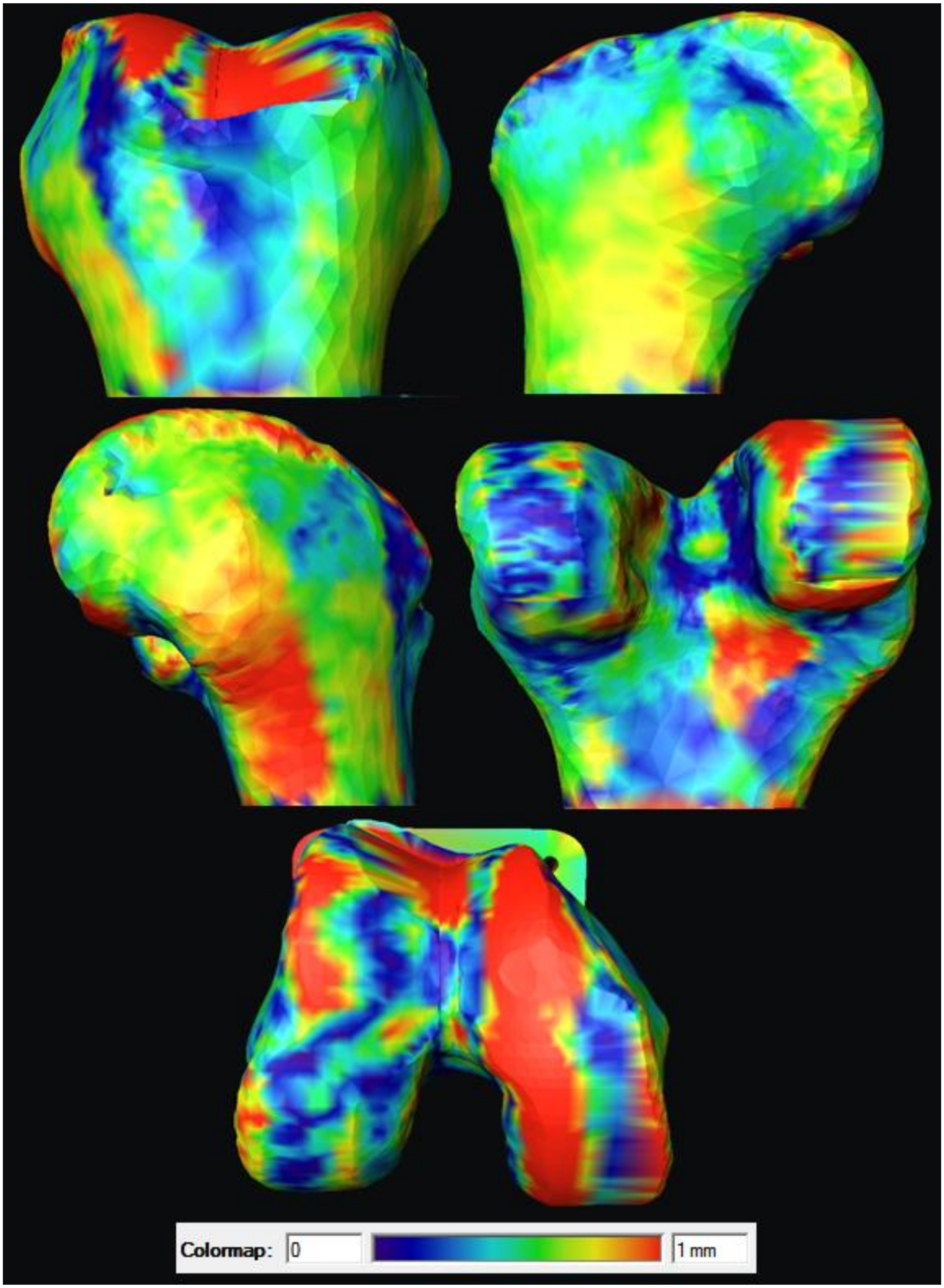

Figure 7.4. Distance map between original and digitized femur models after cartilage removal (global mean 0.58 mm).

7.4. Results Analysis

Rapidform 2006 was used to remove the cartilage surface from the digitized femur model. The cartilage surface was then placed over the digitized processed femur model in Amira 3.0 Figure 7.5 so that the thickness of the cartilage removed could be assessed Figure 7.6. The mean cartilage thickness removed was 0.91 mm with a maximum of 5.04 mm as compared to the simulated results which yielded a mean cartilage thickness removed of 0.38 mm with a maximum of 3.6 mm.

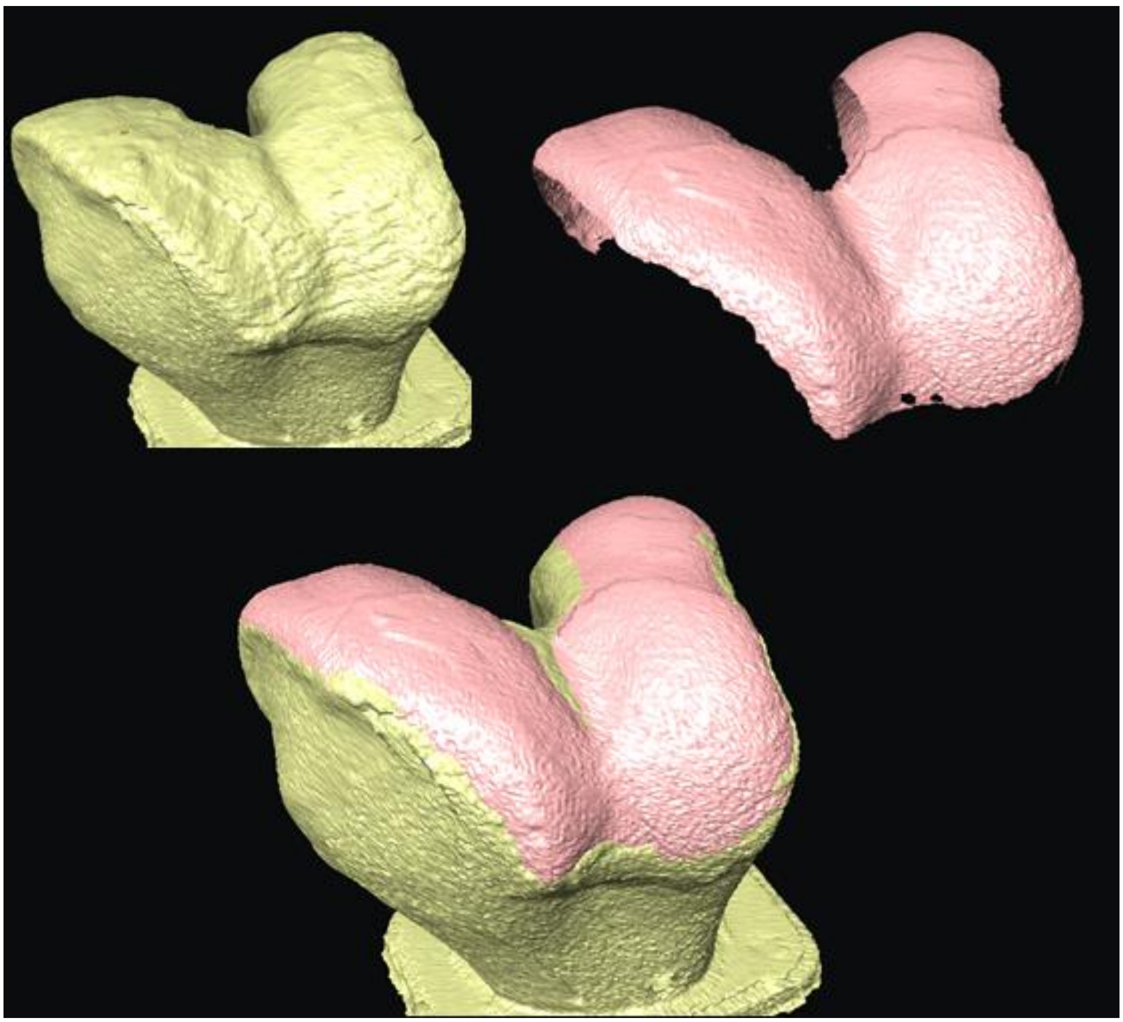

Figure 7.5. Digitized femur model after cartilage removal and removed cartilage section

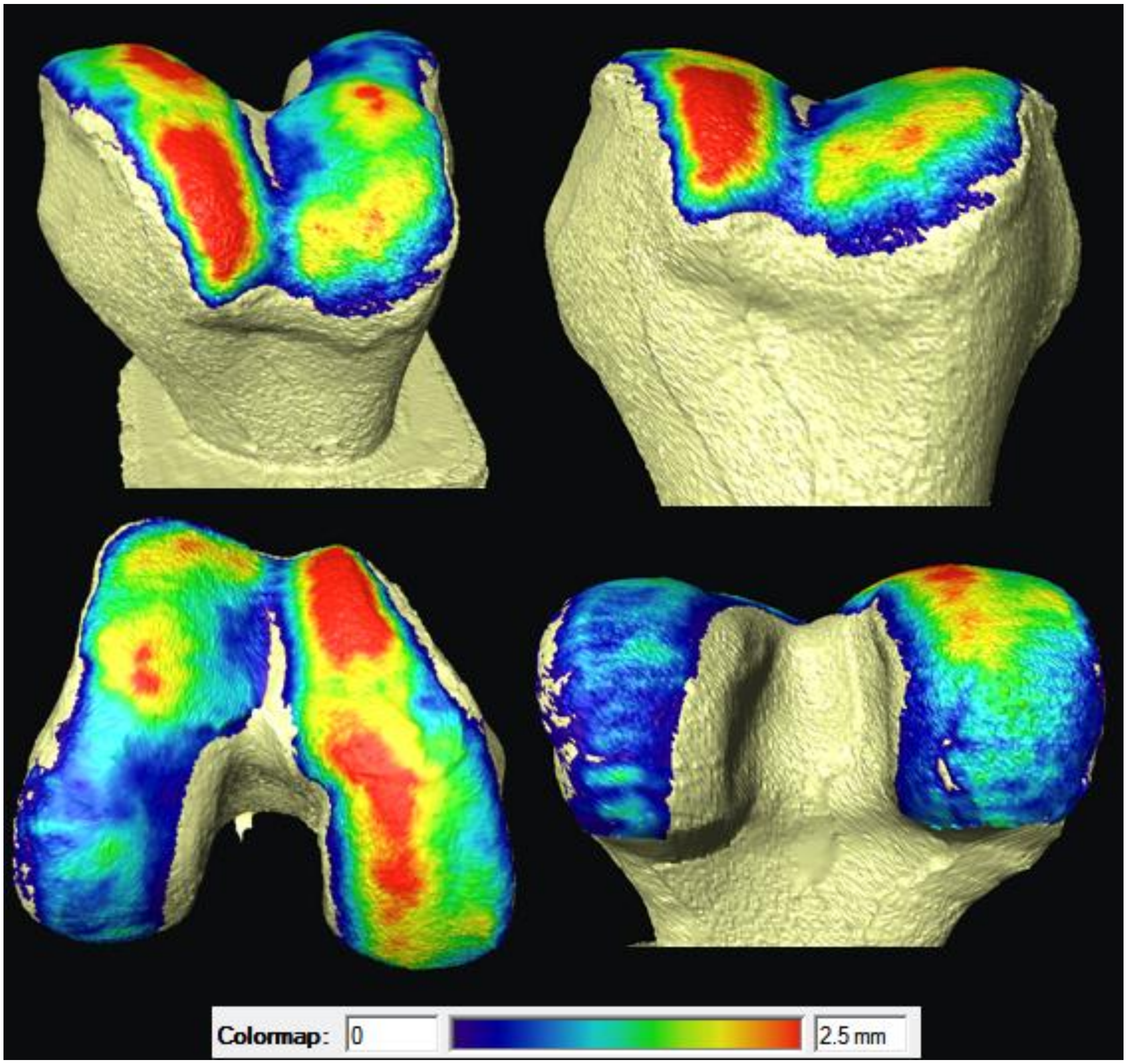

Figure 7.6. Distance map between the removed cartilage and digitized femur model (mean cartilage removed is 0.9mm).

7.5. Conclusions

The iCS generated jig modified with the tongue component was able to accurately position the base component with respect to the femur. The base component fit solidly to the femur model and did not change position through the procedure. The fixation arm was successfully constrained by the base component.

Although the design was able to successfully guide the drill through the intended cutting area, several design issues were discovered.The AP track was not constrained acceptably by the fixation arm. This was due to the ABS plastic of the fixation arm shifting during the experiment.

The AP slider was able to travel along each AP track and provide a rigid support for the ML tracks. The ML tracks were not rigid enough to support the drill and holster without deflection during use. Also, the surface contact between the ABS plastic surface of the ML tracks and steel surface of the ML slider did not allow the drill bit to freely slide along the ML track. The shifting of the ABS plastic ML tracks and fixation arm was the most outstanding cause of the difference in cutting depth between the simulation and experimental results.

Chapter 8

Future Work

8.1. Design Improvements

While the slider component performed as a rigid frame to mount the holster and ML tracks, it should be further refined to improve its ability to glide over the AP and ML tracks. The roughness of the inner surface contributed in decreasing the ability of the Slider component to travel easily across the tracks. This can be accomplished by either including further polishing techniques such as sand blasting to further smooth the surface or incorporating roller bearings as the contact between the slider and AP tracks. Both approaches could be tested in the future by attaching a simple force gauge to each Slider design and measuring the force required to move the Slider along the AP and ML tracks.

The ML tracks and fixation arm were not acceptably rigid, which allowed the drill bit to deviate from its intended path. The surface interaction between the steel slider components and ABS plastic was also not acceptably smooth. The contact between the steel sliders and track was more successful in providing a smooth gliding action than between the abs plastic track and steel slider. Because of this, the ML tracks should be manufactured from steel as well.

While the Dremel was able to remove the resin material that the femur model was manufactured of, it is considerably more bulky than the microsurgical drill that a surgeon would likely use. In addition, the holster created to fit the drill should be further refined to be made of steel and include a more form fit method of attachment to the drill than that currently used.

8.2. Smart Microsurgical Robot

Although the discussed design improvements should increase the usability and accuracy of the cutting tool, the design is still limited to utilizing a separate rigid AP and ML track for each condyle. This results in the depth of the cutting tool not being able to conform locally to the bone contour. With future work, this design limitation can be eliminated by replacing the ML tracks and drill and holster assembly with a smart microsurgical robot. The proposed robot would be translated about the femur by the surgeon's hand in the ML and AP directions. The cutting depth of the drill bit would adjust depending on the location of the robot with respect to the femur, allowing a contoured resection.

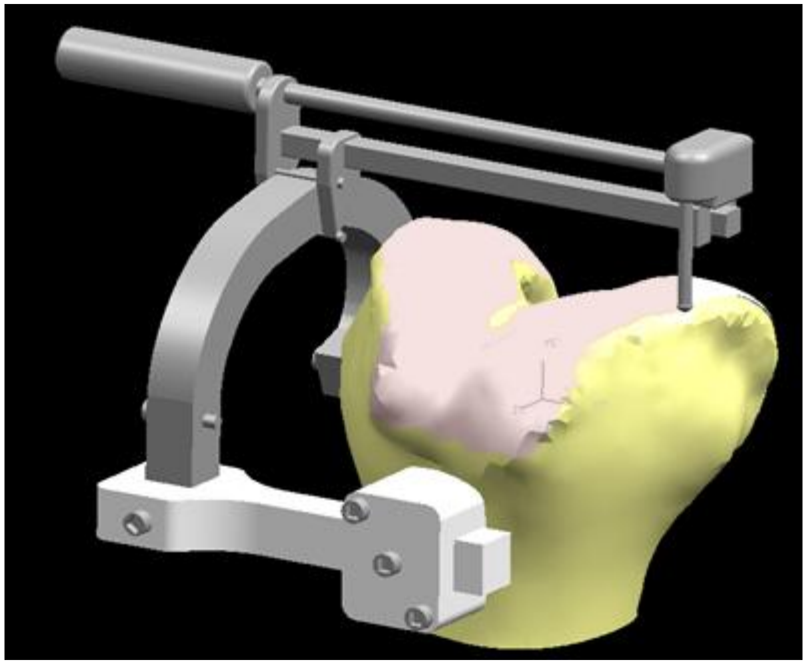

Figure 8.1 Microsurgical Robot

The location of the drill bit could be tracked in the AP and ML directions via a linear cable extension transducer. The output voltage of the transducer varies as the length of cable drawn from the transducer changes. The transducer is connected to reference points on the robot and the AP track Figure 8.2. As the robot is translated about the AP track, the output voltage of the transducer accordingly changes and the position of the robot is known. Similarly, the location of the robot in the mediolateral direction is also determined by a linear cable extension transducer. The transducer is connected to reference points on the robot support frame and the robot exterior Figure 8.3.

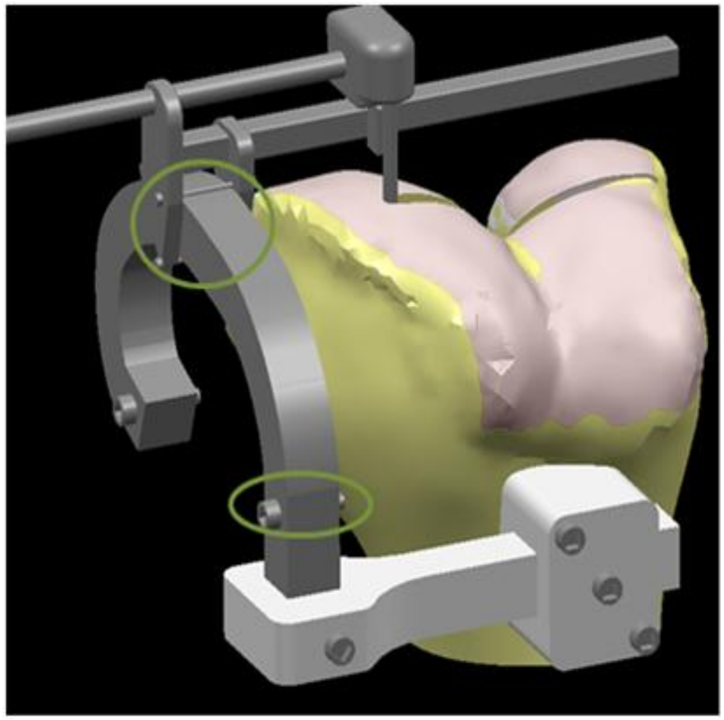
Figure 8.2 Reference points for the AP linear cable extension transducer

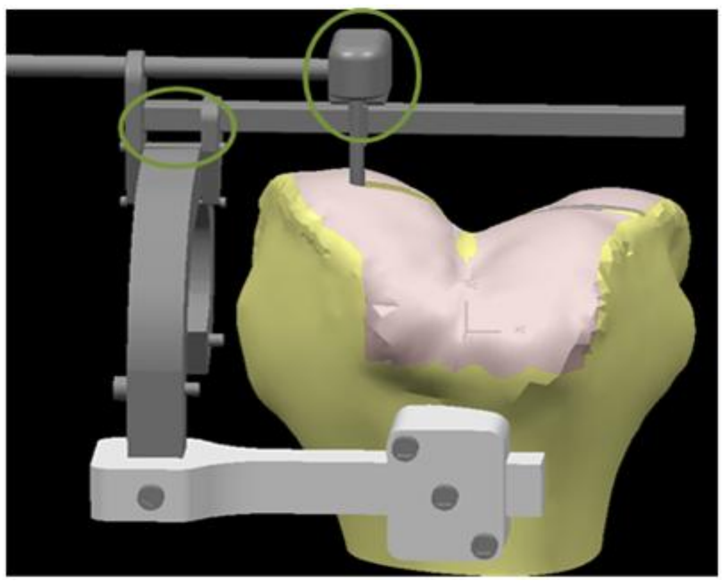
Figure 8.3 Reference points for the ML linear cable extension transducer

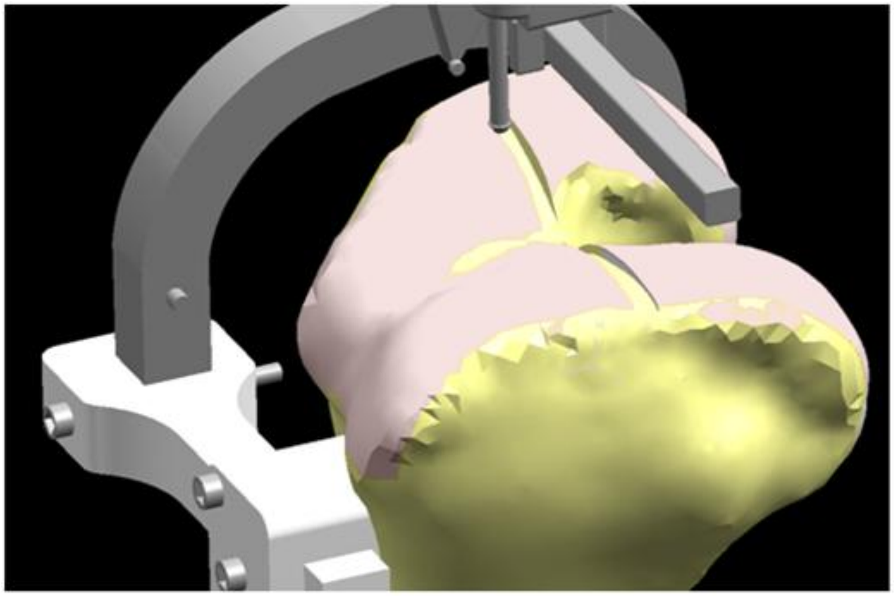

Figure 8.4 Robot contouring to the femur surface

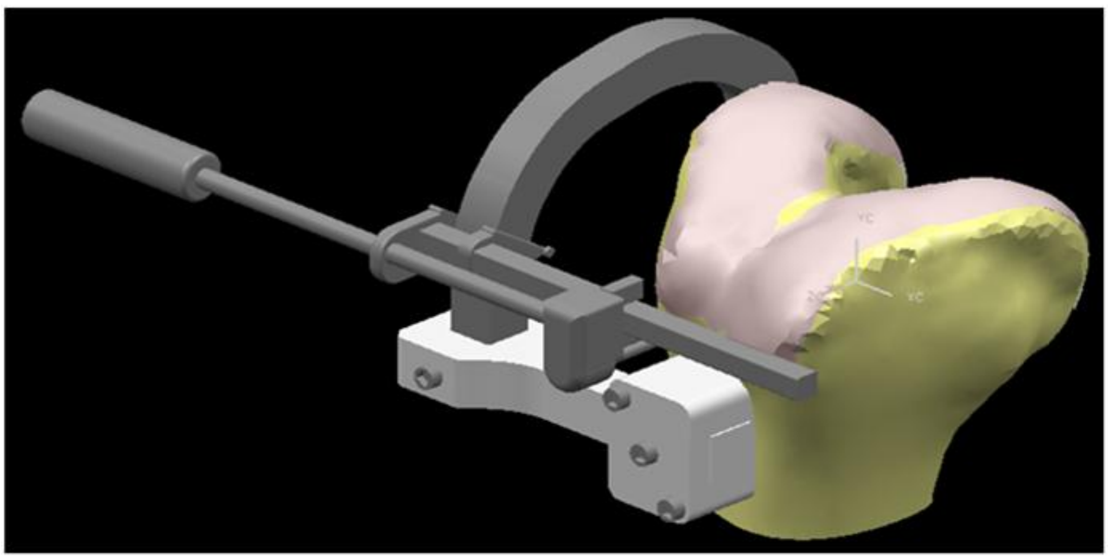

Figure 8.5 Robot in position before resection

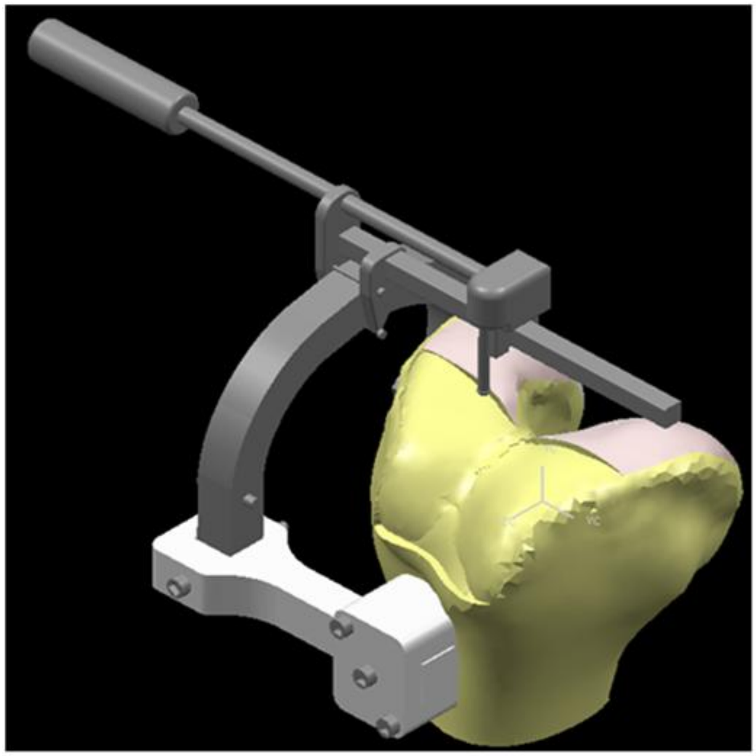

Figure 8.6 Robot contoured resection

Bibliography

References

[1] M.R. Mahfouz, (2009). Implant Design Analysis Suite. USA

[2] T. P. Vail, J.E. Lang,"Surgical Techniques and Instrumentation in Total Knee Arthoplasty,"*Surgery of the Knee (4th edition, Vol 2)*, Churchill Livingstone, ISBN 0-443-6671-X, pp. 1455-1521.

[3] M.A. Hafez, B. Jaramaz, A DiGioia III, "Computer-Assisted Knee Surgery: An Overview,"*Surgery of the Knee (4th edition, Vol 2)*, Churchill Livingstone, ISBN 0-443-6671-X, pp. 1655-1674.

[4] S.D. Stulberg "Computer-Navigated Total Knee Arthoplasty,"*Surgery of the Knee (4th edition, Vol 2)*, Churchill Livingstone, ISBN 0-443-6671-X, pp. 1675-1688.

[5] M. Roche, "MAKOplasty® Unicompartmental Knee Surgery: Early Clinical Results," in *Orthopaedic Product News*, 2006.

[6] M. Conditt "Outcomes of Initial Series of MAKOplasty® Unicompartmental Knee Arthroplasty"

[7] A. V. Lombardi, K. R. Berend,J. B. Adams," Patient-specific Approach in Total Knee Arthroplasty" *Orthopedics,*vol. 30,pp. 927, 2008.

[8] J. Slamin, D. Steins, "Bringing Personalized Medicine to Orthopedics"

[9] CT Protocol Reference Guide for the ConforMIS Family of Knee Resurfacing Implants

[10] Conformis iUniG2 Surgical Technique Guide

[11] M.R. Mahfouz, E. Fatah,L. S. Bowers, G. Scuderi, "Three-Dimensional Morphology of the Knee, an Ethnic Study," *Clinical Orthopaedics and Related Research*.

[12] N. Roidis, T. Karachalios, K. Malizos, and E. McPherson, "Incision stretching in primary TKA: what is the real length of our approach?," *Orthopedics*, vol. 30, pp. 397-398, 2007.

[13] R. S. Laskin, "Minimally Invasive Total Knee Arthroplasty: The Results Justify Its Use," *Clinical Orthopaedics and Related Research*, vol. 440, pp. 54-59 2005

[14] S. K. Kane RL, Wilt TJ, Bershadsky B, Cross WW III, MacDonald RM, Rutks I., "Total Knee Replacement. Evidence Report/Technology Assessment No. 86," *Agency for Healthcare Research and Quality*, 2003.

[15] G. Sabbioni, N. Rani, N. Del Piccolo, R. Ben Ayad, C. Carubbi, and D. Tigani, "Gap balancing versus measured resection technique using a mobile-bearing prosthesis in computer-assisted surgery," in *Musculoskeletal Surgery*, vol. 95: Springer Milan, 2011, pp. 25-30.

[16] W. Fitz, R.D. Scott,"Unicompartmental Knee Arthoplasty,"*Surgery of the Knee (4th edition, Vol 2)*, Churchill Livingstone, ISBN 0-443-6671-X, pp. 1409-1420.

[17] D. Saragaglia, G. Estour, C. Nemer, and P.-E. Colle, "Revision of 33 unicompartmental knee prostheses using total knee arthroplasty: strategy and results," in *International Orthopaedics*, vol. 33: Springer Berlin / Heidelberg, pp. 969-974, 2009.

[18] J. N. Insall, G. R. Scuderi, R. D. Komistek, K. Math, D. A. Dennis, and D. T. Anderson, "Correlation Between Condylar Lift-Off and Femoral Component Alignment," *Clinical Orthopaedics and Related Research*, vol. 403, 2002.

[19] F Johnson, S Leitl, W Waugh 'The distribution of load across the knee. *'A comparison of static and dynamic measurements'*. Journal of Bone and Joint Surgery - British Volume, Vol 62-B, Issue 3,pp. 346-349 1980

[20] Zimmer Natural-Knee® II Primary System Surgical Technique

[21] J. Saksena, V. Kosmopoulos, and C. Schizas, "An intramedullary alignment guide lodging within the femoral canal during total knee arthroplasty: a case report.," *J Orthop Surg (Hong Kong)*, vol. 16, pp. 114-6, 2008.

[22] Depuy Orthopedics Measured Resection Fixed Reference Surgical Technique

[23] Stryker precisioN Knee Navigation Operative Technique

[24] J.B. Stiehl, W.H. Konermann, R.G. Haaker, A.M. DiGioia (2006): *'Navigation and MIS in Orthopedic Surgery,'* Springer Publishing Company, ISBN 3-540-36690-3

[25] M. Roche, P. F. O'Loughlin, D. Kendoff, V. Musahl,A. D. Pearle, "Robotic Arm–Assisted Unicompartmental Knee Arthroplasty: Preoperative Planning and Surgical Technique," *Am J Orthop,*vol. 38 (2 Suppl),pp. 10-15, 2009

[26] P. Ritschl, F. Machacek, R. Fuiko, "Modern Navigated Ligament Balancing in Total Knee Arthroplasty with the PiGalileo System," in *'Navigation and MIS in Orthopedic Surgery,'* Springer Publishing Company, ISBN 3-540-36690-3

[27] C. Plaskos, P. Cinquin, S. Lavallée,A.K. Hodgson, 'Praxiteles: a miniature bone-mounted robot for minimal access total knee arthroplasty,' *The International Journal of Medical Robotics and Computer Assisted Surgery,* vol. 4, pp.67-79, 2005

[28] S.M. Howell, K. Kuznik, M. L. Hull, R. A. Siston, "Results of an Initial Experience with Custom-fit Positioning Total Knee Arthroplasty in a Series of 48 Patients," *Orthopedics*, vol. 31, pp. 857-863, 2008.

[29] M. R. Mahfouz, R. E. Booth, Jr., J. N. Argenson, B. C. Merkl, M. J. Kuhn, E. Fatah, E. R. Pritchard. "Utilization of Biplanar X-Ray Images in 3D Reconstruction of Patient-Specific Bones and Automatic Morphometric Measurements," 7th International Symposium on Computer Methods in Biomechanics and Biomedical Engineering, Antibes, Cote d?Azur, France, 2006.

[30] M. R. Mahfouz, "Three-Dimensional Morphology of the Knee" *Surgery of the Knee* 2011

[31] C. Runge: "Über empirische Funktionen und die Interpolation zwischen äquidistanten Ordinaten," *Zeitschrift für Mädematik und Physik*, vol. 46, pp. 224–243, 1901

[32] J.H. Mathews, K.K. Fink (2004): *'Numerical Methods Using Matlab (4th Edition),'* Prentice Hall, ISBN 0-130-65248-2

[33] G.D. Knott (1999):*'Interpolating cubic splines,'* Birkhäuser Boston, ISBN 0-817-64100-9

[34] MATLAB version R2010a Documentation, Natick, Massachusetts: The MathWorks Inc., 2011

Image Sources

{1} D.W. LENNOX, L.H. RILEY Jr. "Elective Surgery of the knee" in *Atlas of Orthopaedic Surgery*, Vol. 3, Lower Extremity. C.A. Laurin, L.H. Riley Jr., R Roy-Camille, Ed. Paris, Masson, 1991

{2} R.S. Gorab "Minimally Invasive Knee Replacement Incisions," Internet: http://www.robertgorab.com/minimallyinvasive-kneearthroplasty.html, Jul. 14, 2011

{3} Internet: http://www.conformis.com/Patients/ConforMIS-Patient-Specific-Implants , Jul. 14, 2011

{4} M.R. Mahfouz, (2009). Implant Design Analysis Suite. USA

{5} Zimmer Natural-Knee® II Primary System Surgical Technique

{6} Depuy Orthopedics Measured Resection Fixed Reference Surgical Technique

{7} Stryker precisioN Knee Navigation Operative Technique

{8} Internet: http://files.solidworks.com/InternalMarketing/PressRoom/medical/RIO%20Robotic%20Arm.jpg Jul. 14, 2011

{9} Internet: http://files.solidworks.com/InternalMarketing/PressRoom/medical/RIO_one.jpg Jul. 14, 2011

{10} P. Ritschl, F. Machacek, R. Fuiko, "Modern Navigated Ligament Balancing in Total Knee Arthroplasty with the PiGalileo System," in *'Navigation and MIS in Orthopedic Surgery,'* Springer Publishing Company, ISBN 3-540-36690-3

{11} C. Plaskos, P. Cinquin, S. Lavallée,A.K. Hodgson, 'Praxiteles: a miniature bone-mounted robot for minimal access total knee arthroplasty,' *The International Journal of Medical Robotics and Computer Assisted Surgery,* vol. 4, pp.67-79, 2005

Vita

Wes was born on January 17, 1987 in Levonia, Michigan. When he was four, Wes and his family moved to Columbia, Tennessee where he grew up. After graduating high school, he came to the University of Tennessee in fall of 2004 where he majored in Biomedical Engineering and eventually joined The Center for Musculoskeletal Research (CMR). Upon completing his bachelor's degree in the spring of 2008 he remained at CMR and pursued his master's degree under the direction of Dr. Mohamed Mahfouz. Wes is now ready to pursue a career in biomedical engineering.